

Noname manuscript No.
 (will be inserted by the editor)

A New Decomposition Paradigm for Graph-structured Nonlinear Programs via Message Passing

Kuangyu Ding · Marie Maros · Gesualdo Scutari

Abstract We study finite-sum nonlinear programs with localized variable coupling encoded by a (hyper)graph. We introduce a graph-compliant decomposition framework that brings message passing into continuous optimization in a rigorous, implementable, and provable way. The (hyper)graph is partitioned into tree clusters (hypertree factor graphs). At each iteration, agents update in parallel by solving local subproblems whose objective splits into an *intra*-cluster term summarized by cost-to-go messages from one min-sum sweep on the cluster tree, and an *inter*-cluster coupling term handled Jacobi-style using the latest out-of-cluster variables. To reduce computation/communication, the method supports graph-compliant surrogates that replace exact messages/local solves with compact low-dimensional parametrizations; in hypergraphs, the same principle enables surrogate hyperedge splitting, to tame heavy hyperedge overlaps while retaining finite-time intra-cluster message updates and efficient computation/communication. We establish convergence for (strongly) convex and nonconvex objectives, with topology- and partition-explicit rates that quantify curvature/coupling effects and guide clustering and scalability. To our knowledge, this is the first convergent message-passing method on loopy graphs.

Keywords Distributed optimization · Graph decomposition · Message passing · Block Jacobi · Hypergraph

Mathematics Subject Classification (2020) 90C30 · 90C25 · 68W15 · 05C85

1 Introduction

We study optimization problems with graphical structure, modeling localized interactions among decision variables. These interactions are encoded by a (hyper)graph. Let $\mathcal{G} = (\mathcal{V}, \mathcal{E})$ be a hypergraph with node set \mathcal{V} of cardinality $|\mathcal{V}| = m$; nodes will henceforth be referred to as *agents*. The hyperedge set is $\mathcal{E} \subset 2^{\mathcal{V}}$. Agent i controls a vector $x_i \in \mathbb{R}^d$; we stack $\mathbf{x} = [x_1^\top, \dots, x_m^\top]^\top \in \mathbb{R}^{md}$. For any hyperedge

K. Ding
 Edwardson School of Industrial Engineering, Purdue University, West Lafayette, IN. E-mail: ding433@purdue.edu.

M. Maros
 Wm Michael Barnes '64 Department of Industrial and Systems Engineering, Texas A&M University, College Station, TX. E-mail: mmaros@tamu.edu.

G. Scutari
 Edwardson School of Industrial Engineering & Elmore Family School of Electrical and Computer Engineering, Purdue University, West Lafayette, IN. E-mail: gscutari@purdue.edu.

The work of Ding and Scutari has been supported by the ONR Grant # N00014-24-1-2751.

$\omega \in \mathcal{E}$, denote by $x_\omega = (x_i)_{i \in \omega} \in \mathbb{R}^{d|\omega|}$ the subvector indexed by ω . Each agent i and hyperedge $\omega \in \mathcal{E}$ is associated with the smooth functions $\phi_i : \mathbb{R}^d \rightarrow \mathbb{R}$ and $\psi_\omega : \mathbb{R}^{|\omega|d} \rightarrow \mathbb{R}$, respectively. The optimization problem reads

$$\min_{\mathbf{x} \in \mathbb{R}^{md}} \Phi(\mathbf{x}) := \sum_{i=1}^m \phi_i(x_i) + \sum_{\omega \in \mathcal{E}} \psi_\omega(x_\omega). \quad (\text{P})$$

Throughout the paper, we assume (P) admits a solution.

A common special case is *pairwise* coupling, where $\mathcal{E} \subseteq \{\{i, j\} : i \neq j\}$ (every hyperedge has size two). The graphical model reduces to an undirected graph with pairwise interactions, and (P) specializes to

$$\min_{\mathbf{x} \in \mathbb{R}^{md}} \Phi(\mathbf{x}) = \sum_{i=1}^m \phi_i(x_i) + \sum_{(i,j) \in \mathcal{E}} \psi_{ij}(x_i, x_j), \quad (\text{P}')$$

where $\psi_{ij} : \mathbb{R}^{2d} \rightarrow \mathbb{R}$ is symmetric in its arguments, i.e., $\psi_{ij}(x_i, x_j) = \psi_{ji}(x_j, x_i)$.

While many problems can be cast in the form (P) (e.g., by using a single factor over all variables), our focus is on *sparse* graphical structure, meaning each coupling term ψ_ω depends only on a small subset of agents variables. Such sparsity is central in applications ranging from Markov random fields in statistical physics to graph-based signal processing, communication and power networks, and large-scale decentralized optimization; see Sec. 1.3 for motivating examples.

Leveraging graphical sparsity, our goal is to design decentralized algorithms that decompose (P) into weakly coupled subproblems solved via *localized computation* and *single-hop* neighbor communication. Key desiderata are: (i) communication efficiency (costs scale with local degree, not network size), (ii) scalability to large graphs, and (iii) minimal coordination overhead (no central coordinator). As we detail next, existing approaches generally fall short.

(i) Graph-agnostic decentralizations. Naively decentralizing gradient descent or classical block methods (Jacobi/Gauss–Seidel) [1] is communication inefficient and ignores the graphical structure. In gradient descent, agent i needs

$$\nabla_i \Phi(\mathbf{x}) = \nabla \psi_i(x_i) + \sum_{\omega \in \mathcal{E}: i \in \omega} \nabla_i \psi_\omega(x_\omega),$$

which depends on all variables in each factor scope ω containing i ; thus agents must collect and broadcast information beyond single-hop neighborhoods, incurring heavy coordination overhead. Likewise, vanilla Jacobi requires dense, iteration-by-iteration neighbor synchronization, while Gauss–Seidel enforces sequential updates and global scheduling. In both cases, per-iteration communication scales with network size rather than local degree.

(ii) Consensus-based methods. Problem (P) can be cast as min-sum program over networks—i.e., $\min_x \sum_{i=1}^m f_i(x)$ —for which a vast literature of gossip/consensus schemes exists, including decentralized gradient methods [9, 25, 26, 48], gradient tracking-based algorithms [10, 24, 35, 39] and primal-dual variants [36, 37, 50]; we refer to the tutorial [23] and the monograph [32] for further references. Despite their differences, these methods share a common *lifting*: each agent maintains a local copy x_i of the *full* decision vector \mathbf{x} and enforces agreement via gossip averaging or dual reformulations. This is ill-suited for *sparsely coupled* problems like (P): (a) *memory/communication inflation*—agents store and exchange md -dimensional vectors regardless of their degree or size of local factor scopes; and (b)

consensus-limited rates—convergence is governed by the mixing spectral properties (e.g., spectral gap), which can be slow on poorly connected graphs and scale poorly with m on some topologies [6, 33, 47]. This motivates methods that operate on *single-hop, scope-sized* messages without replicating the entire decision vector.

(iii) Methods for overlapping neighborhood objectives. The line of work [4, 5, 8, 18, 38] develops decentralized algorithms tailored to *neighborhood-scoped* cost functions—a special instance of (P)—of the form

$$\min_{\mathbf{x} \in \mathbb{R}^{md}} \Phi(\mathbf{x}) = \sum_{i=1}^m \phi_i(x_{\mathcal{N}_i}), \quad (\text{P}'')$$

where $x_{\mathcal{N}_i}$ is the vector containing the variables of agents i and its immediate neighbors. The difficulty here is that a local update at agent i (or on $x_{\mathcal{N}_i}$) requires *current* information on blocks *controlled by other agents*. The following are existing strategies to cope with this multi-hop coupling (hyperedge).

(a) *Overlapping domain decomposition/Schwarz-type patch updates.* These methods form *overlapping* subproblems by enlarging each *block of variables* (patch) by creating *local copies* of the variables in the overlap (one copy per patch), thereby decoupling the local minimizations. The algorithm then alternates block updates with the exchange of overlap values (or boundary interfaces) across neighboring patches to reconcile overlap-inconsistency; see [38] and Schwarz/domain-decompositions [4, 40]. In graph settings as (P''), this yields decentralized (asynchronous) Jacobi- or Gauss-Seidel-like updates on overlapping neighborhoods. Their convergence is established most notably for strongly convex *quadratic* objectives [38]—typically under implicit contractivity/diagonal-dominance-type conditions that are difficult to verify a priori. Moreover, when convergence rates are provided, they are rarely explicit: the contraction factor is usually buried in graph- and overlap-dependent constants (e.g., spectral radii of certain operators), making it hard to extract clean scaling laws with respect to d, m , or the degree of overlapping.

(b) *Asynchrony, delays, and event-triggered exchanges.* A complementary line of work reduces the communication burden by limiting *when* and *which* information (primal blocks, gradients, or local models) is exchanged, via asynchronous updates, randomized activations, or event-triggered communication; see, e.g., [5, 8, 18] and references therein. These works typically prove convergence making the effect of asynchrony explicit through delay/activation parameters. However, the *structural* dependence of the rate on overlap-induced coupling—e.g., hyperedge size $|\mathcal{N}_i|$, overlap multiplicity, or topology features such as diameter/expansion—is rarely exposed. Instead, scalability is absorbed into global constants (Lipschitz/monotonicity moduli, operator norms, error-bound parameters, etc.) that conflate graph and overlap effects and are hard to interpret or certify a priori. Consequently, these schemes provide limited guidance on how communication savings trade off against convergence as m grows or overlap increases.

1.1 A message-passing viewpoint for graph-structured optimization

This paper takes a fundamentally different route than existing graph-compliant decompositions: we develop (to our knowledge) the first framework for nonlinear programs on graphs and hypergraphs that is *rigorously built around message passing*, with an explicit focus on computational and communication efficiency.

Message passing originates in statistics and information theory for inference on graphical models [42]. Its direct transplant to continuous nonlinear programs

typically leads to methods that may fail to converge on loopy graphs and incur prohibitive communication overhead. These bottlenecks help explain why message passing has remained peripheral in optimization, despite its appealing locality.

To make this perspective precise, next we provide a brief primer on min-sum/message passing and then review existing min-sum-type methods for non-linear programs and their limited convergence guarantees.

Message passing on acyclic graphs: a primer. Consider the pairwise instance of (P') over a path graph $\mathcal{G} = (\mathcal{V}, \mathcal{E})$, $\mathcal{V} = \{1, \dots, m\}$ and $\mathcal{E} = \{\{i, i+1\} : i = 1, \dots, m-1\}$:

$$\underset{x_1, \dots, x_m \in \mathbb{R}^d}{\text{minimize}} \sum_{i=1}^m \phi_i(x_i) + \sum_{j=1}^{m-1} \psi_{j,j+1}(x_j, x_{j+1}). \quad (1)$$

Here, each node i controls the variable x_i , has access to ϕ_i , $\psi_{i-1,i}$, $\psi_{i,i+1}$, and communicates with its immediate neighbors (nodes $i-1$ and $i+1$).

When the graph is *cycle-free* as above, min-sum/sum-product message passing reduces to dynamic programming, leveraging the following decomposition of (1):

$$x_i^* \in \underset{x_i \in \mathbb{R}^d}{\text{argmin}} \phi_i(x_i) + \mu_{i-1 \rightarrow i}^*(x_i) + \mu_{i+1 \rightarrow i}^*(x_i), \quad \forall i = 1, \dots, m, \quad (2)$$

where

$$\mu_{i-1 \rightarrow i}^*(x_i) := \underset{x_1, \dots, x_{i-1} \in \mathbb{R}^d}{\min} \sum_{j=1}^{i-1} \phi_j(x_j) + \sum_{j=1}^{i-1} \psi_{j,j+1}(x_j, x_{j+1}), \quad (3a)$$

$$\mu_{i+1 \rightarrow i}^*(x_i) := \underset{x_{i+1}, \dots, x_m \in \mathbb{R}^d}{\min} \sum_{j=i+1}^m \phi_j(x_j) + \sum_{j=i+1}^{m-1} \psi_{j,j+1}(x_j, x_{j+1}), \quad (3b)$$

with boundary conditions $\mu_{0 \rightarrow 1}^*(\cdot) \equiv 0$ and $\mu_{m+1 \rightarrow m}^*(\cdot) \equiv 0$.

The functions $\mu_{i-1 \rightarrow i}^*$ and $\mu_{i+1 \rightarrow i}^*$ are the optimal costs of the left and right subchains of node i , conditioned on x_i through the boundary factors $\psi_{i-1,i}$ and $\psi_{i,i+1}$, respectively. It is assumed that $\mu_{i-1 \rightarrow i}^*(\cdot)$ and $\mu_{i+1 \rightarrow i}^*(\cdot)$ are sent to node i from its neighbors $i-1$ and $i+1$, respectively; hence the name “messages”.

Given the pairwise model in (3a)-(3b), the messages factorizes as:

$$\mu_{i-1 \rightarrow i}^*(x_i) = \underset{x_{i-1} \in \mathbb{R}^d}{\min} \phi_{i-1}(x_{i-1}) + \psi_{i-1,i}(x_{i-1}, x_i) + \mu_{i-2 \rightarrow i-1}^*(x_{i-1}), \quad (4a)$$

$$\mu_{i+1 \rightarrow i}^*(x_i) = \underset{x_{i+1} \in \mathbb{R}^d}{\min} \phi_{i+1}(x_{i+1}) + \psi_{i,i+1}(x_i, x_{i+1}) + \mu_{i+2 \rightarrow i+1}^*(x_{i+1}). \quad (4b)$$

This recursive decomposition suggests a simple iterative procedure for the computation of these functions over the path graph, using only neighboring exchanges: given the iteration index $\nu = 0, 1, 2, \dots$ and arbitrary initialization of all messages (with $\mu_{0 \rightarrow 1}^0 \equiv 0$ and $\mu_{m+1 \rightarrow m}^0 \equiv 0$), at iteration $\nu + 1$, perform a *forward* pass

$$\mu_{i \rightarrow i+1}^{\nu+1}(x_{i+1}) = \underset{x_i}{\min} \left\{ \phi_i(x_i) + \psi_{i,i+1}(x_i, x_{i+1}) + \mu_{i-1 \rightarrow i}^\nu(x_i) \right\}, \quad i = 1, \dots, m-1,$$

and a *backward* pass: for $i = m-1, \dots, 1$,

$$\mu_{i+1 \rightarrow i}^{\nu+1}(x_i) = \underset{x_{i+1}}{\min} \left\{ \phi_{i+1}(x_{i+1}) + \psi_{i,i+1}(x_i, x_{i+1}) + \mu_{i+2 \rightarrow i+1}^\nu(x_{i+1}) \right\}.$$

The algorithm above reaches the fixed point (4a)-(4b) in at most $m-1$ iterations (each composed of one forward pass plus one backward pass), each communicating $2(m-1)$ messages total. Finally each node i compute x_i^* via (2).

The above idea and convergence guarantees extend to graph-structured problems (P') whose \mathcal{G} is an *acyclic* factor graph; see, e.g., [17]. This is the clean regime in which message-passing-based methods are both exact and well understood.

Message passing on loopy graphs. On graphs with cycles, convergence guarantees exist only in *restricted regimes*, mostly for *pairwise* models (not directly applicable to (P)). (i) *Scaled diagonal dominance*: The most general convergence results for min-sum message passing methods are for *pairwise-separable convex* objectives (as in (P')), satisfying the so-called *scaled diagonal dominance* condition, which enforces that local curvature dominates pairwise couplings; under this assumption, (a)synchronous min-sum converges, and explicit convergence rate bounds are derived [21, 51]. However, the dominance requirement significantly restricts the class of problems that can be handled. (ii) *Quadratic objectives (Gaussian)*: For strictly convex quadratics, *correctness* and *convergence* decouple: if loopy Gaussian Belief Propagation/min-sum converges, it yields the exact minimizer on graphs of arbitrary topology [46]. However, convergence itself requires additional structure such as *walk-summability/convex decomposability* (and compatible initializations), and not every strongly convex quadratic function satisfies these conditions [19, 20]. Graph-cover analyses explain failure modes and motivate reweighted/parameterized variants; yet, convergence for *arbitrary* strongly convex quadratic is not established beyond empirical evidence [31]. (iii) *Higher-order (hypergraph) couplings*: Min-sum extends to higher-order factor graphs (as in (P)) and remains exact on acyclic graphs [17], but for *loopy* nonlinear programs, convergence theory remains far less developed—beyond dominance-type assumptions for convex factors [21], topology-/arity-explicit rate characterizations are essentially missing.

Pervasive bottlenecks. Across (i)-(iii), a first obstacle is *practical implementability*: messages are *functional* objects in continuous domains, and even for vector-valued quadratics parametrizations can require exchanging *dense* second-order information (matrices) [20, 21, 31]. This issue is exacerbated over hypergraphs: factor-to-variable updates entail multi-variable partial minimizations over hyperedges, so both computation and communication grow rapidly with the hyperedge size [21]. Second, *rate interpretability*: when bounds exist, they are typically stated through global dominance/spectral constants that entangle topology and problem parameters, so clean scalability laws in graph features (degree, overlap, diameter, separators, etc.) remain unknown in full generality [20, 51].

1.2 Main contributions

The main contributions of the paper are as follows.

- **MP-Jacobi: A message-passing-based decomposition.** We introduce a new decomposition principle for graph-structured nonlinear programs in the form (P') , built *rigorously* on the machinery of message passing. Starting from a new graph-compliant fixed-point characterization induced by a partition of the graph into *tree clusters*, we decouple interactions into: (i) *intra-cluster* couplings, captured by one min-sum sweep on the selected intra-cluster trees, and (ii) *inter-cluster* couplings, handled *Jacobi-style* using out-of-cluster neighbors' most recent variables. The resulting *Message-Passing Jacobi* (MP-Jacobi) method is a *single-loop*, fully decentralized scheme that, per iteration, performs one (damped) local Jacobi minimization together with one step of intra-cluster message updates. This yields (to

our knowledge) the first *provably convergent* message-passing-based decomposition for continuous optimization on *loopy graphs* that is graph-compliant and implementable with purely local, single-hop communication. From the Jacobi viewpoint, it also resolves a long-standing obstacle: realizing a genuine block-Jacobi decomposition without multi-hop replication or consensus-style global coordination.

- **Novel convergence analysis and topology-explicit rates.** By casting MP-Jacobi as a delayed block-Jacobi method on a partition-induced operator, we establish *linear* (resp. *sublinear*) convergence for strongly convex (resp. merely convex or nonconvex) objectives. Our theory provides (to our knowledge) the *first* convergence guarantees for a *message-passing-based* algorithm on *loopy graphs*, which do *not* rely on structural properties of the loss function such as diagonal dominance or walk-summability, but only on stepsize tuning. Such unrestricted convergence is ensured by the Jacobi correction that stabilizes cross-cluster interactions while allowing message passing to run on tree components only. Moreover, unlike existing message-passing analyses where rates are buried in global spectral/-dominance constants, our contraction factor is explicit in terms of (i) local and coupling regularity/curvature parameters and (ii) *topological features of the chosen partition* (e.g., intra-cluster trees and boundary interfaces), thereby offering concrete guidance for partition design and scalability with the network size.
- **Surrogation.** To overcome the main bottleneck of classical message passing in optimization—high per-iteration computation/communication due to functional messages—we develop *surrogate MP-Jacobi*, a variant of MP-Jacobi, based on surrogation. It preserves the same decentralized architecture and convergence guarantees while enabling lightweight message parametrizations (at the level of vectors/low-dimensional summaries) and offering explicit cost–rate trade-offs. We provide practical surrogate constructions that cover common smooth/convex structures and substantially reduce per-iteration complexity, yet preserving fast convergence.
- **Hypergraphs.** We extend the framework to hypergraph models (P), by deriving a decomposition method employing hypergraph message-passing *within* hypergraph *factor graph tree* clusters and Jacobi-like updates over *inter*-cluster hyperedge factors. For cycle-rich hypergraphs with heavy overlaps, we propose a *surrogate hyperedge-splitting* strategy that removes intra-cluster loops so that tree-based message updates remain applicable, while retaining fast convergence provably.
- **Empirical validation and practical gains.** Extensive experiments on graph and hypergraph instances corroborate the theory, quantify the impact of clustering and surrogate design, and demonstrate substantial gains over gradient-type baselines and decentralized consensus methods, highlighting MP-Jacobi as a scalable primitive for distributed optimization with localized couplings.

1.3 Motivating applications

- (i) **Laplacian Linear systems.** Graph-Laplacian systems arise across scientific computing and data science (e.g., electrical flows [22], random-walk quantities such as hitting times, and Markov-chain stationarity [27]). A standard formulation is

$$\min_{\mathbf{x} \in \mathbb{R}^m} - \sum_{i=1}^m b_i x_i + \frac{1}{2} \sum_{i=1}^m \sum_{j=1}^m L_{ij} x_i x_j,$$

where $L = [L_{ij}]_{i,j=1}^m$ is the graph Laplacian. This is an instance of (P'').

(ii) Signal processing on graphs [28, 45] extends traditional signal processing techniques to graph-structured data. A signal on a graph is a function that assigns a value to each node on a graph, representing data. The graph structure encodes relations among the data that are represented through edges. A key task is recovering a graph signal z from a noisy observation $y = z + n$, where $n \sim \mathcal{N}(0, \Sigma)$, under the smoothness prior that neighboring nodes should have similar values. A canonical estimator solves the following neighborhood-scoped problem [16]:

$$\min_{\mathbf{x} \in \mathbb{R}^{md}} \sum_{i=1}^m d_i \|y_i - x_i\|^2 + \frac{1}{2\mu} \sum_{(i,j) \in \mathcal{E}} w_{ij} \|x_i - x_j\|^2.$$

(iii) Personalized and multi-task learning: each agent owns a local private dataset and aims to learn a personalized model according to their own learning objective. Neighboring agents have similar objectives and therefore, agents benefit from interacting with their neighbors. This is captured by the problem [11, 43]:

$$\min_{\mathbf{x} \in \mathbb{R}^{md}} \sum_{i=1}^m d_i \mathcal{L}_i(x_i) + \frac{1}{2\mu} \sum_{(i,j) \in \mathcal{E}} w_{ij} \|x_i - x_j\|^2,$$

where $\mathcal{L}_i : \mathbb{R}^d \rightarrow \mathbb{R}$ denotes agent i 's private loss, and $\mu > 0$ is a trade-off parameter. The above formulation also arises in multi-task learning with soft coupling among tasks [30], where adjacency in the graph now represents tasks that share similarities and thus should inform one another during training.

(iv) Distributed optimization. In the classical decentralized optimization setting, agents solve $\min_{x \in \mathbb{R}^d} \sum_{i=1}^m f_i(x)$, with each agent i having access to f_i only and communicating with its immediate neighbors. Two notorious algorithms are the DGD-CTA (Decentralized Gradient Descent - Combine Then Adapt) [49] and the DGD-ATC (DGD-Adapt Then Combine) [7]; they can be interpreted as gradient descent applied to lifted, graph-regularized problems

$$\min_{\mathbf{x} \in \mathbb{R}^{md}} \sum_{i=1}^m f_i(x_i) + \frac{1}{2\gamma} \|\mathbf{x}\|_{\mathbf{I}_{md} - \mathbf{W} \otimes \mathbf{I}_d}^2, \quad (5)$$

and

$$\min_{\mathbf{x} \in \mathbb{R}^{md}} \sum_{i=1}^m f_i \left(\sum_{j \in \mathcal{N}_i} w_{ij} x_j \right) + \frac{1}{2\gamma} \|\mathbf{x}\|_{\mathbf{I}_{md} - \mathbf{W}^2 \otimes \mathbf{I}_d}^2. \quad (6)$$

(v) MAP (maximum a posteriori) on graphical models: Let \mathbf{x} be latent variables and \mathbf{y} measurements, with posterior

$$p(\mathbf{x} | \mathbf{y}) \propto \prod_{\omega \in \mathcal{E}} \pi_\omega(x_\omega) \prod_{\omega \in \mathcal{E}} p_\omega(y_\omega | x_\omega),$$

where ω indexes a factor scope, x_ω is the subset of latent variables associated with ω , and y_ω are the measurements associated with x_ω . The MAP estimator is obtained by minimizing the negative log-posterior $\min_{\mathbf{x}} -\log p(\mathbf{x} | \mathbf{y})$, which fits (P) and underpins many applications, such as robotics, speech processing, bio-informatics, finance and computer vision.

(a) Robot localization and motion planning (e.g., [3]). The variables $x_1, \dots, x_m \in \mathbb{R}^d$ represent a discrete-time trajectory of robot poses (and possibly landmark states). The robot acquires a set of $|\mathcal{E}|$ measurements, each involving a subset of

states \mathbf{x} : $y_\omega = h_\omega(x_\omega) + \varepsilon_\omega$, $\varepsilon_\omega \sim \mathcal{N}(0, \Sigma_\omega)$, with known measurement model h_ω . Assuming conditional independence across factors given x_ω , the MAP is obtained by setting $p_\omega(y_\omega \mid x_\omega) \propto \exp(-\frac{1}{2}\|h_\omega(x_\omega) - y_\omega\|_{\Sigma_\omega^{-1}}^2)$, while $\pi_\omega(x_\omega)$ encodes priors/regularizers (e.g., motion priors, landmark priors), and can be omitted to obtain a maximum-likelihood (ML) estimator. The resulting MAP/ML problem is a core computational primitive in simultaneous localization and mapping.

(b) Hidden Markov Models (HMMs) Consider a HMM (X, Y) with hidden states $\{X_i\}$ and observations $\{Y_i\}$, where X_{i+1} depends only on X_i and the observation model links Y_i to X_i . Given observations (y_1, \dots, y_m) , the goal is to recover the most likely hidden sequence (x_1, \dots, x_m) . The induced dependence structure is a line graph, with factors $\pi_1(x_1) = \mu(x_1)$, $\pi_{(i,i+1)}(x_i, x_{i+1}) = q_{(i+1,i)}(x_{i+1} \mid x_i)$, where μ is the initial-state density and $q_{(i+1,i)}$ the transition density. The likelihood factors as $p_\omega(y_\omega \mid x_\omega) = \prod_{i \in \omega} q'_i(y_i \mid x_i)$, where q'_i is the emission density. MAP then reduces to a structured instance of (P) (pairwise on a chain).

(c) Image denoising/inpainting via Fields of Experts (FoE) [29, 44]. Pixels (or patches) in an image \mathbf{x} are treated as nodes in a graph, and a neighborhood system induces high-order cliques: each neighborhood/patch ω defines a maximal clique x_ω and hence a hyperedge. FoE specifies a high-order Markov random field prior through the product of L expert factors $\pi_\omega(x_\omega) = \prod_{i=1}^L \phi(J_i^\top x_\omega, \alpha_i)$ where $\{J_\ell\}$ is a learned filter bank and $\{\alpha_\ell\}$ are learned parameters; e.g., [44] uses $\phi(J_\ell^\top x_\omega, \alpha_\ell) = (1 + \frac{1}{2}(J_\ell^\top x_\omega)^2)^{-\alpha_\ell}$. Given a noisy image \mathbf{y} , the goal is to find a faithful denoised image \mathbf{x} . For this, set $\prod_{\omega \in \varepsilon} p_\omega(y_\omega \mid x_\omega) \propto \exp(-\frac{\lambda}{\sigma^2} \|\mathbf{x} - \mathbf{y}\|^2)$, so the MAP estimate balances fidelity to \mathbf{y} and the FoE prior, yielding a hypergraph-structured instance of (P).

1.4 Notation

The power set of a set \mathcal{S} is denoted by $2^\mathcal{S}$. Given an undirected hypergraph $\mathcal{G} = (\mathcal{V}, \mathcal{E})$ (assumed throughout the paper having no selfloops), with node-set $\mathcal{V} = \{1, 2, \dots, m\}$ and hyperedge-set $\mathcal{E} \subseteq 2^\mathcal{V}$, the hyperedge neighborhood of agent i is defined as $\mathcal{N}_i := \{\omega \in \mathcal{E} \mid i \in \omega\}$. For any $\mathcal{S} \subseteq \mathcal{V}$, we denote its complement by $\overline{\mathcal{S}} := \mathcal{V} \setminus \mathcal{S}$. In particular, when $|\omega| = 2$, for any $\omega \in \mathcal{E}$, \mathcal{G} reduces to the pairwise graph—the neighborhood of agent i reads $\mathcal{N}_i = \{j \in \mathcal{V} \mid (i, j) \in \mathcal{E}\}$. The diameter of \mathcal{G} is denoted by $d_{\mathcal{G}}$. For any integer $s > 0$, we write $[s] := \{1, \dots, s\}$.

Given $\mathbf{x} \in \mathbb{R}^{md}$, $\mathcal{C} \subseteq \mathcal{V}$, we write $\mathbf{x}_{\mathcal{C}} \in \mathbb{R}^{|\mathcal{C}|d}$ for the subvector formed by the blocks of \mathbf{x} indexed by \mathcal{C} ; for given $\mathbf{x} = [x_1, \dots]$ and $[\mathbf{d}_1, \dots]$ of suitable dimensions (clear from the context), with $x_i \in \mathbb{R}^d$, $\mathbf{d}_i \in \mathbb{N}$, and given $\nu \in \mathbb{N}$, we use the shorthand $x_{\mathcal{C}}^{\nu-\mathbf{d}} := (x_i^{\nu-\mathbf{d}_i})_{i \in \mathcal{C}}$. For any set of indices $\mathcal{C} \subseteq [m]$, define a selection matrix $U_{\mathcal{C}}$ that extracts the d -dimensional blocks in \mathbf{x} indexed by \mathcal{C} : $U_{\mathcal{C}}^\top \mathbf{x} = \mathbf{x}_{\mathcal{C}}$. The orthogonal projector onto the coordinates indexed by \mathcal{C} is then $P_{\mathcal{C}} := U_{\mathcal{C}} U_{\mathcal{C}}^\top$. For $\Phi : \mathbb{R}^{md} \rightarrow \mathbb{R}$ and $\mathcal{C} \subseteq \mathcal{V}$, we denote by $\nabla_{\mathcal{C}} \Phi(\mathbf{x}) \in \mathbb{R}^{|\mathcal{C}|d}$ the gradient of Φ with respect to $\mathbf{x}_{\mathcal{C}}$. For index sets $\mathcal{A}, \mathcal{B} \subseteq \mathcal{V}$, $\nabla_{\mathcal{A}, \mathcal{B}}^2 \Phi(\mathbf{x}) \in \mathbb{R}^{|\mathcal{A}|d \times |\mathcal{B}|d}$ is the corresponding block Hessian, whose (i, j) -th $(d \times d)$ block is $\nabla_j(\nabla_i \Phi(\mathbf{x}))^\top$, $i \in \mathcal{A}$ and $j \in \mathcal{B}$. We say $\Phi \in C^k$ if Φ is k -times differentiable. If, in addition, its k -th derivative is (globally) Lipschitz, we write $\Phi \in LC^k$. Given two functions $f(x, y)$ and $g(x, y)$, we say that f and g are equivalent with respect to x , denoted $f(x, y) \xrightarrow{x} g(x, y)$, if the difference $f(x, y) - g(x, y)$ is independent of x . When the variable is clear from context, we simply write $f \sim g$. The set of $d \times d$ positive semidefinite (resp. definite) matrices is denoted by \mathbb{S}_+^d (resp. \mathbb{S}_{++}^d).

2 Decomposition via Message Passing: Pairwise Problem (P')

This section focuses on the design of decomposition algorithms for the pairwise formulation (P'). Our approach exploits a key property of message-passing algorithms (see Sec. 1.1): on loopless graphs, they converge in a finite number of steps. This motivates the following graph partition and assumption.

Definition 1 (condensed graph) Given $\mathcal{G} = (\mathcal{V}, \mathcal{E})$ and $p \in [m]$, let $\mathcal{C}_1, \dots, \mathcal{C}_p$ be a partition of \mathcal{V} , with associated intra-cluster edge-sets $\mathcal{E}_1, \dots, \mathcal{E}_p$, where

$$\mathcal{E}_r := \{(i, j) \in \mathcal{E} \mid i, j \in \mathcal{C}_r\}, \quad r \in [p]; \quad (7)$$

this results in the subgraphs $\mathcal{G}_r = (\mathcal{C}_r, \mathcal{E}_r)$, $r \in [p]$.

The condensed graph relative to $\{\mathcal{G}_r\}_{r=1}^p$ is defined as $\mathcal{G}_C := (\mathcal{V}_C, \mathcal{E}_C)$, where

- $\mathcal{V}_C := \{\mathbf{c}_1, \dots, \mathbf{c}_p\}$ is the set of supernodes, with \mathbf{c}_r associated with \mathcal{C}_r ; and
- $\mathcal{E}_C \subseteq \mathcal{V}_C \times \mathcal{V}_C$ is the set of superedges: $(\mathbf{c}_r, \mathbf{c}_s) \in \mathcal{E}_C$ iff $(i, j) \in \mathcal{E}$, for some $i \in \mathcal{C}_r$ and $j \in \mathcal{C}_s$, with $i \neq j$.

For each $i \in \mathcal{C}_r$, define

$$\mathcal{N}_i^{\text{in}} := \mathcal{N}_i \cap \mathcal{C}_r, \quad \mathcal{N}_i^{\text{out}} := \mathcal{N}_i \setminus \mathcal{C}_r, \quad \text{and} \quad \mathcal{N}_{\mathcal{C}_r} := \cup_{i \in \mathcal{C}_r} \mathcal{N}_i^{\text{out}};$$

$\mathcal{N}_i^{\text{in}}$ (resp. $\mathcal{N}_i^{\text{out}}$) is the neighborhood of $i \in \mathcal{C}_r$ within (resp. outside) \mathcal{G}_r and $\mathcal{N}_{\mathcal{C}_r}$ is the external neighborhood of \mathcal{C}_r . Finally, $D_r := \text{diam}(\mathcal{G}_r)$ is the diameter of \mathcal{G}_r , with $D := \max_{r \in [p]} D_r$; and $\mathcal{B}_r := \{i \in \mathcal{C}_r : |\mathcal{N}_i^{\text{in}}| = 1\}$ is set of leaves of \mathcal{G}_r .

Assumption 1 Each subgraph \mathcal{G}_r in \mathcal{G}_C is a tree. Singleton clusters ($\mathcal{E}_r = \emptyset$) are regarded as trees.

Notice that we posit tree-partitions that are *edge-maximal*: each cluster contains all edges between its internal nodes.

Equipped with the tree partition $\{\mathcal{G}_r\}_{r=1}^p$ (Assumption 1), we decompose any solution \mathbf{x}^* of (P') over the subgraphs according to the fixed-point inclusion:

$$x_i^* \in \underset{x_i}{\operatorname{argmin}} \phi_i(x_i) + \mu_{\mathcal{N}_i^{\text{in}} \rightarrow i}^*(x_i) + \mu_{\mathcal{N}_i^{\text{out}} \rightarrow i}^*(x_i), \quad i \in \mathcal{C}_r, \quad r \in [p], \quad (8)$$

where

$$\begin{aligned} \mu_{\mathcal{N}_i^{\text{in}} \rightarrow i}^*(x_i) := \\ \min_{x_{\mathcal{C}_r \setminus \{i\}}} \left(\sum_{j \in \mathcal{C}_r \setminus \{i\}} \phi_j(x_j) + \sum_{(j, k) \in \mathcal{E}_r} \psi_{jk}(x_j, x_k) + \sum_{j \in \mathcal{C}_r \setminus \{i\}} \sum_{k \in \mathcal{N}_j^{\text{out}}} \psi_{jk}(x_j, x_k^*) \right) \end{aligned} \quad (9)$$

and

$$\mu_{\mathcal{N}_i^{\text{out}} \rightarrow i}^*(x_i) := \sum_{k \in \mathcal{N}_i^{\text{out}}} \psi_{ik}(x_i, x_k^*) \quad (10)$$

represent, respectively, the optimal cost contributions of the intra-cluster and inter-cluster neighbors of node $i \in \mathcal{C}_r$ —see Fig. 1(a). They constitute the only “summaries” that node i needs in order to solve Problem (P') locally via (8)—we term them as *messages*, because it is information to be routed to agent i . Exploiting the pairwise structure in (9), we show next that the intra-cluster message $\mu_{\mathcal{N}_i^{\text{in}} \rightarrow i}^*$ can be obtained recursively from pairwise messages along the tree.

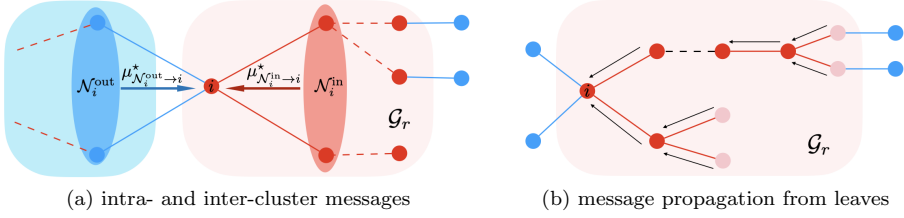


Fig. 1: (a) Intra-cluster and inter-cluster messages at node i : $\mu_{\mathcal{N}_i^{\text{in}} \rightarrow i}^*$ collects contributions from neighbors within \mathcal{G}_r (red nodes) while $\mu_{\mathcal{N}_i^{\text{out}} \rightarrow i}^*$ collects those from neighbors outside the cluster (blue nodes). (b) Message propagation within \mathcal{G}_r : messages are initialized at the leaves (light red nodes) and propagated along the tree according to the recursion(11).

For every two nodes i, j in \mathcal{G}_r connected by an edge, $(i, j) \in \mathcal{E}_r$, define the pairwise message from j to i as

$$\mu_{j \rightarrow i}^*(x_i) = \min_{x_j} \left\{ \psi_{ij}(x_i, x_j) + \phi_j(x_j) + \sum_{k \in \mathcal{N}_j^{\text{in}} \setminus \{i\}} \mu_{k \rightarrow j}^*(x_j) + \sum_{k \in \mathcal{N}_j^{\text{out}}} \psi_{jk}(x_j, x_k^*) \right\}. \quad (11)$$

Note that the recursion is well-defined because $\mathcal{N}_j^{\text{in}} \setminus \{i\} = \emptyset$ for every leaf node j of \mathcal{G}_r and $i \in \mathcal{C}_r$. In fact, for such nodes, (11) reduces to

$$\mu_{j \rightarrow i}^*(x_i) := \min_{x_j} \left\{ \psi_{ij}(x_i, x_j) + \phi_j(x_j) + \sum_{k \in \mathcal{N}_j^{\text{out}}} \psi_{jk}(x_j, x_k^*) \right\}, \quad j \in \mathcal{B}_r, i \in \mathcal{C}_r. \quad (12)$$

Therefore, every pairwise messages along the tree \mathcal{G}_r can be expressed recursively in terms of the incoming messages routed from the leaves. Fig. 1(b) illustrates the message-passing construction on a tree cluster. In particular, the intra-cluster message $\mu_{\mathcal{N}_i^{\text{in}} \rightarrow i}^*$ can be then represented as the aggregate of the pairwise messages from the neighbors of node i within \mathcal{G}_r , i.e.,

$$\mu_{\mathcal{N}_i^{\text{in}} \rightarrow i}^*(x_i) = \sum_{j \in \mathcal{N}_i^{\text{in}}} \mu_{j \rightarrow i}^*(x_i). \quad (13)$$

Substituting (13) in (8), we obtain the final decomposition of a solution of (P') compliant with the graph structure:

$$x_i^* \in \operatorname{argmin}_{x_i} \left\{ \phi_i(x_i) + \sum_{j \in \mathcal{N}_i^{\text{in}}} \mu_{j \rightarrow i}^*(x_i) + \sum_{j \in \mathcal{N}_i^{\text{out}}} \psi_{ij}(x_i, x_j^*) \right\}, \quad i \in \mathcal{C}_r, r \in [p]. \quad (14)$$

The proposed decentralized algorithm is obtained by viewing (14) as a fixed-point system in the messages $\mu_{j \rightarrow i}^*$ and variables x_i^* , and iterating on these relations; the resulting scheme is summarized in Algorithm 1. To control convergence, we further incorporate the over-relaxation step (15b) in the update of the agents block-variables. The method combines intra-cluster message passing with inter-cluster block-Jacobi updates, in a fully decentralized fashion.

Algorithm 1: Message Passing-Jacobi (MP-Jacobi)

Initialization: $x_i^0 \in \mathbb{R}^d$, for all $i \in \mathcal{V}$; initial message $\mu_{i \rightarrow j}^0(\cdot)$ arbitrarily chosen (e.g., $\mu_{i \rightarrow j}^0 \equiv 0$), for all $(i, j) \in \mathcal{E}_r$ and $r \in [p]$.

for $\nu = 0, 1, 2, \dots$ **do**

each agent $i \in \mathcal{V}$ **in parallel:**

Performs the following updates:

$\hat{x}_i^{\nu+1} \in \operatorname{argmin}_{x_i} \left\{ \phi_i(x_i) + \sum_{j \in \mathcal{N}_i^{\text{in}}} \mu_{j \rightarrow i}^{\nu}(x_i) + \sum_{k \in \mathcal{N}_i^{\text{out}}} \psi_{ik}(x_i, x_k^{\nu}) \right\}, \quad (15a)$

$x_i^{\nu+1} = x_i^{\nu} + \tau_r^{\nu}(\hat{x}_i^{\nu+1} - x_i^{\nu}), \quad (15b)$

$\mu_{i \rightarrow j}^{\nu+1}(x_j) = \min_{x_i} \left\{ \phi_i(x_i) + \psi_{ij}(x_j, x_i) + \sum_{k \in \mathcal{N}_i^{\text{in}} \setminus \{j\}} \mu_{k \rightarrow i}^{\nu}(x_i) + \sum_{k \in \mathcal{N}_i^{\text{out}}} \psi_{ik}(x_i, x_k^{\nu}) \right\}, \forall j \in \mathcal{N}_i^{\text{in}}; \quad (15c)$

Sends out $x_i^{\nu+1}$ to all $j \in \mathcal{N}_i^{\text{out}}$ and $\mu_{i \rightarrow j}^{\nu+1}(x_j)$ to all $j \in \mathcal{N}_i^{\text{in}}$.

Fig. 2 summarizes the key principle. The original graph is partitioned into tree subgraphs (clusters) $\mathcal{G}_r = (\mathcal{C}_r, \mathcal{E}_r)$, inducing the condensed graph \mathcal{G}_C with one supernode (possibly a singleton) per cluster. The coupling among agents *within* each (non-singleton) cluster \mathcal{C}_r (i.e., inside each non-singleton supernode of \mathcal{G}_C) is handled via a min-sum-type message-passing scheme over the edges \mathcal{E}_r ; this corresponds to the “intra-cluster” interaction term $\sum_{j \in \mathcal{N}_i^{\text{in}}} \mu_{j \rightarrow i}^{\nu}(x_i)$ in agent i ’s subproblem (15a). In contrast, the coupling *across* clusters is handled in a Jacobi-like fashion: in the local minimization step (15a), each agent i accounts for the cross-terms ψ_{ij} from its inter-cluster neighbors $j \in \mathcal{N}_i^{\text{out}}$ (the singleton supernodes in \mathcal{G}_C connected to i) via the contribution $\sum_{k \in \mathcal{N}_i^{\text{out}}} \psi_{ik}(x_i, x_k^{\nu})$.

In a nutshell, message passing accounts for all agents’ interactions within each tree cluster, while block-Jacobi updates account for the interactions between clusters through the boundary nodes only. The rationale for this design is that, on a tree, min-sum message passing is known to converge in a finite number of iterations (e.g., [12, 41])—on the order of the tree diameter—provided all other quantities are kept fixed. In our algorithm, however, we do *not* run an inner message-passing routine to convergence at each outer iteration: only a single forward-backward sweep of messages is performed per round, and these sweeps are interleaved with the block-Jacobi updates. Hence, the overall procedure is a single-loop decentralized algorithm relying solely on single-hop communications.

Notice that when all clusters are singletons ($\mathcal{E}_r = \emptyset$), no messages are exchanged and Algorithm 1 becomes a damped Jacobi method. At the opposite extreme, when the entire graph is a tree (i.e., $\mathcal{E}_r = \mathcal{E}$), the scheme (with $\tau_r^{\nu} \equiv 1$) reduces to standard min-sum message passing on a tree.

3 Convergence analysis of Algorithm 1

In this section, we establish convergence of Algorithm 1, under the following assumptions on the graph \mathcal{G} and Problem (P').

Assumption 2 *The graph $\mathcal{G} = (\mathcal{V}, \mathcal{E})$ is undirected and connected. Nodes can only communicate with their immediate neighbors \mathcal{N}_i ’s.*

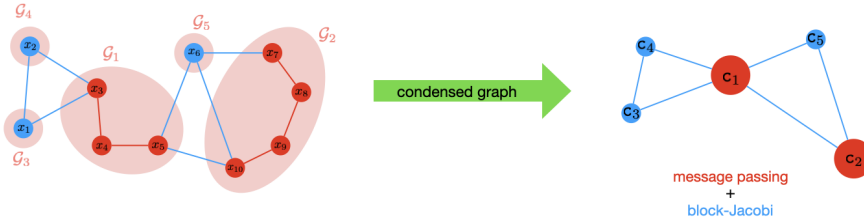


Fig. 2: Birds-eye view of Algorithm 1. The graph is decomposed into tree clusters $(\mathcal{C}_i)_{i=1}^5$. Intra-cluster interactions are handled via message passing within the nonsingleton supernodes c_1 and c_2) whereas inter-cluster interactions are handled by Jacobi-type updates at boundary (singleton) supernodes c_3 and c_4 , and c_5 . At the the condensed graph level, the iterations approximate a block-Jacobi.

Assumption 3 Given the partition $(\mathcal{G}_r)_{r=1}^p$, each \mathcal{C}_r has no external neighbors that connect to more than one node in \mathcal{C}_r :

$$|\mathcal{N}_k \cap \mathcal{C}_r| \leq 1, \quad \forall k \in \bar{\mathcal{C}}_r, \forall r \in [p]. \quad (16)$$

Condition (16) enforces single-node contacts between clusters: any external node can connect to a cluster through at most one gateway node. While not necessary, this assumption is posited to simplify the notation in some derivations.

For each $r \in [p]$, let $P_r := U_{\mathcal{C}_r} U_{\mathcal{C}_r}^\top$ be the orthogonal projector onto the coordinates in \mathcal{C}_r . Moreover, define $P_{\partial r} := U_{\mathcal{N}_{\mathcal{C}_r}} U_{\mathcal{N}_{\mathcal{C}_r}}^\top$ as the projector onto the external neighborhood coordinates $\mathcal{N}_{\mathcal{C}_r}$.

Assumption 4 Given the partition $(\mathcal{G}_r)_{r=1}^p$, the following hold:

- (i) $\Phi \in LC^1$ is lower bounded and μ -strongly convex (with $\mu \geq 0$); for each $r \in [p]$, $x_{\mathcal{C}_r} \mapsto \Phi(x_{\mathcal{C}_r}, z_{\mathcal{C}_r})$ is μ_r -strongly convex uniformly w.r.t. $z_{\mathcal{C}_r}$, with $\mu_r \geq 0$.
- (ii) For each $r \in [p]$, there exist constants $L_r > 0$ and $L_{\partial r} > 0$ such that:

$$\|P_r \nabla \Phi(\mathbf{x}) - P_r \nabla \Phi(\mathbf{y})\| \leq L_r \|P_r(\mathbf{x} - \mathbf{y})\|, \quad \forall \mathbf{x}, \mathbf{y} \text{ s.t. } (I - P_r)\mathbf{x} = (I - P_r)\mathbf{y}; \quad (17)$$

$$\|P_r \nabla \Phi(\mathbf{x}) - P_r \nabla \Phi(\mathbf{y})\| \leq L_{\partial r} \|P_{\partial r}(\mathbf{x} - \mathbf{y})\|, \quad \forall \mathbf{x}, \mathbf{y} \text{ s.t. } P_r \mathbf{x} = P_r \mathbf{y}. \quad (18)$$

When $\mu > 0$, we define the global condition number $\kappa := (\max_{r \in [p]} L_r)/\mu$. When $\mu = 0$, the problem admits a solution.

Notice that the existence of L_r follows directly from the block-Lipschitz continuity of $\nabla \Phi$, whereas the definition of $L_{\partial r}$ additionally exploits the graph-induced sparsity. More specifically, for fixed $P_r \mathbf{x}$, $P_r \nabla \Phi(\mathbf{x})$ depends only on the blocks of $(I - P_r)\mathbf{x}$ (i.e., $x_{\bar{\mathcal{C}}_r}$) indexed by $\mathcal{N}_{\mathcal{C}_r}$ (i.e., $P_{\partial r} \mathbf{x}$). Then, for any \mathbf{x}, \mathbf{y} with $P_r \mathbf{x} = P_r \mathbf{y}$,

$$P_r(\nabla \Phi(\mathbf{x}) - \nabla \Phi(\mathbf{y})) = P_r(\nabla \Phi(P_r \mathbf{x} + P_{\partial r} \mathbf{x}) - \nabla \Phi(P_r \mathbf{y} + P_{\partial r} \mathbf{y})),$$

which, by the smoothness of Φ , proves the existence of $L_{\partial r}$.

Next we study convergence of Algorithm 1; we organize the analysis in two steps: (i) first, we establish the equivalence between the algorithm and a (damped) block-Jacobi method with delayed inter-cluster information; then, (ii) we proceed proving convergence of such a Jacobi method.

3.1 Step 1: Algorithm 1 as a block-Jacobi method with delays

This reformulation builds on eliminating in (15a) the messages and making explicit the underlying intra-cluster minimization. Specifically, substitute (15c), i.e.,

$$\mu_{j \rightarrow i}^\nu(x_i) = \min_{x_j} \left\{ \phi_j(x_j) + \psi_{ij}(x_i, x_j) + \sum_{k \in \mathcal{N}_j^{\text{in}} \setminus \{i\}} \mu_{k \rightarrow j}^{\nu-1}(x_j) + \sum_{k \in \mathcal{N}_j^{\text{out}}} \psi_{jk}(x_j, x_k^{\nu-1}) \right\}. \quad (19)$$

into (15a). For each $j \in \mathcal{N}_i^{\text{in}}$, this introduces the new variable x_j together with the inner messages $\mu_{k \rightarrow j}^{\nu-1}$, $k \in \mathcal{N}_j^{\text{in}} \setminus \{i\}$.

We reapply (19) to these new messages and repeat the substitution recursively along the tree \mathcal{G}_r . Each application of (19) moves one hop farther from i inside \mathcal{G}_r : it adds one local function ϕ_j , one pairwise factor ψ_{jk} , and replaces the expanded message by messages incoming from the next layer of neighbors plus the boundary terms. When the recursion hits a boundary edge (j, k) , $j \in \mathcal{C}_r$ and $(j, k) \notin \mathcal{E}_r$, the expansion stops along that branch and produces the factor $\psi_{jk}(x_j, x_k^{\nu-\mathbf{d}})$, where \mathbf{d} is the depth of the recursion. Since \mathcal{G}_r is a tree, every intra-cluster node and edge is reached at most once, so the recursion terminates after finitely many substitutions and aggregates all intra-cluster factors exactly once. Therefore, one can write

$$\begin{aligned} & \sum_{j \in \mathcal{N}_i^{\text{in}}} \mu_{j \rightarrow i}^\nu(x_i) \\ &= \min_{x_{\mathcal{C}_r \setminus \{i\}}} \left\{ \sum_{j \in \mathcal{C}_r} \phi_j(x_j) + \sum_{(j, k) \in \mathcal{E}_r} \psi_{jk}(x_j, x_k) + \sum_{j \in \mathcal{C}_r, k \in \mathcal{N}_j^{\text{out}}} \psi_{jk}(x_j, x_k^{\nu-\mathbf{d}(i, j)}) \right\}, \end{aligned}$$

where $d(i, j) \in \mathbb{N}$ is the length of the unique path between i and j in \mathcal{G}_r .

Using the above expression in (15a) we obtain the following.

Proposition 1 *Under Assumptions 1 and 2, Algorithm 1 can be rewritten in the equivalent form: for any $i \in \mathcal{C}_r$ and $r \in [p]$,*

$$x_i^{\nu+1} = x_i^\nu + \tau_r^\nu (\hat{x}_i^{\nu+1} - x_i^\nu), \quad (20a)$$

$$\hat{x}_i^{\nu+1} \in \operatorname{argmin}_{x_i} \min_{x_{\mathcal{C}_r \setminus \{i\}}} \left\{ \sum_{j \in \mathcal{C}_r} \phi_j(x_j) + \sum_{(j, k) \in \mathcal{E}_r} \psi_{jk}(x_j, x_k) + \sum_{j \in \mathcal{C}_r, k \in \mathcal{N}_j^{\text{out}}} \psi_{jk}(x_j, x_k^{\nu-\mathbf{d}(i, j)}) \right\}. \quad (20b)$$

If, in addition, Assumption 3 holds, (20b) reduces to the following block-Jacobi update with delays:

$$\hat{x}_i^{\nu+1} \in \operatorname{argmin}_{x_i} \min_{x_{\mathcal{C}_r \setminus \{i\}}} \Phi(x_{\mathcal{C}_r}, x_{\bar{\mathcal{C}}_r}^{\nu-\mathbf{d}_i}), \quad (21)$$

where $\mathbf{d}_i \in \mathbb{N}^{|\bar{\mathcal{C}}_r|}$ is defined as

$$(\mathbf{d}_i)_k := \begin{cases} d(i, j_k), & k \in \mathcal{N}_{\mathcal{C}_r}, \\ 0, & k \in \bar{\mathcal{C}}_r \setminus \mathcal{N}_{\mathcal{C}_r}, \end{cases}$$

and, for $k \in \mathcal{N}_{\mathcal{C}_r}$, $j_k \in \mathcal{B}_r$ is the unique node such that $(j_k, k) \in \mathcal{E}$.

Proof See Appendix A. □

The distance $d(i, j)$ of $j \in \mathcal{C}_r$ from the updating index i along the tree \mathcal{G}_r satisfies $d(i, j) \leq \text{diam}(\mathcal{G}_r) \leq |\mathcal{C}_r| - 1$. Clearly, if $|\mathcal{C}_r| = 1$ then $d(i, j) = 0$.

The equivalence of the algorithm updates (20b) with (21) (under Assumption 3) along with the postulated lower boundedness of Φ (Assumption 4(i)) readily implies the existence of a minimizer for the subproblems (21).

Proposition 2 *Suppose Assumptions 1, 3, and 4 hold. Then Algorithm 1 is well-defined: at every iteration ν , all message-update subproblems (15c) and variable-update subproblems (15) admit minimizers. If, in addition, Φ is strongly convex, these minimizers are unique.*

We emphasize that Assumption 3 is used only to enable the compact notation in (21) and to streamline the convergence analysis. When it fails, the surrogation technique in Sec. 4 preserves well-posedness and convergence.

3.2 Step 2: Convergence analysis of block-Jacobi method with bounded delays

Now, we establish convergence for the delayed block-Jacobi scheme in (21).

Given $\hat{x}_i^{\nu+1}$, the minimizer produced by agent i at iteration ν satisfying (21), define the assembled vector $\hat{\mathbf{x}}^{\nu+1} := [(\hat{x}_1^{\nu+1})^\top, \dots, (\hat{x}_m^{\nu+1})^\top]^\top$. For each cluster, set $\hat{x}_{\mathcal{C}_r}^{\nu+1} := (\hat{x}_i^{\nu+1})_{i \in \mathcal{C}_r}$. Notice that $\hat{x}_{\mathcal{C}_r}^{\nu+1}$ is an assembled vector: its blocks may correspond to different delay patterns \mathbf{d}_i . Using the projector operator $P_r := U_{\mathcal{C}_r} U_{\mathcal{C}_r}^\top$, the update of the algorithm can be written in vector form as:

$$\mathbf{x}^{\nu+1} = \mathbf{x}^\nu + \sum_{r \in [p]} \tau_r^\nu P_r (\hat{\mathbf{x}}^{\nu+1} - \mathbf{x}^\nu). \quad (22)$$

We also introduce the virtual *non-delayed* block updates: for each $r \in [p]$, let

$$\bar{x}_{\mathcal{C}_r}^{\nu+1} \in \underset{x_{\mathcal{C}_r}}{\operatorname{argmin}} \Phi(x_{\mathcal{C}_r}, x_{\mathcal{C}_r}^\nu), \quad \text{and} \quad \bar{x}_i^{\nu+1} = [\bar{x}_{\mathcal{C}_r}^{\nu+1}]_i, \quad \forall i \in \mathcal{C}_r; \quad (23)$$

and the assembled vector $\bar{\mathbf{x}}^{\nu+1} := [(\bar{x}_1^{\nu+1})^\top, \dots, (\bar{x}_m^{\nu+1})^\top]^\top$. Notice that since the clusters form a partition, each $x_i^{\nu+1}$ above is uniquely defined.

The first result is the descent of Φ along the iterates $\{\mathbf{x}^\nu\}$, summarized next.

Lemma 1 *Under Assumption 4 and any stepsize choice satisfying $\tau_r^\nu \geq 0$ and $\sum_{r=1}^p \tau_r^\nu \leq 1$, the following holds:*

$$\Phi(\mathbf{x}^{\nu+1}) \leq \Phi(\mathbf{x}^\nu) + \sum_{r \in [p]} \tau_r^\nu \left[-\frac{\|P_r \nabla \Phi(\mathbf{x}^\nu)\|^2}{2L_r} + \frac{L_r}{2} \|P_r(\hat{\mathbf{x}}^{\nu+1} - \bar{\mathbf{x}}^{\nu+1})\|^2 \right]. \quad (24)$$

Proof For each $r \in [p]$, $x_{\mathcal{C}_r} \mapsto \Phi(x_{\mathcal{C}_r}, x_{\mathcal{C}_r}^\nu)$ is L_r -smooth (Assumption 4(ii)). Therefore

$$\begin{aligned} \Phi(\mathbf{x}^\nu + P_r(\hat{\mathbf{x}}^{\nu+1} - \mathbf{x}^\nu)) &\leq \Phi(\mathbf{x}^\nu + P_r(\bar{\mathbf{x}}^{\nu+1} - \mathbf{x}^\nu)) \\ &+ \underbrace{\left\langle \nabla \Phi(\mathbf{x}^\nu + P_r(\bar{\mathbf{x}}^{\nu+1} - \mathbf{x}^\nu)), P_r(\hat{\mathbf{x}}^{\nu+1} - \bar{\mathbf{x}}^{\nu+1}) \right\rangle}_{=0} + \frac{L_r}{2} \|P_r(\hat{\mathbf{x}}^{\nu+1} - \bar{\mathbf{x}}^{\nu+1})\|^2, \\ &\leq \Phi(\mathbf{x}^\nu) - \frac{\|P_r \nabla \Phi(\mathbf{x}^\nu)\|^2}{2L_r} + \frac{L_r}{2} \|P_r(\hat{\mathbf{x}}^{\nu+1} - \bar{\mathbf{x}}^{\nu+1})\|^2, \end{aligned} \quad (25)$$

where the zero inner-product comes from $P_r \nabla \Phi(\mathbf{x}^\nu + P_r(\bar{\mathbf{x}}^{\nu+1} - \mathbf{x}^\nu)) = 0$, due to

$$\Phi(\mathbf{x}^\nu + P_r(\bar{\mathbf{x}}^{\nu+1} - \mathbf{x}^\nu)) = \min_{x_{\mathcal{C}_r}} \Phi(x_{\mathcal{C}_r}, x_{\bar{\mathcal{C}}_r}^\nu). \quad (26)$$

Next, rewrite the update (22) as

$$\mathbf{x}^{\nu+1} = \left(1 - \sum_{r=1}^p \tau_r^\nu\right) \mathbf{x}^\nu + \sum_{r=1}^p \tau_r^\nu \left(\mathbf{x}^\nu + P_r(\hat{\mathbf{x}}^{\nu+1} - \mathbf{x}^\nu)\right).$$

Invoking the Jensens' inequality (and subtracting $\Phi(\mathbf{x}^\nu)$ from both sides), yields

$$\Phi(\mathbf{x}^{\nu+1}) - \Phi(\mathbf{x}^\nu) \leq \sum_{r=1}^p \tau_r^\nu \left(\Phi(\mathbf{x}^\nu + P_r(\hat{\mathbf{x}}^{\nu+1} - \mathbf{x}^\nu)) - \Phi(\mathbf{x}^\nu) \right). \quad (27)$$

Finally, applying (25) to each term of the sum on the RHS of (27) gives (24). \square

Lemma 1 provides a descent estimate for Φ driven by the projected gradient norm, up to the delay-induced discrepancy $\|P_r(\bar{\mathbf{x}}^{\nu+1} - \hat{\mathbf{x}}^{\nu+1})\|^2$. For the subsequent contraction analysis, we also need a complementary sufficient decrease inequality that produces a negative quadratic term in the actual block displacement $\|P_r(\mathbf{x}^{\nu+1} - \mathbf{x}^\nu)\|^2$. This is obtained next exploiting strong convexity of Φ .

Lemma 2 *Under Assumption 4 and any stepsize choice satisfying $\tau_r^\nu \geq 0$ and $\sum_{r=1}^p \tau_r^\nu \leq 1$, the following holds:*

$$\Phi(\mathbf{x}^{\nu+1}) \leq \Phi(\mathbf{x}^\nu) + \sum_{r \in [p]} \tau_r^\nu \left[-\frac{\mu_r}{4} \|P_r(\hat{\mathbf{x}}^{\nu+1} - \mathbf{x}^\nu)\|^2 + \frac{L_r + \mu_r}{2} \|P_r(\bar{\mathbf{x}}^{\nu+1} - \hat{\mathbf{x}}^{\nu+1})\|^2 \right]. \quad (28)$$

Proof Invoking (26) and strong convexity of Φ , yields

$$\Phi(\mathbf{x}^\nu + P_r(\bar{\mathbf{x}}^{\nu+1} - \mathbf{x}^\nu)) \leq \Phi(\mathbf{x}^\nu) - \frac{\mu_r}{2} \|P_r(\bar{\mathbf{x}}^{\nu+1} - \mathbf{x}^\nu)\|^2.$$

Using (25), we have

$$\Phi(\mathbf{x}^\nu + P_r(\hat{\mathbf{x}}^{\nu+1} - \mathbf{x}^\nu)) \leq \Phi(\mathbf{x}^\nu) - \frac{\mu_r}{2} \|P_r(\hat{\mathbf{x}}^{\nu+1} - \mathbf{x}^\nu)\|^2 + \frac{L_r}{2} \|P_r(\bar{\mathbf{x}}^{\nu+1} - \hat{\mathbf{x}}^{\nu+1})\|^2. \quad (29)$$

Note that

$$-\|P_r(\bar{\mathbf{x}}^{\nu+1} - \mathbf{x}^\nu)\|^2 \leq -\frac{1}{2} \|P_r(\hat{\mathbf{x}}^{\nu+1} - \mathbf{x}^\nu)\|^2 + \|P_r(\bar{\mathbf{x}}^{\nu+1} - \hat{\mathbf{x}}^{\nu+1})\|^2.$$

Grouping together, we have

$$\Phi(\mathbf{x}^\nu + P_r(\hat{\mathbf{x}}^{\nu+1} - \mathbf{x}^\nu)) \leq \Phi(\mathbf{x}^\nu) - \frac{\mu_r}{4} \|P_r(\hat{\mathbf{x}}^{\nu+1} - \mathbf{x}^\nu)\|^2 + \frac{L_r + \mu_r}{2} \|P_r(\bar{\mathbf{x}}^{\nu+1} - \hat{\mathbf{x}}^{\nu+1})\|^2.$$

Applying above inequality to each term of the sum on the RHS of (27) gives (28). \square

Note that both Lemma 1 and Lemma 2 contains the delay-induced discrepancy term $\|\bar{x}_{\mathcal{C}_r}^{\nu+1} - \hat{x}_{\mathcal{C}_r}^{\nu+1}\|^2$, which is bounded by the accumulated boundary variations over a window of length at most D_r . We have the following lemma.

Lemma 3 *In the setting of Lemma 1 and Lemma 2, assume $\mu_r > 0$ for all $r \in [p]$. Then, the following holds: for any $r \in [p]$,*

$$\|P_r(\hat{\mathbf{x}}^{\nu+1} - \bar{\mathbf{x}}^{\nu+1})\|^2 \leq \frac{L_{\partial r}^2 |\mathcal{C}_r| D_r}{\mu_r^2} \sum_{\ell=\nu-D_r}^{\nu-1} \|P_{\partial r}(\mathbf{x}^{\ell+1} - \mathbf{x}^\ell)\|^2. \quad (30)$$

Proof Define the auxiliary variable

$$\hat{x}_{\mathcal{C}_r, i}^{\nu+1} := \operatorname{argmin}_{x_i} \min_{x_{\mathcal{C}_r \setminus i}} \Phi(x_{\mathcal{C}_r}, x_{\mathcal{C}_r}^{\nu-\mathbf{d}_i}), \text{ with } \hat{x}_i^{\nu+1} = [\hat{x}_{\mathcal{C}_r, i}^{\nu+1}]_i.$$

By optimality the condition,

$$\begin{aligned} 0 &= \nabla_{\mathcal{C}_r} \Phi(\hat{x}_{\mathcal{C}_r, i}^{\nu+1}, x_{\mathcal{C}_r}^{\nu-\mathbf{d}_i}) - \nabla_{\mathcal{C}_r} \Phi(\bar{x}_{\mathcal{C}_r}^{\nu+1}, x_{\mathcal{C}_r}^{\nu}) \\ &= \underbrace{\nabla_{\mathcal{C}_r} \Phi(\hat{x}_{\mathcal{C}_r, i}^{\nu+1}, x_{\mathcal{C}_r}^{\nu-\mathbf{d}_i}) - \nabla_{\mathcal{C}_r} \Phi(\bar{x}_{\mathcal{C}_r}^{\nu+1}, x_{\mathcal{C}_r}^{\nu-\mathbf{d}_i})}_{\text{in-block change}} + \underbrace{\nabla_{\mathcal{C}_r} \Phi(\bar{x}_{\mathcal{C}_r}^{\nu+1}, x_{\mathcal{C}_r}^{\nu-\mathbf{d}_i}) - \nabla_{\mathcal{C}_r} \Phi(\bar{x}_{\mathcal{C}_r}^{\nu+1}, x_{\mathcal{C}_r}^{\nu})}_{\text{cross-block change}}. \end{aligned}$$

Taking inner product with $\hat{x}_{\mathcal{C}_r, i}^{\nu+1} - \bar{x}_{\mathcal{C}_r}^{\nu+1}$, using μ_r -strong convexity in $x_{\mathcal{C}_r}$ and the cross-Lipschitz bound of Assumption 4(ii), we obtain

$$\begin{aligned} \mu_r \|\hat{x}_{\mathcal{C}_r, i}^{\nu+1} - \bar{x}_{\mathcal{C}_r}^{\nu+1}\|^2 &\leq - \left\langle \nabla_{\mathcal{C}_r} \Phi(\bar{x}_{\mathcal{C}_r}^{\nu+1}, x_{\mathcal{C}_r}^{\nu-\mathbf{d}_i}) - \nabla_{\mathcal{C}_r} \Phi(\bar{x}_{\mathcal{C}_r}^{\nu+1}, x_{\mathcal{C}_r}^{\nu}), \hat{x}_{\mathcal{C}_r, i}^{\nu+1} - \bar{x}_{\mathcal{C}_r}^{\nu+1} \right\rangle \\ &\leq \|\nabla_{\mathcal{C}_r} \Phi(\bar{x}_{\mathcal{C}_r}^{\nu+1}, x_{\mathcal{C}_r}^{\nu-\mathbf{d}_i}) - \nabla_{\mathcal{C}_r} \Phi(\bar{x}_{\mathcal{C}_r}^{\nu+1}, x_{\mathcal{C}_r}^{\nu})\| \|\hat{x}_{\mathcal{C}_r, i}^{\nu+1} - \bar{x}_{\mathcal{C}_r}^{\nu+1}\| \\ &\leq L_{\partial r} \|x_{\mathcal{N}_{\mathcal{C}_r}}^{\nu-\mathbf{d}_i} - x_{\mathcal{N}_{\mathcal{C}_r}}^{\nu}\| \|\hat{x}_{\mathcal{C}_r, i}^{\nu+1} - \bar{x}_{\mathcal{C}_r}^{\nu+1}\|, \end{aligned}$$

which proves $\|\hat{x}_{\mathcal{C}_r, i}^{\nu+1} - \bar{x}_{\mathcal{C}_r, i}^{\nu+1}\| \leq \frac{L_{\partial r}}{\mu_r} \|x_{\mathcal{N}_{\mathcal{C}_r}}^{\nu-\mathbf{d}_i} - x_{\mathcal{N}_{\mathcal{C}_r}}^{\nu}\|$. Then, we have

$$\begin{aligned} \|\hat{x}_{\mathcal{C}_r}^{\nu+1} - \bar{x}_{\mathcal{C}_r}^{\nu+1}\|^2 &= \sum_{i \in \mathcal{C}_r} \|\hat{x}_i^{\nu+1} - \bar{x}_i^{\nu+1}\|^2 \leq \sum_{i \in \mathcal{C}_r} \|\hat{x}_{\mathcal{C}_r, i}^{\nu+1} - \bar{x}_{\mathcal{C}_r, i}^{\nu+1}\|^2 \\ &\leq \sum_{i \in \mathcal{C}_r} \left(\frac{L_{\partial r}}{\mu_r} \right)^2 \|x_{\mathcal{N}_{\mathcal{C}_r}}^{\nu-\mathbf{d}_i} - x_{\mathcal{N}_{\mathcal{C}_r}}^{\nu}\|^2 \leq \frac{L_{\partial r}^2 |\mathcal{C}_r| D_r}{\mu_r^2} \sum_{\ell=\nu-D_r}^{\nu-1} \|x_{\mathcal{N}_{\mathcal{C}_r}}^{\ell+1} - x_{\mathcal{N}_{\mathcal{C}_r}}^{\ell}\|^2. \end{aligned}$$

This completes the proof. \square

Notice that when $|\mathcal{C}_r| = 1$, $D_r = 0$, and the right-hand side of (30) equals 0.

Lemma 3 shows that, for each cluster, the delay discrepancy is controlled only by variations of the iterates on the *external neighborhood* $\mathcal{N}_{\mathcal{C}_r}$ of that cluster (equivalently, through the projector $P_{\partial r}$ onto $\mathcal{N}_{\mathcal{C}_r}$). Hence, delay accumulation acts only on the coordinates in $\bigcup_{r \in [p]: |\mathcal{C}_r| > 1} \mathcal{N}_{\mathcal{C}_r}$. To make this explicit, we introduce a minimal cover of this set by clusters. Let $\mathcal{J} \subseteq [p]$ be the minimal index set of clusters whose union covers all external neighbors, i.e.,

$$\bigcup_{r \in [p]: |\mathcal{C}_r| > 1} \mathcal{N}_{\mathcal{C}_r} \subseteq \bigcup_{r \in \mathcal{J}} \mathcal{C}_r. \quad (31)$$

We call $\{\mathcal{C}_r\}_{r \in \mathcal{J}}$ the *external-neighborhood clusters*. In sparse graphs, this set is typically much smaller than the full partition ($|\mathcal{J}| \ll p$ and $\sum_{r \in \mathcal{J}} |\mathcal{C}_r| \ll m$), so the delay accumulation affects only a small subset of coordinates.

Using the above results, we can now state the first convergence result.

Theorem 1 Suppose Assumption 1, 2, and 4 hold, with $p > 1$ and $\mu_r > 0$, for all $r \in [p]$. Let $\{\mathbf{x}^\nu\}$ be the iterates generated by the method (20a) and (21). Then,

$$\Phi(\mathbf{x}^\nu) - \Phi^* \leq c\rho^\nu, \text{ for any } \nu \in \mathbb{N},$$

where $c \in (0, \infty)$ is a universal constant, and $\rho \in (0, 1)$ is defined as follows.

(i) (heterogeneous stepsizes): Under $\sum_{r \in [p]} \tau_r^\nu = 1$, $\tau_r^\nu > 0$; and

$$2D + 1 \leq \min \left\{ \frac{2 \max_{r \in [p], \nu \geq 1} \frac{L_r}{\tau_r^\nu}}{\mu}, \frac{\min_{r \in \mathcal{J}, \nu \geq 1} \frac{\mu_r}{8\tau_r^\nu}}{\max_{\nu \geq 1} A_{\mathcal{J}}^\nu} \right\}, \quad (32)$$

the rate is given by

$$\rho = 1 - \frac{\mu}{2} \min_{r \in [p], \nu \geq 1} \frac{\tau_r^\nu}{L_r}. \quad (33)$$

Here

$$A_{\mathcal{J}}^\nu := \max_{i \in \cup_{j \in \mathcal{J}} \mathcal{C}_j} \sum_{r: |\mathcal{C}_r| > 1, i \in \mathcal{N}_{\mathcal{C}_r}} (\tau_r^\nu A_r), \text{ with } A_r := \frac{(2L_r + \mu_r)L_{\partial r}^2 |\mathcal{C}_r| D_r}{4\mu_r^2}.$$

(ii) (uniform stepsizes) : if $\tau_r^\nu \equiv \tau$ and

$$\tau \leq \min \left\{ \frac{1}{p}, \frac{2\kappa}{2D + 1}, \sqrt{\frac{\min_{r \in \mathcal{J}} \mu_r}{8(2D + 1)A_{\mathcal{J}}}} \right\}, \quad (34)$$

then

$$\rho = 1 - \frac{\tau}{2\kappa}. \quad (35)$$

Here

$$A_{\mathcal{J}} := \max_{i \in \cup_{j \in \mathcal{J}} \mathcal{C}_j} \sum_{r: |\mathcal{C}_r| > 1, i \in \mathcal{N}_{\mathcal{C}_r}} A_r. \quad (36)$$

Proof Fix $\nu \in \mathbb{N}$. For any index set $S \subseteq [m]$, write $\Delta_S^\nu := \sum_{\ell=\nu-D}^{\nu-1} \|x_S^{\ell+1} - x_S^\ell\|^2$. By (24), (28), and Lemma 3,

$$\Phi(\mathbf{x}^{\nu+1}) \leq \Phi(\mathbf{x}^\nu) - \sum_{r \in [p]} \frac{\tau_r^\nu}{4L_r} \|\nabla_{\mathcal{C}_r} \Phi(\mathbf{x}^\nu)\|^2 - \sum_{r \in [p]} \frac{\mu_r}{8\tau_r^\nu} \|x_{\mathcal{C}_r}^{\nu+1} - x_{\mathcal{C}_r}^\nu\|^2 + \sum_{r \in [p]} \tau_r^\nu A_r \Delta_{\mathcal{N}_{\mathcal{C}_r}}^\nu.$$

Discarding the vanishing terms with $|\mathcal{C}_r| = 1$ and using the disjointness of $\{\mathcal{C}_j\}_{j \in \mathcal{J}}$,

$$\sum_{r: |\mathcal{C}_r| > 1} (\tau_r^\nu A_r) \Delta_{\mathcal{N}_{\mathcal{C}_r}}^\nu = \sum_{\ell=\nu-D}^{\nu-1} \sum_{i \in \cup_{j \in \mathcal{J}} \mathcal{C}_j} \left(\sum_{r: |\mathcal{C}_r| > 1, i \in \mathcal{N}_{\mathcal{C}_r}} (\tau_r^\nu A_r) \right) \|x_i^{\ell+1} - x_i^\ell\|^2.$$

By definition of $A_{\mathcal{J}}^\nu$, we have

$$\sum_{r: |\mathcal{C}_r| > 1} (\tau_r^\nu A_r) \Delta_{\mathcal{N}_{\mathcal{C}_r}}^\nu \leq A_{\mathcal{J}}^\nu \sum_{\ell=\nu-D}^{\nu-1} \sum_{i \in \cup_{j \in \mathcal{J}} \mathcal{C}_j} \|x_i^{\ell+1} - x_i^\ell\|^2 = A_{\mathcal{J}}^\nu \sum_{j \in \mathcal{J}} \Delta_{\mathcal{C}_j}^\nu.$$

Finally, by strong convexity, $\|\nabla\Phi(\mathbf{x}^\nu)\|^2 \geq 2\mu(\Phi(\mathbf{x}^\nu) - \Phi^*)$, and thus

$$\begin{aligned}\Phi(\mathbf{x}^{\nu+1}) - \Phi^* &\leq \left(1 - \frac{\mu}{2} \min_{r \in [p], \nu \geq 1} \frac{\tau_r^\nu}{L_r}\right)(\Phi(\mathbf{x}^\nu) - \Phi^*) - \sum_{r \in \mathcal{J}} \frac{\mu_r}{8\tau_r^\nu} \|x_{\mathcal{C}_r}^{\nu+1} - x_{\mathcal{C}_r}^\nu\|^2 \\ &\quad + A_{\mathcal{J}}^\nu \sum_{r \in \mathcal{J}} \Delta_{\mathcal{C}_r}^\nu.\end{aligned}$$

Invoking the standard delay-window inequality (e.g. [15, Lemma 5]) yields linear convergence, subject to (32). Using heterogeneous (resp. uniform) stepsize values along with (32) yields the linear convergence rates as given in (33) (resp. (34)). \square

Remark 1 When \mathcal{G} is a tree, $p = 1$ (i.e., message passing on the entire \mathcal{G}), and $\tau_r^\nu \equiv 1$, the iterates terminate in finitely many (diameter of \mathcal{G}) rounds, thus recovering the classical finite-time property of min-sum/message passing on trees.

Remark 2 The linear rate established in the theorem does not hinge on edge-maximality or Assumption 9 per se. It is suffices that each cluster “aggregate surrogate”—obtained collecting all terms involving $x_{\mathcal{C}_r}$ —is strongly convex in $x_{\mathcal{C}_r}$ (see Assumption 5 in Sec. 4 for the formal statement). That said, dropping maximality/ non-overlap may jeopardize well-posedness of the algorithmic subproblems (existence of minimizers). Both issues are resolved by the surrogate construction in Sec. 4, which enforces strong convexity and well-posed local updates.

3.3 Discussion

Theorem 1 establishes global *linear* convergence of $\{\Phi(\mathbf{x}^\nu)\}$, with a contraction factor $\rho \in (0, 1)$, under heterogeneous stepsizes (subject to (32)) or homogeneous ones (satisfying (34)). For the sake of conciseness, next we comment only the latter case; for the former, we only recall that, under $\tau_r^\nu = 1/p$, the contraction factor (32) becomes $\rho = 1 - (1/(2\kappa p))$, matching that of the *centralized p-block Jacobi*.

The rate expression (35), under (34), reads

$$\rho = 1 - \frac{1}{2\kappa} \cdot \min \left\{ \underbrace{\frac{1}{p}}_{(\text{I})}, \underbrace{\frac{2\kappa}{2D+1}}_{(\text{II})}, \underbrace{\sqrt{\frac{\min_{r \in \mathcal{J}} \mu_r}{8(2D+1) A_{\mathcal{J}}}}}_{(\text{III})} \right\}. \quad (37)$$

Here, (I) captures the cluster-level effect—typical of Jacobi-type schemes with p playing the role of the number of blocks; (II) reflects the *intra*-cluster geometry via the delay/diameter parameter D , along with the loss landscape (uniformly across all partitions) through the condition number κ ; and (III) captures the *inter*-cluster coupling through $A_{\mathcal{J}}$, which aggregates the external interactions *only* over the block-coordinates belonging to the external-neighborhood clusters $\{\mathcal{C}_r\}_{r \in \mathcal{J}}$ (i.e., the subset where delay accumulation can occur).

Eq. (37) shows a trade-off: Term (I) increases as p decreases, whereas terms (II)–(III) raise as D decreases. For a fixed graph, these quantities are coupled by the partition $\{\mathcal{G}_r\}_{r \in [p]}$: coarser clustering (smaller p) typically increase the diameters D and may also increase the coefficient $A_{\mathcal{J}}$, while finer partitions (larger p) reduce D but can enlarge p . Table 1 suggests the following partition-design principles. If (I) is active, the bound is *block-count limited* and one should reduce

Active term (interpretation)	Margin $1 - \rho$
(I) (block-count limited)	$1 - \rho = \frac{1}{4\kappa p}$
(II) (delay/diameter limited)	$1 - \rho = \frac{1}{2D + 1}$
(III) (external-coupling limited)	$1 - \rho = \frac{1}{2\kappa} \sqrt{\frac{\min_{r \in \mathcal{J}} \mu_r}{8(2D + 1)A_{\mathcal{J}}}}$

Table 1: Operating regimes of (37). Each tuning knob improves the bound only while its associated term is active; otherwise the rate saturates.

the number of clusters p (coarser clustering), while controlling the induced growth of D and $A_{\mathcal{J}}$. If (II) is active, the bound is *delay/diameter limited* and the priority is to keep clusters shallow (small D); in this regime the contraction is essentially κ -insensitive. If (III) is active, the bound is *external-coupling limited* and one should reduce $A_{\mathcal{J}}$ by placing cuts on weak inter-cluster couplings (small $L_{\partial r}$). Figures 3–5 empirically illustrate these mechanisms: Fig. 3 shows that, when (I) is active, reducing p yields faster convergence (until saturation); Fig. 4 isolates the effect of $A_{\mathcal{J}}$ and confirms the monotone improvement predicted by the (III)-regime; and Fig. 5 highlights that, once (II) is active, the observed iteration count becomes nearly insensitive to κ .

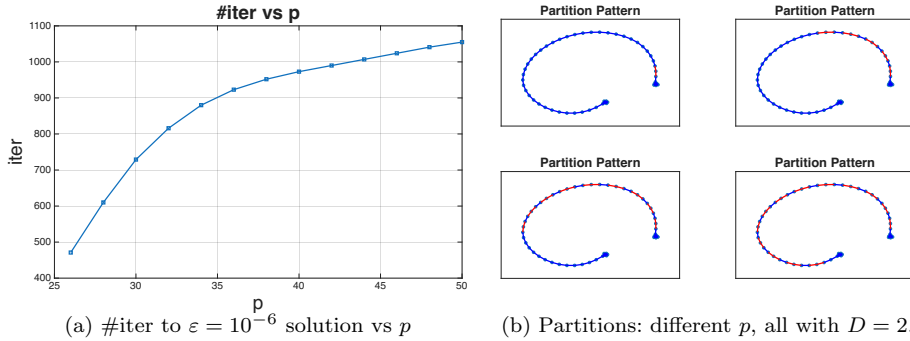


Fig. 3: Graph with two cliques (degree 6) connected by a long path (length 42). All partitions (different p) share the same D , $A_{\mathcal{J}}$, $(\mu_r)_{r \in \mathcal{J}}$ and κ .

3.4 Optimal rate scaling for ring and 2D graphs

We specialize here the general rate expression (37) to two representative graph families (rings and 2D grids) and to simple parametric partition patterns. Our goal is not to characterize *all* possible partitions, but to show how (37) guides the design and leads to explicit *rate scalings* in terms of the network size.

3.4.1 Ring graphs

Let \mathcal{G} be a ring. We study two partition strategies, namely: (\mathcal{P}_1) *one path plus singletons*, and (\mathcal{P}_2) *equal length paths*.

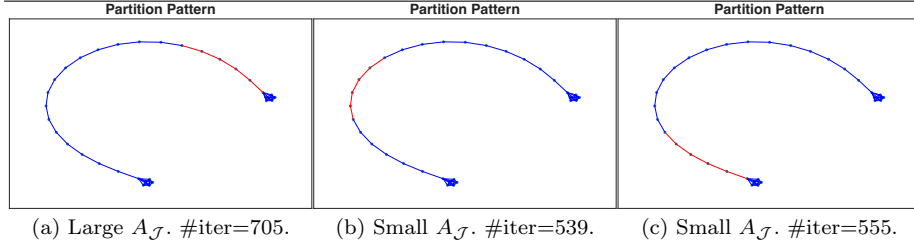


Fig. 4: Graph with two cliques connected by a long path (length =20); $A_{\mathcal{J}}$ varies, with constant p , D , $(\mu_r)_{r \in \mathcal{J}}$ and κ .

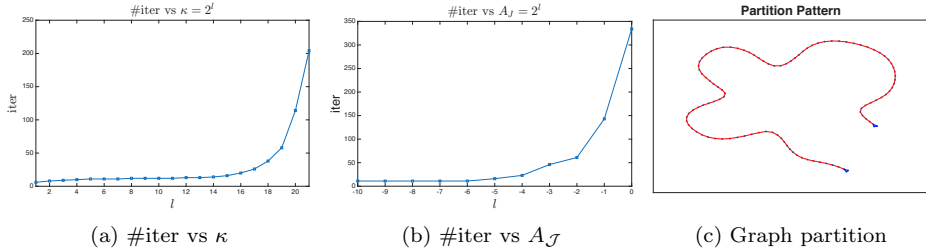


Fig. 5: Graph as in panel (c). In (a), κ varies while keeping all the other parameters fixed, whereas in (b) only $A_{\mathcal{J}}$ changes.

(P₁) one path plus singletons: Fix $D \in \{1, \dots, m-2\}$ and define one non-singleton cluster $\mathcal{C}_1 = \{s, s+1, \dots, s+D\} \pmod{m}$ and all remaining nodes as singletons. For $D \leq m-2$, one has $p = m-D$, $|\mathcal{C}_1| = D+1$, $\mathcal{N}_{\mathcal{C}_1} = \{s-1, s+D+1\}$, and $\mathcal{J} = \{s-1, s+D+1\}$; hence $A_{\mathcal{J}}$ in (36) reads

$$A_{\mathcal{J}} = A_1 = \frac{(2L_1 + \mu_1)L_{\partial 1}^2(D+1)D}{4\mu_1^2}.$$

Substituting the expression of $A_{\mathcal{J}}$ in term (III) in (37), we obtain

$$(III)(D) = \sqrt{\frac{\min_{j \in \mathcal{J}} \mu_j}{8(2D+1)A_{\mathcal{J}}(D)}} = \frac{c_1}{\sqrt{(2D+1)D(D+1)}} = \Theta(D^{-3/2}),$$

where $c_1 := \sqrt{(\min_{j \in \mathcal{J}} \mu_j)/2} \cdot \frac{\mu_1}{L_{\partial 1} \sqrt{2L_1 + \mu_1}}$ is independent of D .

We proceed to minimize (37) with respect to $D \in \{1, m-2\}$, for large m . To choose D , note that (I)(D) = 1/(m-D) increases with D , while (II)(D) = 2 κ /(2D+1) and (III)(D) decrease with D . Hence the maximizer of $\min\{(I), (II), (III)\}$ is obtained by equating (I) with the smallest decreasing term. For large m , taking $D = \Theta(m)$ makes (III)(D) = $\Theta(m^{-3/2}) \ll (I)(D) = \Theta(m^{-1})$, so (III) becomes the bottleneck; thus the relevant balance is (I) \asymp (III). Solving 1/(m-D) \asymp $D^{-3/2}$ yields the asymptotic optimizer

$$D^* = \Theta(m^{2/3}), \quad p^* = m - D^* = m - \Theta(m^{2/3}),$$

and the resulting rate scaling

$$1 - \rho(D^*) = \Theta\left(\frac{1}{\kappa m}\right), \quad (1 - \rho(D^*))^{-1} = \Theta(\kappa m).$$

Notice that the resulting contraction scaling exhibits the same Jacobi-type dependence on the number of blocks, since $p = m - D \approx m$. Indeed, \mathcal{P}_1 partitions the ring into one main cluster and many singletons, so the condensed graph remains nearly as large as the original one, and the rate is therefore bottlenecked by term (I) = $1/p$. Despite $|\mathcal{J}| = 2$ localizes delay accumulation, this affects only term (III) and cannot overcome the global limitation imposed by $p \approx m$. Motivated by this observation, we next analyze a balanced partition \mathcal{P}_2 , which leverages the ring symmetry to enforce $p \ll m$ while keeping D controlled.

(\mathcal{P}_2) equal length paths: Assume $(D+1) \mid m$ and set $p = m/(D+1)$. Partition the ring into p disjoint contiguous paths (clusters): for each $r \in [p]$,

$$\mathcal{C}_r = \{(r-1)(D+1) + 1, (r-1)(D+1) + 2, \dots, r(D+1)\} \pmod{m},$$

so that $|\mathcal{C}_r| = D+1$ and $D_r = D$ for all $r \in [p]$.

Fix $r \in [p]$. Since \mathcal{C}_r is a contiguous path segment on the ring, the only edges leaving \mathcal{C}_r are the two boundary edges adjacent to its endpoints. Therefore, the neighbor outside \mathcal{C}_r is

$$\mathcal{N}_{\mathcal{C}_r} = \{(r-1)(D+1), r(D+1) + 1\} \pmod{m}.$$

Observe that $(r-1)(D+1)$ is the last node of cluster \mathcal{C}_{r-1} , and $r(D+1) + 1$ is the first node of cluster \mathcal{C}_{r+1} (with indices modulo p). Therefore, taking the union over $r \in [p]$ yields exactly the set of all cluster endpoints, namely the nodes of the form $r(D+1)$ and $(r-1)(D+1) + 1$:

$$\bigcup_{r: |\mathcal{C}_r| > 1} \mathcal{N}_{\mathcal{C}_r} = \{r(D+1) : r \in [p]\} \cup \{(r-1)(D+1) + 1 : r \in [p]\}.$$

Finally, each endpoint belongs to exactly one cluster, so any cover of this set by clusters must include every \mathcal{C}_r , and the minimal such cover is $\mathcal{J} = [p]$.

Let us derive the explicit expression of $A_{\mathcal{J}}$. Notice that $i \in \mathcal{N}_{\mathcal{C}_r}$ holds iff i equals one of these two boundary-neighbor nodes (mod m). Since $\{\mathcal{N}_{\mathcal{C}_r}\}_{r=1}^p$ are disjoint in the ring equal-length construction, for every fixed i , the sum in (36) contains at most one nonzero term, and equals either A_r for a unique r or 0. Maximizing over i and using $|\mathcal{C}_r| = D+1$ and $D_r = D$ in A_r yield

$$A_{\mathcal{J}} = \max_{r \in [p]} A_r = (D+1)D \cdot \max_{r \in [p]} \frac{(2L_r + \mu_r)L_{\partial r}^2}{4\mu_r^2}.$$

Using the above expression of $A_{\mathcal{J}}$, term (III) becomes

$$(III)(D) = \sqrt{\frac{\min_{r \in [p]} \mu_r}{8(2D+1)A_{\mathcal{J}}(D)}} = \frac{c_2}{\sqrt{(2D+1)D(D+1)}} = \Theta(D^{-3/2}),$$

for some constant $c_2 > 0$ independent of D . Moreover $p = m/(D+1)$ gives $(I)(D) = (D+1)/m = \Theta(D/m)$. Balancing (I) \asymp (III) yields

$$\frac{D}{m} \asymp D^{-3/2} \implies D^* = \Theta(m^{2/5}), \quad p^* = \frac{m}{D^* + 1} = \Theta(m^{3/5}).$$

At this choice, for fixed κ , $(II)(D^*) = \Theta(\kappa m^{-2/5}) \gg \Theta(m^{-3/5}) = (I)(D^*) \asymp (III)(D^*)$, so (II) is inactive and $\min\{(I), (II), (III)\} = \Theta(m^{-3/5})$. The resulting rate reads

$$1 - \rho(D^*) = \Theta\left(\frac{1}{\kappa} m^{-3/5}\right), \quad (1 - \rho(D^*))^{-1} = \Theta(\kappa m^{3/5}).$$

This rate scaling strictly improves over the one-path-plus-singletons partition \mathcal{P}_1 . This comes from exploiting the translational symmetry of the ring to reduce the number of blocks from $p \approx m$ (under \mathcal{P}_1) to $p = \Theta(m^{3/5})$ (under \mathcal{P}_2), without letting the intra-cluster diameter D grow too aggressively; the optimal choice $D^* = \Theta(m^{2/5})$ balances the block limitation (I) against the coupling-driven term (III).

Overall, on rings (and more generally on homogeneous circulant topologies), balanced partitions that distribute cluster diameters evenly are preferable: they leverage symmetry to simultaneously reduce p and keep D controlled, yielding a provably better asymptotic rate. Unbalanced partitions such as \mathcal{P}_1 are mainly useful when structural or modeling considerations single out a localized strongly-coupled region to be kept within one cluster, but they do not improve the Jacobi-type scaling inherent to having $p \approx m$.

3.4.2 2D-grid graphs

Let \mathcal{G} be a $\sqrt{m} \times \sqrt{m}$ grid (assume m is a perfect square) with row-wise indexing. Fix $D \in \{1, \dots, \sqrt{m} - 1\}$. We consider *horizontal path* clusters of length D :

$$\mathcal{C}_r = \{(r-1)\sqrt{m} + 1, (r-1)\sqrt{m} + 2, \dots, (r-1)\sqrt{m} + (D+1)\}, \quad r \in [\sqrt{m}];$$

and let all remaining nodes be singletons. The number of clusters is

$$p = \sqrt{m} + (m - (D+1)\sqrt{m}) = m - D\sqrt{m}.$$

Moreover, $|\mathcal{C}_r| = D+1$ and $D_r = D$ for all $r \in [n]$ (while singletons have diameter 0), hence $D = \max_{r \in [p]} D_r$.

We now compute \mathcal{J} and $A_{\mathcal{J}}$ for this partition and minimize (37) over D .

Fix a row-cluster \mathcal{C}_r . Since \mathcal{C}_r lies in columns $1, \dots, D+1$, its external neighborhood $\mathcal{N}_{\mathcal{C}_r}$ consists of: (i) the right neighbor of its row-endpoint, that is $(r-1)\sqrt{m} + (D+2)$ (when $D \leq \sqrt{m} - 2$); (ii) the vertical neighbors (rows $r \pm 1$) of all nodes in \mathcal{C}_r (when those rows exist). Thus, for $D \leq \sqrt{m} - 2$,

$$\begin{aligned} \mathcal{N}_{\mathcal{C}_r} = & \{(r-1)\sqrt{m} + (D+2)\} \cup \{(r-2)\sqrt{m} + c : c = 1, \dots, D+1 : r \geq 2\} \\ & \cup \{r\sqrt{m} + c : c = 1, \dots, D+1 : r \leq \sqrt{m} - 1\}. \end{aligned}$$

Therefore,

$$\bigcup_{r: |\mathcal{C}_r| > 1} \mathcal{N}_{\mathcal{C}_r} = \bigcup_{r=1}^{\sqrt{m}} \mathcal{C}_r \cup \{(r-1)\sqrt{m} + (D+2) : r = 1, \dots, \sqrt{m}\}. \quad (38)$$

(The second set is absent when $D = \sqrt{m} - 1$.) Any cover of (38) by clusters must include all row-clusters $\mathcal{C}_1, \dots, \mathcal{C}_{\sqrt{m}}$; and when $D \leq \sqrt{m} - 2$, it must also include the \sqrt{m} singleton clusters at column $D+2$. Hence, for $D \leq \sqrt{m} - 2$,

$$\mathcal{J} = \{1, \dots, \sqrt{m}\} \cup \{\text{singleton clusters } \{(r-1)\sqrt{m} + (D+2)\} : r \in [\sqrt{m}]\}, \quad (39)$$

and $|\mathcal{J}| = 2\sqrt{m} \ll p$; whereas for $D = \sqrt{m} - 1$ one has $\mathcal{J} = [\sqrt{m}]$.

The only clusters with $|\mathcal{C}_r| > 1$ are the \sqrt{m} row-clusters, and for each such r ,

$$A_r(D) = \frac{(2L_r + \mu_r)L_{\partial r}^2 |\mathcal{C}_r| D_r}{4\mu_r^2} = \frac{(2L_r + \mu_r)L_{\partial r}^2 (D+1)D}{4\mu_r^2}.$$

We derive the expression of $A_{\mathcal{J}}$ as function of the above quantities. Fix $i \in \cup_{j \in \mathcal{J}} \mathcal{C}_j$. If i is a node in column $D + 2$, then $i \in \mathcal{N}_{\mathcal{C}_r}$ for a *unique* row r , and the corresponding sum in (36) equals $A_r(D)$. If instead i lies in columns $1, \dots, D + 1$, then i can be adjacent (vertically) to at most two row-clusters (the ones in the rows immediately above and below), so the sum contains at most two terms. Therefore,

$$\max_{1 \leq r \leq \sqrt{m}} A_r(D) \leq A_{\mathcal{J}} \leq 2 \max_{1 \leq r \leq \sqrt{m}} A_r(D), \quad (40)$$

and in particular $A_{\mathcal{J}} = \Theta(D(D + 1))$. Consequently,

$$(\text{III})(D) = \sqrt{\frac{\min_{r \in \mathcal{J}} \mu_r}{8(2D + 1)A_{\mathcal{J}}}} = \frac{c_{\text{grid}}}{\sqrt{(2D + 1)D(D + 1)}} = \Theta(D^{-3/2}),$$

for some constant $c_{\text{grid}} > 0$ independent of D .

We now maximize $\min\{(\text{I})(D), (\text{II})(D), (\text{III})(D)\}$ over $D \in [\sqrt{m} - 1]$ for large m . Recall, $(\text{I})(D) = 1/(m - D\sqrt{m})$ and $(\text{II})(D) = 2\kappa/(2D + 1)$. For fixed κ and large \sqrt{m} , the balance $(\text{I}) \asymp (\text{II})$ would give $D = \Theta(\sqrt{m})$ and thus $(\text{II}) = \Theta(\kappa/\sqrt{m})$, whereas $(\text{III}) = \Theta(m^{-3/4}) \ll \kappa/\sqrt{m}$, so (III) becomes the bottleneck. Therefore the relevant balance is $(\text{I}) \asymp (\text{III})$.

To solve it, write

$$D = \sqrt{m} - \Delta, \quad \Delta \in \{1, \dots, \sqrt{m} - 1\}.$$

Then $p = \Delta\sqrt{m}$, so $(\text{I})(D) = 1/(\Delta\sqrt{m})$. Moreover, for $D = \sqrt{m} - \Delta$ with $\Delta = o(\sqrt{m})$ one has $(\text{III})(D) = \Theta(D^{-3/2}) = \Theta(m^{-3/4})$. Equating $(\text{I}) \asymp (\text{III})$ gives

$$(\Delta\sqrt{m})^{-1} \asymp m^{-3/4} \implies \Delta \asymp m^{1/4}.$$

Therefore,

$$D^* = \sqrt{m} - \Theta(m^{1/4}), \quad p^* = m - D^*\sqrt{m} = \Theta(m^{3/4}).$$

At this choice,

$$(\text{II})(D^*) = \Theta(\kappa m^{-1/2}) \gg \Theta(m^{-3/4}) = (\text{I})(D^*) \asymp (\text{III})(D^*),$$

so (II) is inactive and $\min\{(\text{I}), (\text{II}), (\text{III})\} = \Theta(m^{-3/4})$. Substituting into (37) yields

$$1 - \rho(D^*) = \Theta(\kappa^{-1} m^{-3/4}), \quad (1 - \rho(D^*))^{-1} = \Theta(\kappa m^{3/4}).$$

This results shows that, for this one-directional partition family, the exponent $3/4$ in the rate scaling is the unavoidable outcome of the tradeoff between reducing p and the simultaneous deterioration of (III) driven by the growth of $A_{\mathcal{J}}$. In fact, the only way to decrease the Jacobi-type term $(\text{I}) = 1/p$ is to make the row paths as long as possible, since $p = m - D\sqrt{m}$ shrinks only when D approaches \sqrt{m} . However, longer paths also enlarge the delay-coupling penalty: $A_r \propto |\mathcal{C}_r|D_r = (D + 1)D$, so $A_{\mathcal{J}}$ grows like $D(D + 1)$ and term (III) decays as $\Theta(D^{-3/2})$. Balancing these two opposing effects forces D to be “almost” \sqrt{m} but not equal to it, specifically $D^* = \sqrt{m} - \Theta(m^{1/4})$, which leaves a residual block count $p^* = \Theta(m^{3/4})$ and yields the overall rate scaling $(1 - \rho)^{-1} = \Theta(\kappa m^{3/4})$.

4 Enhancing computation and communication via surrogation

We introduce a surrogate-based variant of Algorithm 1 to reduce both per-iteration computation and communication as well as ensure well-posed local updates when Assumption 3 does not hold. Updates in the form (15a) and (15c) require solving local minimization problems *exactly*, each intra-cluster message $\mu_{j \rightarrow i}^\nu(\cdot)$ is a function of the receiver's variable, which can be expensive to compute and transmit. This is particularly acute beyond quadratic function-messages, which are generally infinite-dimensional objects. Even for quadratic objectives, exact messages are quadratic functions parameterized by matrices that may be dense, hence communication demanding for large block-dimensions. Our approach is to replace the local costs by suitable surrogates: this ensures the existence of local minimizers, makes the subproblems cheap to solve, and induces messages with lightweight parameterizations (e.g., affine or structured-quadratic).

More formally, at iteration ν , each agent i uses reference values $y_i := x_i^\nu$, $i \in \mathcal{V}$ and $y_{\mathcal{N}_i} := \{x_j^\nu\}_{j \in \mathcal{N}_i}$, and employs model surrogates $\tilde{\phi}_i(\cdot; y_i)$ and $\tilde{\psi}_{ij}(\cdot, \cdot; y_i, y_j)$ around the reference values, replacing $\phi_i(\cdot)$ and $\psi_{ij}(\cdot, \cdot)$, respectively. The resulting scheme is summarized in Algorithm 2.

Algorithm 2: Message Passing-Jacobi (MP-Jacobi) with Surrogate

Initialization: $x_i^0 \in \mathbb{R}^d$, for all $i \in \mathcal{V}$; initial message $\tilde{\mu}_{i \rightarrow j}^0(\cdot)$ arbitrarily chosen (e.g.,

$\tilde{\mu}_{i \rightarrow j}^0 \equiv 0$), for all $(i, j) \in \mathcal{E}_r$ and $r \in [p]$.

for $\nu = 0, 1, 2, \dots$ **do**

each agent $i \in \mathcal{V}$ **in parallel:**

Performs the following updates:

$$\hat{x}_i^{\nu+1} \in \operatorname{argmin}_{x_i} \left\{ \tilde{\phi}_i(x_i; x_i^\nu) + \sum_{j \in \mathcal{N}_i^{\text{in}}} \tilde{\mu}_{j \rightarrow i}^\nu(x_i) + \sum_{k \in \mathcal{N}_i^{\text{out}}} \tilde{\psi}_{ik}(x_i, x_k^\nu; x_i^\nu, x_k^\nu) \right\}, \quad (41a)$$

$$x_i^{\nu+1} = x_i^\nu + \tau_r^\nu (\hat{x}_i^{\nu+1} - x_i^\nu), \quad (41b)$$

$$\tilde{\mu}_{i \rightarrow j}^{\nu+1}(x_j) = \min_{x_i} \left\{ \tilde{\phi}_i(x_i; x_i^\nu) + \tilde{\psi}_{ji}(x_j, x_i; x_j^\nu, x_i^\nu) + \sum_{k \in \mathcal{N}_i^{\text{in}} \setminus \{j\}} \tilde{\mu}_{k \rightarrow i}^\nu(x_i) + \sum_{k \in \mathcal{N}_i^{\text{out}}} \tilde{\psi}_{ik}(x_i, x_k^\nu; x_i^\nu, x_k^\nu) \right\}, \forall j \in \mathcal{N}_i^{\text{in}}; \quad (41c)$$

Sends out $x_i^{\nu+1}$ to all $j \in \mathcal{N}_i^{\text{out}}$ and $\tilde{\mu}_{i \rightarrow j}^{\nu+1}(x_j)$ to all $j \in \mathcal{N}_i^{\text{in}}$.

Remark 3 While Algorithm 2 is presented using the same surrogate models in both the variable and message updates, surrogation can be applied selectively. For instance, one may keep the variable update (41a) exact while surrogating the message update (41c) to reduce communication; conversely, surrogating (41a) primarily targets local computational savings. The same convergence guarantees can be established for these mixed exact/surrogate variants, but we omit the details for brevity—some numerical results involving these instances are presented in Sec. 6.

4.1 Surrogate regularity conditions

We request mild regularity conditions on the surrogates functions to guarantee convergence of Algorithm 2. We state these conditions directly on the *cluster surrogate objective* induced by the local models, as formalized next.

For any cluster $r \in [p]$ and $\mathbf{x} \in \mathbb{R}^{md}$, recall the partition $\mathbf{x} = (x_{\mathcal{C}_r}, x_{\bar{\mathcal{C}}_r})$, where $x_{\mathcal{C}_r}$ are the cluster variables and $x_{\bar{\mathcal{C}}_r}$ are the variables outside the cluster. Define the cluster-relevant portion of the global objective:

$$\Phi_r(\mathbf{x}) := \sum_{i \in \mathcal{C}_r} \phi_i(x_i) + \sum_{(i,j) \in \mathcal{E}_r} \psi_{ij}(x_i, x_j) + \sum_{i \in \mathcal{C}_r} \sum_{k \in \mathcal{N}_i^{\text{out}}} \psi_{ik}(x_i, x_k). \quad (42)$$

Given surrogates $\tilde{\phi}_i(\cdot; \cdot)$ and $\tilde{\psi}_{ij}(\cdot, \cdot; \cdot, \cdot)$, we build an aggregated surrogate for Φ_r around the *reference points* collected into

$$\zeta_r := (y_{\mathcal{C}_r}, y_{\bar{\mathcal{C}}_r}, y_{\mathcal{E}_r}),$$

where $y_{\mathcal{C}_r} := \{y_i\}_{i \in \mathcal{C}_r}$ (cluster nodes), $y_{\bar{\mathcal{C}}_r} := \{y_k\}_{k \in \bar{\mathcal{C}}_r}$ (outside nodes), and $y_{\mathcal{E}_r}$ is the intra-cluster edge reference stack

$$y_{\mathcal{E}_r} := ((y_e, y'_e))_{e \in \mathcal{E}_r}.$$

Fixing an arbitrary ordering of \mathcal{E}_r , we identify each edge-stack $y_{\mathcal{E}_r} = ((y_e, y'_e))_{e \in \mathcal{E}_r}$ with its stacked vector in $\mathbb{R}^{2|\mathcal{E}_r|d}$ (endowed with the Euclidean norm); with a slight abuse of notation, we use the same symbol $y_{\mathcal{E}_r}$ for these vectors.

The aggregated surrogate around ζ_r is defined as

$$\begin{aligned} \tilde{\Phi}_r(\mathbf{x}; \zeta_r) := & \sum_{i \in \mathcal{C}_r} \tilde{\phi}_i(x_i; y_i) + \sum_{(i,j) \in \mathcal{E}_r} \tilde{\psi}_{ij}(x_i, x_j; y_{(i,j)}, y'_{(i,j)}) \\ & + \sum_{i \in \mathcal{C}_r} \sum_{k \in \mathcal{N}_i^{\text{out}}} \tilde{\psi}_{ik}(x_i, x_k; y_i, y_k). \end{aligned} \quad (43)$$

When the ‘‘exact surrogates’’ are used ($\tilde{\phi}_i \equiv \phi_i$ and $\tilde{\psi}_{ij} \equiv \psi_{ij}$), one has $\tilde{\Phi}_r \equiv \Phi_r$.
Consistency: We say that ζ_r is *consistent with* \mathbf{x} if all references coincide with the associated blocks of \mathbf{x} , i.e.,

$$y_{\mathcal{C}_r} = x_{\mathcal{C}_r}, \quad y_{\bar{\mathcal{C}}_r} = x_{\bar{\mathcal{C}}_r}, \quad \text{and} \quad y_{\mathcal{E}_r} = x_{\mathcal{E}_r} := ((x_i, x_j))_{(i,j) \in \mathcal{E}_r}.$$

We request the following conditions on the aggregate surrogates $\tilde{\Phi}_r$, $r \in [p]$.

Assumption 5 (cluster surrogate regularity) *Each surrogate $\tilde{\Phi}_r$ in (43) satisfies the following conditions:*

(i) *(gradient consistency)* *For all $\mathbf{x} = (x_{\mathcal{C}_r}, x_{\bar{\mathcal{C}}_r})$ and all ζ_r consistent with \mathbf{x} ,*

$$\nabla_{\mathcal{C}_r} \tilde{\Phi}_r(\mathbf{x}; \zeta_r) = \nabla_{\mathcal{C}_r} \Phi_r(\mathbf{x}). \quad (44)$$

(ii) *For all $\mathbf{x} = (x_{\mathcal{C}_r}, x_{\bar{\mathcal{C}}_r})$ and all reference tuples ζ_r ,*

$$\Phi_r(\mathbf{x}) \leq \tilde{\Phi}_r(\mathbf{x}; \zeta_r), \quad (45)$$

with equality whenever ζ_r is consistent with \mathbf{x} .

(iii) (*uniform strong convexity and smoothness in $x_{\mathcal{C}_r}$*) There exist constants $\tilde{\mu}_r, \tilde{L}_r \in (0, \infty)$ such that, for all $x_{\bar{\mathcal{C}}_r}$ and all tuple ζ_r , the mapping

$$u \mapsto \tilde{\Phi}_r((u, x_{\bar{\mathcal{C}}_r}); \zeta_r), \quad u \in \mathbb{R}^{d|\mathcal{C}_r|},$$

is $\tilde{\mu}_r$ -strongly convex and has \tilde{L}_r -Lipschitz continuous gradient. Define the surrogate condition number $\tilde{\kappa}$ as $\tilde{\kappa} := (\max_{r \in [p]} \tilde{L}_r)/\mu$.

(iv) (*sensitivity to intra-cluster edge references*) There exists $\tilde{\ell}_r \in (0, \infty)$ such that, for all $\mathbf{x} = (x_{\mathcal{C}_r}, x_{\bar{\mathcal{C}}_r})$ and all $y_{\mathcal{C}_r}$, the mapping

$$v \mapsto \nabla_{\mathcal{C}_r} \tilde{\Phi}_r(\mathbf{x}; (y_{\mathcal{C}_r}, x_{\bar{\mathcal{C}}_r}, v)), \quad v \in \mathbb{R}^{2|\mathcal{E}_r|d},$$

is $\tilde{\ell}_r$ -Lipschitz, i.e., for all $v, v' \in \mathbb{R}^{2|\mathcal{E}_r|d}$,

$$\left\| \nabla_{\mathcal{C}_r} \tilde{\Phi}_r(\mathbf{x}; (y_{\mathcal{C}_r}, x_{\bar{\mathcal{C}}_r}, v)) - \nabla_{\mathcal{C}_r} \tilde{\Phi}_r(\mathbf{x}; (y_{\mathcal{C}_r}, x_{\bar{\mathcal{C}}_r}, v')) \right\| \leq \tilde{\ell}_r \|v - v'\|.$$

(v) (*locality through boundary variables*) There exists a constant $\tilde{L}_{\partial r} \in (0, \infty)$ such that, for all $x_{\mathcal{C}_r}$, $y_{\mathcal{C}_r}$, and $y_{\mathcal{E}_r}$, the mapping

$$w \mapsto \nabla_{\mathcal{C}_r} \tilde{\Phi}_r((x_{\mathcal{C}_r}, w); (y_{\mathcal{C}_r}, w, y_{\mathcal{E}_r})), \quad w \in \mathbb{R}^{|\bar{\mathcal{C}}_r|d},$$

is $\tilde{L}_{\partial r}$ -Lipschitz along $P_{\partial r}$, i.e.,

$$\begin{aligned} & \left\| \nabla_{\mathcal{C}_r} \tilde{\Phi}_r((x_{\mathcal{C}_r}, w); (y_{\mathcal{C}_r}, w, y_{\mathcal{E}_r})) - \nabla_{\mathcal{C}_r} \tilde{\Phi}_r((x_{\mathcal{C}_r}, w'); (y_{\mathcal{C}_r}, w', y_{\mathcal{E}_r})) \right\| \\ & \leq \tilde{L}_{\partial r} \|P_{\partial r}(w - w')\| \quad \forall w, w' \in \mathbb{R}^{|\bar{\mathcal{C}}_r|d}. \end{aligned} \quad (46)$$

Condition (i) is the cluster-level analogue of first-order consistency: when the reference tuple is consistent with the current point, the surrogate matches the *cluster gradient* of the original objective. This is the key property ensuring that any fixed point of the algorithm is a solution for the original problem. Condition (ii) is a standard majorization requirement: it makes each cluster update a descent step for Φ (up to the delay terms accounted for in the analysis), and is the main mechanism behind monotonicity/contractivity. Condition (iii) ensures strong-convexity and smoothens of the cluster subproblems. This guarantees that each cluster subproblem has a unique minimizer, and it provides the curvature/smoothness constants $(\tilde{\mu}_r, \tilde{L}_r)$ affecting the convergence rate. Conditions (iv) controls throughout the constants $\tilde{\ell}_r$'s how much the *cluster gradients* change when the intra-cluster *edge-reference stack* is perturbed; it governs the error induced by using delayed/stale edge references in the surrogate messages. One can make $\tilde{\ell}_r$ small by employing edge surrogates whose gradients depend weakly (Lipschitzly) on their reference arguments—for instance, quadratic/linearized models where the reference enters only through a Hessian approximation that is stable along the iterates. Condition (v) quantifies the dependence of the cluster gradient on the *outside block* (and its boundary reference), measured only through the boundary projector $P_{\partial r}$. This matches the graph structure locality: in (43), the outside block enters $\tilde{\Phi}_r$ only through cross-cluster terms $\{\tilde{\psi}_{ik} : i \in \mathcal{C}_r, k \in \mathcal{N}_i^{\text{out}}\}$. Consequently, changing components of $x_{\bar{\mathcal{C}}_r}$ (and of the corresponding outside reference $y_{\bar{\mathcal{C}}_r}$) outside $\mathcal{N}_{\mathcal{C}_r}$ does not affect $\tilde{\Phi}_r$ and hence does not affect $\nabla_{\mathcal{C}_r} \tilde{\Phi}_r$.

Sufficient local conditions: A simple recipe to enforce Assumption 5 is on the *local* surrogates. For instance, *touching/gradient-consistency* and *majorization* properties on $\tilde{\phi}_i$ and $\tilde{\psi}_{ij}$ lift to **(i)**–**(ii)**. Strong convexity and smoothness in **(iii)** can be ensured by choosing all the cluster surrogates to include enough curvature in the optimized variables (e.g., via quadratic/proximal regularization in the node models and/or in the edge surrogates) and smoothness. The sensitivity bounds **(iv)**–**(v)** are typically obtained by requiring that the relevant *gradients* of the local edge surrogates depend Lipschitz-continuously on their *reference arguments*.

However, enforcing majorization or strong convexity *termwise* can be unnecessarily restrictive, especially when the couplings ψ_{ij} are nonconvex. Assumption 5 requires these properties only for the *aggregated* cluster surrogates $\tilde{\Phi}_r$, so that curvature and upper-bounding can be achieved *collectively* at the cluster level. This is a key departure from the surrogation conditions adopted in decomposition-based methods, which are usually imposed on the individual local models [13, 14, 34]. We next give examples of local surrogates that may fail Assumption 5 term-wise, yet inducing aggregated cluster surrogates that do satisfy Assumption 5.

4.2 Some surrogate examples

The following are practical designs satisfying Assumption 5 and useful to reduce computation and/or communication costs. Throughout, at iteration ν we employ reference points $y_i = x_i^\nu$ and $y_{\mathcal{E}_r} = ((x_i^\nu, x_j^\nu))_{(i,j) \in \mathcal{E}_r}$, for all $i \in \mathcal{V}$ and $r \in [p]$.

(i) first-order surrogates: Choose, for some $\alpha > 0$ and any $\nu \geq 0$,

$$\tilde{\phi}_i(x_i; x_i^\nu) := \phi_i(x_i^\nu) + \langle \nabla \phi_i(x_i^\nu), x_i - x_i^\nu \rangle + \frac{1}{2\alpha} \|x_i - x_i^\nu\|^2, \quad (47a)$$

$$\begin{aligned} \tilde{\psi}_{ij}(x_i, x_j; x_i^\nu, x_j^\nu) := & \psi_{ij}(x_i^\nu, x_j^\nu) + \langle \nabla_i \psi_{ij}(x_i^\nu, x_j^\nu), x_i - x_i^\nu \rangle \\ & + \langle \nabla_j \psi_{ij}(x_i^\nu, x_j^\nu), x_j - x_j^\nu \rangle, \end{aligned} \quad (47b)$$

for all $i \in \mathcal{V}$ and $(i, j) \in \mathcal{E}$. Using (47a)–(47b) in (41c) yields:

$$\tilde{\mu}_{i \rightarrow j}^{\nu+1}(x_j) \sim \langle \nabla_j \psi_{ij}(x_j^\nu, x_i^\nu), x_j - x_j^\nu \rangle, \quad (47c)$$

Hence each directed message is encoded (up to constants) by a single d -vector.

Using (47c) and (47a)–(47b) in (41a), the variable subproblem (41a) yields the gradient-delayed closed form:

$$\hat{x}_i^{\nu+1} = x_i^\nu - \alpha \left(\nabla \phi_i(x_i^\nu) + \sum_{j \in \mathcal{N}_i^{\text{in}}} \nabla_i \psi_{ij}(x_i^{\nu-1}, x_j^{\nu-1}) + \sum_{k \in \mathcal{N}_i^{\text{out}}} \nabla_i \psi_{ik}(x_i^\nu, x_k^\nu) \right).$$

To implement this surrogate instance of the algorithm, agents only exchange two d -dimensional vectors with their neighbors $\mathcal{N}_i^{\text{in}}$ and $\mathcal{N}_i^{\text{out}}$ per iterations.

Note that the above surrogates satisfy Assumption 5; in particular the majorization condition is ensured by choosing (a sufficiently small) α .

(ii) Quadratic messages and Schur recursion: Let $\tilde{\phi}_i(\cdot; x_i^\nu)$ be any strongly convex quadratic function (e.g., as in (47a) or a second-order model) with Hessian matrix $Q_i \in \mathbb{S}_{++}^d$, $i \in \mathcal{V}$; and let $\tilde{\psi}_{ij}$ be chosen as the quadratic surrogate

$$\begin{aligned} \tilde{\psi}_{ij}(x_i, x_j; x_i^\nu, x_j^\nu) = & \psi_{ij}(x_i^\nu, x_j^\nu) + \langle \nabla_i \psi_{ij}(x_i^\nu, x_j^\nu), x_i - x_i^\nu \rangle + \langle \nabla_j \psi_{ij}(x_i^\nu, x_j^\nu), x_j - x_j^\nu \rangle \\ & + \langle M_{ij}(x_i - x_i^\nu), x_j - x_j^\nu \rangle + \frac{1}{2} \|x_i - x_i^\nu\|_{M_i}^2 + \frac{1}{2} \|x_j - x_j^\nu\|_{M_j}^2, \end{aligned}$$

with each $M_i \in \mathbb{S}_+^d$ and (possibly structured) cross matrices $M_{ij} \in \mathbb{S}^d$. Assume the messages are initialized as quadratic functions:

$$\tilde{\mu}_{i \rightarrow j}^0(x_j) \sim \frac{1}{2} \|x_j\|_{H_{i \rightarrow j}^0}^2 + \langle h_{i \rightarrow j}^0, x_j \rangle, \quad (48a)$$

for some $H_{i \rightarrow j}^0 \in \mathbb{S}_+^d$ and $h_{i \rightarrow j}^0 \in \mathbb{R}^d$. Then, for every $\nu \geq 0$, the updated messages produced by (41c) remain quadratic:

$$\tilde{\mu}_{i \rightarrow j}^{\nu+1}(x_j) \sim \frac{1}{2} \|x_j\|_{H_{i \rightarrow j}^{\nu+1}}^2 + \langle h_{i \rightarrow j}^{\nu+1}, x_j \rangle. \quad (48b)$$

Moreover the curvature matrices satisfy the Schur-complement recursion

$$H_{i \rightarrow j}^{\nu+1} = M_j - M_{ji} \left(Q_i + M_i + \sum_{k \in \mathcal{N}_i^{\text{in}} \setminus \{j\}} H_{k \rightarrow i}^{\nu} \right)^{-1} M_{ji}^{\top}.$$

(The corresponding recursion for $h_{i \rightarrow j}^{\nu+1}$ is explicit as well, but omitted for brevity).

Since each $\tilde{\mu}_{i \rightarrow j}^{\nu+1}(x_j)$ is specified (up to constants) by the pair $(H_{i \rightarrow j}^{\nu+1}, h_{i \rightarrow j}^{\nu+1})$, communication is efficient whenever $H_{i \rightarrow j}^{\nu+1}$ admits a compact parametrization. In particular, by selecting $\{M_i\}$ and $\{M_{ij}\}$ and initializing $\{H_{i \rightarrow j}^0\}$ so that the recursion preserves a *structured* family (e.g., (block-)diagonal, banded, sparse, low-rank+diagonal), each message can be transmitted using $\mathcal{O}(d)$ (or a small multiple thereof) parameters rather than $\mathcal{O}(d^2)$. Also, choosing properly Q_i , M_i , and M_j (typical large) ensures Assumption 5 holds.

(iii) Consensus optimization via CTA-formulation: Consider the consensus optimization problem (5); it is an instance of (P') with

$$\phi_i(x_i) = f_i(x_i) + \frac{1 - w_{ii}}{2\gamma} \|x_i\|^2, \quad \psi_{ij}(x_i, x_j) = -\frac{1}{\gamma} w_{ij} \langle x_i, x_j \rangle, \quad \text{and } w_{ij} = [W]_{ij}.$$

Choose a partial linearization surrogate for ϕ_i and the exact surrogate for ψ_{ij} , i.e.,

$$\begin{aligned} \tilde{\phi}_i(x_i; x_i^{\nu}) &:= f_i(x_i^{\nu}) + \langle \nabla f_i(x_i^{\nu}), x_i - x_i^{\nu} \rangle + \frac{1}{2} \|x_i - x_i^{\nu}\|_{Q_i}^2 + \frac{1 - w_{ii}}{2\gamma} \|x_i\|^2, \\ \tilde{\psi}_{ij}(x_i, x_j; x_i^{\nu}, x_j^{\nu}) &= \psi_{ij}(x_i, x_j) = -\frac{1}{\gamma} w_{ij} \langle x_i, x_j \rangle, \end{aligned} \quad (49)$$

with $Q_i \in \mathbb{S}_+$. If all the initial messages $\tilde{\mu}_{i \rightarrow j}^0(x_j)$ are quadratic as in (48a), all $\tilde{\mu}_{i \rightarrow j}^{\nu+1}(x_j)$ will be quadratic as in (48b), with curvature recursion $H_{i \rightarrow j}^{\nu+1}$ given by the following recursion

$$H_{i \rightarrow j}^{\nu+1} = -\frac{w_{ij}^2}{\gamma^2} \left(Q_i + \frac{1 - w_{ii}}{\gamma} I_d + \sum_{k \in \mathcal{N}_i^{\text{in}} \setminus \{j\}} H_{k \rightarrow i}^{\nu} \right)^{-1}. \quad (50)$$

Therefore, if one chooses Q_i to be (block-)diagonal and initializes $\{H_{i \rightarrow j}^0\}$ as (block-)diagonal, then (50) preserves (block-)diagonality for all ν , so each message can be transmitted using $\mathcal{O}(d)$ parameters (diagonal of $H_{i \rightarrow j}^{\nu}$ plus $h_{i \rightarrow j}^{\nu}$), rather than $\mathcal{O}(d^2)$. In the isotropic choice $Q_i \propto I_d$, (and scalar initializations $\{H_{i \rightarrow j}^0 \propto I_d\}$), even the curvature reduces to a single scalar per message.

When γ is small (the typical regime), the consensus regularizer $\frac{1 - W_{ii}}{2\gamma} \|x_i\|^2$ dominates the curvature of f_i , so the partial linearization surrogate $\tilde{\phi}_i$ in (49) is expected to be an accurate model of f_i . Consequently, the surrogate scheme can

retain near-exact convergence behavior than the algorithm using no surrogation while substantially reducing communication: with quadratic parametrization, each message is encoded by two vectors (diagonal entries and a linear term) rather than a dense matrix plus a vector (or, for non quadratic f_i 's, a full function). Finally, Assumption 5 is ensured choosing each $Q_i - q_i I \in \mathbb{S}_+^d$, for sufficiency large $q_i > 0$.

4.3 Convergence analysis: strongly convex objective

We are ready to present the convergence results of Algorithm 2; we consider for simplicity only the case of homogeneous stepsize and refer to the Appendix B for the case of heterogeneous stepsize values.

Theorem 2 (uniform stepsize) *Suppose Assumptions 1, 2, 3, 4, and 5 hold, with $\mu > 0$ and $\tilde{\mu}_r > 0$, for all $r \in [p]$. Let $\{\mathbf{x}^\nu\}$ be generated by Algorithm 2. Choose $\tau_r^\nu \equiv \tau$ such that*

$$\tau \leq \min \left\{ \frac{1}{p}, \frac{2\tilde{\kappa}}{2D+1}, \sqrt{\frac{\min_{r \in \mathcal{J} \cup \{s \in [p]: |\mathcal{C}_s| > 1\}} \tilde{\mu}_r}{8(2D+1) (A_{\mathcal{J}} + \max_{r: |\mathcal{C}_r| > 1} \tilde{A}_r)}} \right\}, \quad (51)$$

where $A_{\mathcal{J}}$ is defined as in (36), with A_r therein now given by

$$A_r := \frac{(2\tilde{L}_r + \tilde{\mu}_r) \tilde{L}_{\partial r}^2 |\mathcal{C}_r| D_r}{4 \tilde{\mu}_r^2};$$

and

$$\tilde{A}_r := \frac{(2\tilde{L}_r + \tilde{\mu}_r) \tilde{\ell}_r^2 |\mathcal{C}_r| D_r}{4 \tilde{\mu}_r^2} \left(\max_{i \in \mathcal{C}_r} \deg_{\mathcal{G}_r}(i) \right).$$

Then,

$$\Phi(\mathbf{x}^\nu) - \Phi^* \leq c \rho^\nu, \quad \forall \nu \in \mathbb{N},$$

for some universal constant $c \in (0, \infty)$, where

$$\rho = 1 - \frac{\tau}{2\tilde{\kappa}}. \quad (52)$$

Proof See Appendix B. \square

The following remarks are in order. Theorem 2 parallels Theorem 1: linear convergence is guaranteed, with a contraction factor ρ now given by (52), depending on the surrogate condition number $\tilde{\kappa}$. Relative to the exact case (Theorem 1), the stepsize restrictions in (51) retain the same three-way structure as in (37): (I) the block-count limitation $1/p$ (Jacobi-type effect), (II) the delay/diameter limitation $(2D+1)^{-1}$, and (III) an external-coupling limitation.

The main differences are as follows. (i) *larger condition number*. The constants $(L_r, \mu_r, L_{\partial r})$ are replaced by their surrogate counterparts $(\tilde{L}_r, \tilde{\mu}_r, \tilde{L}_{\partial r})$ in A_r and in the admissible range of τ . Since majorization typically inflates curvature $(\tilde{L} \geq L)$, one may have $\tilde{\kappa} \geq \kappa$, hence a slower rate for a given stepsize—the expected price for cheaper local computation/communication. (ii) *A new delay channel through edge-reference sensitivity*. The denominator in the (III)-type

bound now involves $\max\{A_{\mathcal{J}}, \max_{r: |\mathcal{C}_r| > 1} \tilde{A}_r\}$. The term $A_{\mathcal{J}}$ is the same external-neighborhood coupling aggregate as in the exact case, whereas \tilde{A}_r is *new* and quantifies the impact of stale *intra-cluster edge references*. This effect is governed by the reference-sensitivity constant $\tilde{\ell}_r$ in Assumption 5.(iv): tighter edge surrogates (smaller $\tilde{\ell}_r$) reduce \tilde{A}_r and enlarge the admissible stepsize region. **(iii) Partition design must control two coupling measures.** As in the exact case, good partitions balance a small number of clusters p against moderate diameters D_r . In the surrogate setting, one must additionally keep both $A_{\mathcal{J}}$ and $\max_{r: |\mathcal{C}_r| > 1} \tilde{A}_r$ moderate; the latter favors surrogate designs with limited edge-reference sensitivity and/or small non-singleton diameters D_r . An examples is briefly discussed next.

Example (interpreting $\tilde{\ell}_r$). For quadratic edge surrogates (Sec. 4.2(ii)) and C^2 couplings ψ_{jk} , $\tilde{\ell}_r$ is controlled by the mismatch between the surrogate cross-curvature M_{jk} and the true cross-Hessian of ψ_{jk} along the reference points: indeed,

$$\nabla_{(u, u')} \nabla_{(x_j, x_k)} \tilde{\psi}_{jk}((x_j, x_k); (u, u')) = \nabla^2 \psi_{jk}(u, u') - M_{jk}, \quad (j, k) \in \mathcal{E}_r.$$

Hence choosing $M_{jk} \approx \nabla^2 \psi_{jk}(x_j^\nu, x_k^\nu)$ (in operator norm, along the iterates) yields a smaller $\tilde{\ell}_r$, hence reduces \tilde{A}_r . This leads to a milder additional delay penalty in the stepsize condition.

4.4 Convergence analysis: nonstrongly convex objective

When Φ is not strongly convex (and possibly nonconvex), we employ surrogation to ensure that every local subproblem is well-defined. For merely convex objectives, to derive a bound in terms of the *function value gap* $\Phi(\mathbf{x}^\nu) - \Phi(\mathbf{x}^*)$, we need to relate this gap to a squared-distance term involving \mathbf{x}^ν and $\mathbf{x}^* \in \operatorname{argmin}_{\mathbf{x}} \Phi(\mathbf{x})$. This requires a global smoothness property for a *full aggregated* surrogate objective, so that $\Phi(\mathbf{x}^\nu)$ can be related to $\Phi(\mathbf{x}^*)$ through a standard descent inequality.

To this end, we first collect the terms in Φ that are *independent* of the block variable $x_{\mathcal{C}_r}$. For a given cluster \mathcal{C}_r and any $\mathbf{x} \in \mathbb{R}^{md}$, define the remainder

$$R_r(x_{\bar{\mathcal{C}}_r}) := \sum_{i \in \bar{\mathcal{C}}_r} \phi_i(x_i) + \sum_{i, j \in \bar{\mathcal{C}}_r, (i, j) \in \mathcal{E}} \psi_{ij}(x_i, x_j). \quad (53)$$

Then, for a given \mathbf{x} and $\zeta_r = (y_{\mathcal{C}_r}, y_{\bar{\mathcal{C}}_r}, y_{\mathcal{E}_r})$, we introduce the *full aggregated surrogate* associated with \mathcal{C}_r :

$$\tilde{\Phi}_r^{\text{all}}(\mathbf{x}; \zeta_r) := \tilde{\Phi}_r(\mathbf{x}; \zeta_r) + R_r(x_{\bar{\mathcal{C}}_r}). \quad (54)$$

By construction, $\tilde{\Phi}_r^{\text{all}}$ consists of all surrogate terms associated with the subgraph \mathcal{G}_r and all other original objective terms that are independent of $x_{\mathcal{C}_r}$.

Assumption 6 For each $r \in [p]$, the function $\tilde{\Phi}_r^{\text{all}}$ is \bar{L}_r -smooth with respect to its full argument $\mathbf{z} = (\mathbf{x}, \zeta_r)$, i.e., for all \mathbf{z} and \mathbf{z}' ,

$$\|\nabla \tilde{\Phi}_r^{\text{all}}(\mathbf{z}) - \nabla \tilde{\Phi}_r^{\text{all}}(\mathbf{z}')\| \leq \bar{L}_r \|\mathbf{z} - \mathbf{z}'\|.$$

Theorem 3 Suppose Assumptions 1, 2, 3, 4, 5, and 6 hold, with $\mu = 0$ and $\tilde{\mu} > 0$. Let $\{\mathbf{x}^\nu\}$ be generated by Algorithm 2 with uniform stepsize $\tau_r^\nu \equiv \tau$ such that

$$\tau \leq \min \left\{ \frac{1}{p}, \sqrt{\frac{\tilde{\mu}}{16(D+1)(A_{\mathcal{J}} + \max_{r: |\mathcal{C}_r| > 1} \tilde{A}_r)}}, \frac{\tilde{L}_{\min}}{(L + (\sigma+1)(D+1)) \max_{r \in [p]} |\mathcal{C}_r|} \right\},$$

where $\tilde{\mu} = \min_{r \in [p]} \tilde{\mu}_r$, $\tilde{L}_{\min} = \min_{r \in [p]} \tilde{L}_r$, $L = \max_{r \in [p]} L_r$, $\sigma = \max_{r \in [p]} \sigma_r$, and $\sigma_r := \max_{i \in \mathcal{C}_r} \deg_{\mathcal{G}_r}(i)$, $A_{\mathcal{J}}$, and \tilde{A}_r are defined as in Theorem 2. For any

$$\nu \geq \frac{8(\tilde{L} - \tilde{\mu}/\max_{r \in [p]} |\mathcal{C}_r|)}{\tilde{\mu}} + \frac{pK}{A_{\mathcal{J}} + \max_{r: |\mathcal{C}_r| > 1} \tilde{A}_r},$$

with

$$K := \max_{r \in [p]} \left\{ \frac{\bar{L}_r(\sigma_r + 1)(2D_r + 1)}{2} + \frac{|\mathcal{C}_r|^2 D_r (\tilde{L}_{\partial r}^2 + \sigma_r \tilde{L}_r^2)}{2\tilde{\mu}_r^2} \right\},$$

it holds that

$$\Phi(\mathbf{x}^\nu) - \Phi^* \leq \frac{1}{\nu} \left(\Phi(\mathbf{x}^0) - \Phi^* + \frac{\tilde{L}_{\min}}{2\tau \max_{r \in [p]} |\mathcal{C}_r|} \|\mathbf{x}^0 - \mathbf{x}^*\|^2 \right).$$

Proof See Appendix C. \square

Theorem 4 Suppose Assumptions 1, 2, 3, 4.(ii), and 5 hold. Let $\{\mathbf{x}^\nu\}$ be generated by Algorithm 2 with uniform stepsize $\tau_r^\nu \equiv \tau$ satisfying

$$\tau \leq \min \left\{ \frac{1}{p}, \sqrt{\frac{\tilde{\mu}}{8D(A_{\mathcal{J}} + \max_{r: |\mathcal{C}_r| > 1} \tilde{A}_r)}} \right\}.$$

Then

$$\min_{\ell \in \{D, \dots, \nu+D-1\}} \|\nabla \Phi(\mathbf{x}^\ell)\|^2 \leq \frac{4\tilde{L}(\Phi(\mathbf{x}^0) - \Phi^*)}{\tau \nu}, \quad (55)$$

where $\tilde{\mu}$, \tilde{L} , $A_{\mathcal{J}}$, and \tilde{A}_r are defined as in Theorem 3.

Proof See Appendix D. \square

Unlike classical block-Jacobi and min-sum message passing, which typically rely on strong convexity for convergence, Theorems 3 and 4 show that Algorithm 2 is well posed and achieves sublinear convergence in both convex and nonconvex settings. This robustness stems from the use of *strongly convex aggregated surrogate* subproblems. In either regime, the stepsize conditions exhibit the same structural drivers: the block-count factor $1/p$, the delay/diameter constraint, and a bound on the strength of the inter-cluster coupling. As a consequence, the trade-offs and partition-guidance principles in Sec. 3.3 extend verbatim beyond strong convexity.

5 Decomposition via Message Passing: Hypergraph Problem (P)

In this section we extend the proposed framework to the hypergraph formulation (P). We begin introducing basic definitions used throughout the section.

Given the hypergraph $\mathcal{G} = (\mathcal{V}, \mathcal{E})$ underlying (P), we view each hyperedge $\omega \in \mathcal{E}$ as a *factor* representing the coupling term $\psi_\omega(x_\omega)$. This naturally leads to the following bipartite representation, based on the (condensed) factor graph.

Definition 2 (factor graph) The (hypergraph) factor graph associated with $\mathcal{G} = (\mathcal{V}, \mathcal{E})$ is the bipartite graph $\mathcal{F}(\mathcal{G}) := (\mathcal{V} \cup \mathcal{E}, \mathcal{A})$ with variable nodes \mathcal{V} , factor nodes \mathcal{E} , and incidence edges $\mathcal{A} := \{(i, \omega) \in \mathcal{V} \times \mathcal{E} : i \in \omega\}$. For a sub-hypergraph $\mathcal{G}_r = (\mathcal{C}_r, \mathcal{E}_r)$, we denote by $\mathcal{F}_r := \mathcal{F}(\mathcal{G}_r)$ the induced factor graph, i.e., $\mathcal{F}_r = (\mathcal{C}_r \cup \mathcal{E}_r, \mathcal{A}_r)$ with $\mathcal{A}_r := \{(i, \omega) \in \mathcal{C}_r \times \mathcal{E}_r : i \in \omega\}$.

We next introduce the hypergraph analogue of the condensed graph (Def. 1). As in the pairwise setting, we adopt the edge-maximality convention at the level of clusters: each cluster contains *all* factors supported entirely on its variables.

Definition 3 (condensed factor graph) Given $\mathcal{G} = (\mathcal{V}, \mathcal{E})$ and $p \in [m]$, let $\mathcal{C}_1, \dots, \mathcal{C}_p$ be a partition of \mathcal{V} , with associated intra-cluster hyperedge sets

$$\mathcal{E}_r := \{\omega \in \mathcal{E} : \omega \subseteq \mathcal{C}_r\}, \quad r \in [p]; \quad (56)$$

this results in the sub-hypergraphs $\mathcal{G}_r := (\mathcal{C}_r, \mathcal{E}_r)$, with induced factor graphs $\mathcal{F}_r := \mathcal{F}(\mathcal{G}_r)$. Let $\mathcal{E}_{\text{in}} := \bigcup_{r \in [p]} \mathcal{E}_r$ and $\mathcal{E}_{\text{out}} := \mathcal{E} \setminus \mathcal{E}_{\text{in}}$ denote the *intra-cluster* and *inter-cluster* factors, respectively.

The *condensed factor graph* relative to $\{\mathcal{F}_r\}_{r=1}^p$ is the bipartite graph $\mathcal{F}_C := (\mathcal{V}_C \cup \mathcal{E}_{\text{out}}, \mathcal{A}_C)$ where

- $\mathcal{V}_C := \{\mathbf{c}_1, \dots, \mathbf{c}_p\}$ is the set of *supernodes*, with \mathbf{c}_r associated with \mathcal{C}_r ; and
- $\mathcal{A}_C := \{(\mathbf{c}_r, \omega) \in \mathcal{V}_C \times \mathcal{E}_{\text{out}} : \omega \cap \mathcal{C}_r \neq \emptyset\}$ is the set of incidence edges between supernodes and cross-cluster factors.

Fig. 6 illustrates the passage from a hypergraph to its factor graph and to a condensed factor graph under some cluster partitions.

Neighborhoods & factor-graph distance. Neighbors are *incident factors*. For $i \in \mathcal{C}_r$, define (to simplify notation, we keep the same symbols as in the pairwise case)

$$\mathcal{N}_i := \{\omega \in \mathcal{E} : i \in \omega\}, \quad \mathcal{N}_i^{\text{in}} := \mathcal{N}_i \cap \mathcal{E}_r, \quad \mathcal{N}_i^{\text{out}} := \mathcal{N}_i \setminus \mathcal{N}_i^{\text{in}};$$

and let $\mathcal{N}_{\mathcal{C}_r} := \bigcup_{i \in \mathcal{C}_r} \mathcal{N}_i^{\text{out}}$. Note that $\mathcal{N}_i^{\text{in}}$ corresponds to intra-cluster factor nodes adjacent to i in \mathcal{F}_r , whereas $\mathcal{N}_i^{\text{out}}$ collects the inter-cluster factors incident to i (i.e., factors adjacent to the supernode \mathbf{c}_r in \mathcal{F}_C through i). When \mathcal{F}_r is connected, we denote by $D_r := \text{diam}(\mathcal{F}_r)$ its diameter, and let $D := \max_{r \in [p]} D_r$. A *factor-graph path* from u to v in $\mathcal{F}(\mathcal{G})$ (u, v may be variable or factor nodes) is a finite sequence of *distinct* nodes $(z_0, \dots, z_\ell) \subseteq \mathcal{V} \cup \mathcal{E}$ such that $z_0 = u$, $z_\ell = v$, and $(z_{t-1}, z_t) \in \mathcal{A}$, for all $t = 1, \dots, \ell$. The *factor-graph distance* is

$$\text{dist}_{\mathcal{F}}(u, v) := \begin{cases} 0, & u = v, \\ \min\{\ell \geq 1 : \exists \text{ a factor-graph path of length } \ell \text{ from } u \text{ to } v\}, & u \neq v. \end{cases}$$

For variable nodes $i, j \in \mathcal{V}$, define the induced variable-to-variable distance $d(i, j) := (1/2) \text{dist}_{\mathcal{F}}(i, j)$, and for $i \in \mathcal{V}$ and $\omega \in \mathcal{E}$, define the variable-to-factor distance $d(i, \omega) := (1/2)(\text{dist}_{\mathcal{F}}(i, \omega) - 1)$.

As for the pairwise setting, we focus on hypertree partition clusters.

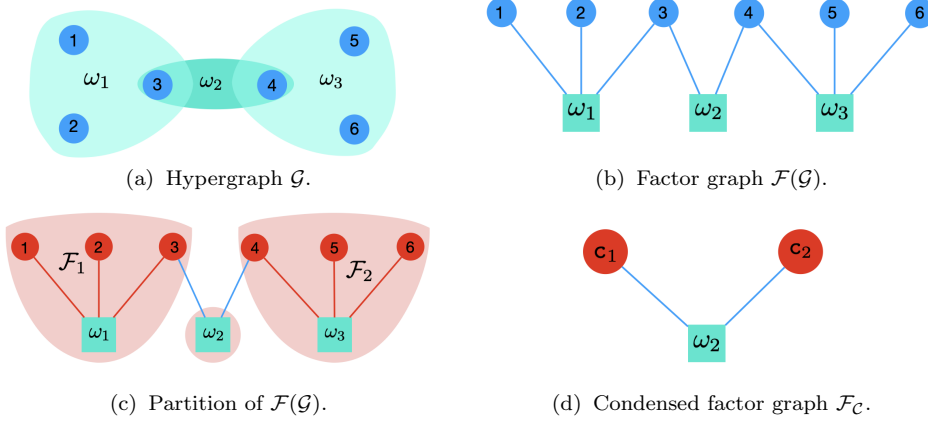


Fig. 6: Hypergraph-to-factor-graph representation and clustering: (a) hypergraph \mathcal{G} ; (b) bipartite factor graph $\mathcal{F}(\mathcal{G})$. (c) example of partition of $\mathcal{F}(\mathcal{G})$ into factor trees \mathcal{F}_r ; (d) condensed factor graph corresponding to the partition in (c).

Definition 4 (Hypertree) A hypergraph $\mathcal{G} = (\mathcal{V}, \mathcal{E})$ is said to be a *(hyper)tree* if its factor graph $\mathcal{F}(\mathcal{G})$ is connected and acyclic (equivalently, $\mathcal{F}(\mathcal{G})$ is a tree).

Notice that the above notion of a hypertree coincides with *Berge-acyclicity* [2].

Assumption 7 (tree-clusters) Let $\{\mathcal{G}_r\}_{r=1}^p$ be a partition satisfying Def. 3; every induced factor graph \mathcal{F}_r is a tree (Singleton clusters $\mathcal{E}_r = \emptyset$ allowed).

Assumption 7 requires that, within each subgraph \mathcal{G}_r , the variable-factor incidence structure is acyclic—see Fig. 6.(b). In Sec. 5.1 we leverage this tree structure to construct min-sum message passing within \mathcal{F}_r yielding finite-round cost-to-go messages for the cluster subproblem. In Sec. 5.2 we will remove Assumption 7 and introduce a hyperedge-splitting construction to handle cycle-rich hypergraphs where such tree partitions may not exist or yield too large clusters/hyperedges.

5.1 Algorithm design for acyclic factor graph-partitioning

Fix a hypertree partition $\{\mathcal{G}_r = (\mathcal{C}_r, \mathcal{E}_r)\}_{r=1}^p$. In analogy with the pairwise case, we separate inter- and intra-cluster interactions, but now in the factor-graph sense. Specifically, we confine min-sum message passing to the intra-cluster factor trees \mathcal{F}_r , so that couplings *within* clusters are aggregated into local cost-to-go messages entering the agents’ subproblems. Couplings *across* clusters are mediated through the *condensed factor graph* \mathcal{F}_C : each inter-cluster factor $\omega \in \mathcal{E}_{\text{out}}$ is incident to the supernodes \mathbf{c}_r it intersects through the incidences $(\mathbf{c}_r, \omega) \in \mathcal{A}_C$, and its contribution is handled in a Jacobi fashion using the most recently out-of-cluster variables.

More formally, for any intra-cluster incidence $(i, \omega) \in \mathcal{A}_r$ (i.e., $\omega \in \mathcal{N}_i^{\text{in}}$), define variable-to-factor and factor-to-variable messages by

$$\mu_{i \rightarrow \omega}^*(x_i) := \phi_i(x_i) + \sum_{\omega' \in \mathcal{N}_i^{\text{in}} \setminus \{\omega\}} \mu_{\omega' \rightarrow i}^*(x_i) + \sum_{\omega' \in \mathcal{N}_i^{\text{out}}} \psi_{\omega'}(x_i, x_{\omega' \setminus \{i\}}^*), \quad (57a)$$

$$\mu_{\omega \rightarrow i}^*(x_i) := \min_{x_{\omega \setminus i}} \left\{ \psi_{\omega}(x_i, x_{\omega \setminus \{i\}}) + \sum_{j \in \omega \setminus \{i\}} \mu_{j \rightarrow \omega}^*(x_j) \right\}, \quad \omega \in \mathcal{N}_i^{\text{in}}. \quad (57\text{b})$$

Then, any solution \mathbf{x}^* of (P') satisfies the cluster-wise optimality decomposition:

$$x_i^* \in \operatorname{argmin}_{x_i} \phi_i(x_i) + \underbrace{\sum_{\omega \in \mathcal{N}_i^{\text{in}}} \mu_{\omega \rightarrow i}^*(x_i)}_{:= \mu_{\mathcal{N}_i^{\text{in}} \rightarrow i}^*(x_i)} + \underbrace{\sum_{\omega \in \mathcal{N}_i^{\text{out}}} \psi_{\omega}(x_i, x_{\omega \setminus \{i\}}^*)}_{:= \mu_{\mathcal{N}_i^{\text{out}} \rightarrow i}^*(x_i)}, \quad i \in \mathcal{C}_r, r \in [p]. \quad (58)$$

Here, $\mu_{\mathcal{N}_i^{\text{in}} \rightarrow i}^*$ is the (factor-to-variable) *cost-to-go* term induced by min-sum on the tree factor graph \mathcal{F}_r , summarizing all interactions *within* \mathcal{C}_r as seen from node i . In contrast, $\mu_{\mathcal{N}_i^{\text{out}} \rightarrow i}^*$ is the *external coupling contribution* collecting all cross-cluster factors $\psi_{\omega}(x_i, x_{\omega \setminus \{i\}}^*)$ incident to i .

We now eliminate the explicit variable→factor messages by substituting (57a) (with i replaced by j) into (57b). This gives, for every $\omega \in \mathcal{E}_r$ and $i \in \omega$,

$$\begin{aligned} \mu_{\omega \rightarrow i}^*(x_i) &= \min_{x_{\omega \setminus \{i\}}} \left\{ \psi_{\omega}(x_i, x_{\omega \setminus \{i\}}) \right. \\ &\quad \left. + \sum_{j \in \omega \setminus \{i\}} \underbrace{\left(\phi_j(x_j) + \sum_{\omega' \in \mathcal{N}_j^{\text{in}} \setminus \{\omega\}} \mu_{\omega' \rightarrow j}^*(x_j) + \sum_{\omega' \in \mathcal{N}_j^{\text{out}}} \psi_{\omega'}(x_j, x_{\omega' \setminus \{j\}}^*) \right)}_{\text{aggregate variable-side cost}} \right\}. \end{aligned} \quad (59)$$

Equation (59) is nothing but the factor-to-variable min-sum update in which each neighbor $j \in \omega \setminus \{i\}$ contributes through its *aggregated variable-side cost*.

The proposed decentralized algorithm—Algorithm 3—is obtained by iterating the fixed-point system (58)–(59) in the variables $\{x_i^*\}$ and intra-cluster messages $\{\mu_{\omega \rightarrow i}^*\}_{(\omega, i) \in \mathcal{A}_r}$, using the same two design principles as in the pairwise MP-Jacobi: (i) the unknown out-of-cluster variables $x_{\omega \setminus \{i\}}^*$ are replaced by the most recently available values $x_{\omega \setminus \{i\}}^\nu$ (Jacobi correction); and (ii) the unknown fixed-point messages $\mu_{\omega' \rightarrow j}^*$ in (59) are replaced by the current iterates $\mu_{\omega' \rightarrow j}^\nu$, yielding one min-sum step within each intra-cluster factor tree \mathcal{F}_r .

Practical implementation of Step (2). In standard message passing, factor nodes are generally not physical computing entities. To implement Step (2) of Algorithm 3 in a single-hop manner, we propose the following two implementations, both realizing the same recursion (61), accommodating different practical settings.

• **option I (no factor processors: hosted factors).** If factors are *logical* and only agents can compute/communicate, then each intra-cluster factor $\omega \in \mathcal{E}_r$ is assigned to a host agent $h(\omega) \in \omega$ (e.g., the smallest index in ω). Each incident agent $j \in \omega$ locally forms the *variable-side aggregate* $\mu_{j \rightarrow \omega}^\nu(\cdot)$ defined in (61), and sends it (one hop within the hyperedge scope) to the host $h(\omega)$. The host emulates the factor computation by evaluating (61) to obtain $\{\mu_{\omega \rightarrow i}^{\nu+1}(\cdot)\}_{i \in \omega}$, and then broadcasts these messages back to all $i \in \omega$. This avoids any cluster-level coordinator while preserving single-hop communication within each hyperedge.

• **option II (factor processors / edge servers).** Assume instead that each factor ω is a computational unit (e.g., an “edge server”) that stores ψ_{ω} and can communicate with all incident agents $j \in \omega$. Then Step (2) is executed directly

Algorithm 3: Hypergraph-Message Passing-Jacobi (H-MP-Jacobi)

Initialization: $x_i^0 \in \mathbb{R}^d$ for all $i \in \mathcal{V}$; initialize $\mu_{\omega \rightarrow i}^0(\cdot)$ and $\mu_{i \rightarrow \omega}^0(\cdot)$ (e.g., $\equiv 0$) for all $i \in \omega$ and $\omega \in \mathcal{E}_r$.

for $\nu = 0, 1, 2, \dots$ **do**

; // (1) Jacobi-style variable update (parallel over $i \in \mathcal{V}$)

each agent $i \in \mathcal{V}$ in parallel:

$$\hat{x}_i^{\nu+1} \in \operatorname{argmin}_{x_i} \left\{ \phi_i(x_i) + \sum_{\omega \in \mathcal{N}_i^{\text{in}}} \mu_{\omega \rightarrow i}^\nu(x_i) + \sum_{\omega \in \mathcal{N}_i^{\text{out}}} \psi_\omega(x_i, x_{\omega \setminus \{i\}}) \right\}, \quad (60a)$$

$$x_i^{\nu+1} = x_i^\nu + \tau_r^\nu (\hat{x}_i^{\nu+1} - x_i^\nu). \quad (60b)$$

Sends $x_i^{\nu+1}$ to all inter-cluster factors $\omega \in \mathcal{N}_i^{\text{out}}$ (or to their implementation);

; // (2) One intra-cluster min-sum (parallel) round on each factor tree \mathcal{F}_r

foreach $r \in [p]$ **do**

foreach $\omega \in \mathcal{E}_r$ **do**

foreach $i \in \omega$ **do**

$$\mu_{\omega \rightarrow i}^{\nu+1}(x_i) = \min_{x_{\omega \setminus \{i\}}} \left\{ \psi_\omega(x_i, x_{\omega \setminus \{i\}}) \right.$$

$$\left. + \sum_{j \in \omega \setminus \{i\}} \left(\phi_j(x_j) + \underbrace{\sum_{\omega' \in \mathcal{N}_j^{\text{in}} \setminus \{\omega\}} \mu_{\omega' \rightarrow j}^\nu(x_j) + \sum_{\omega' \in \mathcal{N}_j^{\text{out}}} \psi_{\omega'}(x_j, x_{\omega' \setminus \{j\}})}_{:= \mu_{j \rightarrow \omega}^\nu(x_j)} \right) \right\}. \quad (61)$$

Send $\mu_{\omega \rightarrow i}^{\nu+1}(\cdot)$ to all $i \in \omega$.

at the factor: each agent $j \in \omega$ sends to ω the same local quantity $\mu_{j \rightarrow \omega}^\nu(\cdot)$. Upon collecting $\{\mu_{j \rightarrow \omega}^\nu(\cdot)\}_{j \in \omega}$, the factor evaluates (61) to compute $\{\mu_{\omega \rightarrow i}^{\nu+1}(\cdot)\}_{i \in \omega}$ and broadcasts them back to the incident agents. In this model, no hosted-factor mechanism is needed: the factor nodes perform the partial minimizations natively.

When all $|\omega| = 2$ (pairwise case), identifying $\mu_{i \rightarrow j}(\cdot) \equiv \mu_{\{i, j\} \rightarrow j}(\cdot)$ reduce both implementation models above to the edge-message updates in Algorithm 1.

We remark that, as in Sec. 4, surrogate constructions can be incorporated to reduce *both* computation and communication costs. Concretely, one may replace the exact intra-cluster min-sum updates in Step (2)-i.e., the factor-to-variable recursion (61) (and, in implementations that materialize them, the corresponding variable-to-factor aggregates implicit in (61))—with surrogate message maps that admit *finite-dimensional* parametrizations. In this way, each incidence (i, ω) exchanges only a lightweight summary (e.g., vectors or structured statistics such as sparse/low-rank matrices) instead of a functional message. When further savings are needed, the same surrogate principle can be applied to the Jacobi subproblem (60a), yielding an inexact/local-model update while preserving the overall decentralized architecture and the cost-rate trade-offs discussed in Sec. 4.

5.1.1 Convergence Analysis

We establish convergence of Algorithm 3 under the following assumptions.

Assumption 8 *The factor graph $\mathcal{F}(\mathcal{G})$ associated with $\mathcal{G} = (\mathcal{V}, \mathcal{E})$ is connected. Moreover, communications are incidence-local: for every (i, ω) with $i \in \omega$, agent i can exchange information with the computing entity implementing factor ω .*

Assumption 9 *Given the partition $\{\mathcal{G}_r = (\mathcal{C}_r, \mathcal{E}_r)\}_{r=1}^p$ satisfying Def. 3, every cross-cluster factor intersects any cluster in at most one node, i.e.,*

$$|\omega \cap \mathcal{C}_r| \leq 1, \quad \forall \omega \in \mathcal{E}_{\text{out}}, \forall r \in [p]. \quad (62)$$

Assumption 9 is not essential for convergence, but it simplifies the delayed block-Jacobi reformulation, which is given below (the proof is omitted).

Proposition 3 *Postulate Assumptions 7 and 8. Then, Algorithm 3 can be rewritten in the equivalent form: for any $i \in \mathcal{C}_r$ and $r \in [p]$,*

$$x_i^{\nu+1} = x_i^\nu + \tau_r^\nu (\hat{x}_i^{\nu+1} - x_i^\nu), \quad (63a)$$

$$\hat{x}_i^{\nu+1} \in \operatorname{argmin}_{x_i} \min_{x_{\mathcal{C}_r \setminus \{i\}}} \left\{ \sum_{i \in \mathcal{C}_r} \phi_i(x_i) + \sum_{\omega \in \mathcal{E}_r} \psi_\omega(x_\omega) + \sum_{j \in \mathcal{C}_r, \omega \in \mathcal{N}_j^{\text{out}}} \psi_\omega(x_j, x_{\omega \setminus \{j\}}^{\nu - d(i,j)}) \right\}. \quad (63b)$$

If, in addition, Assumption 9 holds, (63b) reduces to the following block-Jacobi update with delays:

$$\hat{x}_i^{\nu+1} \in \operatorname{argmin}_{x_i} \min_{x_{\mathcal{C}_r \setminus \{i\}}} \Phi(x_{\mathcal{C}_r}, x_{\bar{\mathcal{C}}_r}^{\nu - \mathbf{d}_i}), \quad (64)$$

where $\mathbf{d}_i \in \mathbb{N}^{|\bar{\mathcal{C}}_r|}$ is defined as

$$(\mathbf{d}_i)_k := \begin{cases} d(i, j_k), & k \in \mathcal{N}_{\mathcal{C}_r}, \\ 0, & k \in \bar{\mathcal{C}}_r \setminus \mathcal{N}_{\mathcal{C}_r}, \end{cases}$$

and $j_k \in \mathcal{B}_r$ is the unique node such that there exists a hyperedge $\omega \in \mathcal{N}_{j_k}^{\text{out}}$ with $k \in \omega \cap \mathcal{N}_{\mathcal{C}_r}$. It holds $\|\mathbf{d}_i\|_\infty \leq \text{diam}(\mathcal{F}_r)/2$, for all $i \in \mathcal{C}_r$.

Under Assumption 9, (64) reduces to a block-Jacobi scheme with bounded delays; hence, Theorem 1 applies. We omit the (essentially identical) details.

5.2 Hyperedge (factor) splitting via surrogation

In this section we address *cycle-rich* hypergraphs, where many factors overlap on multiple variable-nodes. If many pairs of distinct hyperedges $\omega, \omega' \in \mathcal{E}$ satisfy $|\omega \cap \omega'| \geq 2$, then $\mathcal{F}(\mathcal{G})$ is cycle-rich (with short alternating cycles), which may preclude a nontrivial partition into multi-factor hypertree clusters; see Fig. 7.

We handle these hypergraphs via *hyperedge (factor) splitting and surrogation*. First, we perform a combinatorial splitting of hyperedges, replacing each $\omega \in \mathcal{E}$ by component supports $\mathcal{S}(\omega) \subseteq 2^\omega$ and forming the expanded split set $\tilde{\mathcal{E}}$ (hence the split factor graph $\mathcal{F}(\tilde{\mathcal{G}})$). The split is chosen so that, after selecting intra-cluster split hyperedges $\tilde{\mathcal{E}}_r$, each induced split factor graph $\tilde{\mathcal{F}}_r = \mathcal{F}(\mathcal{C}_r, \tilde{\mathcal{E}}_r)$ is a tree. Second, we construct *surrogate split factors* consistent with this split incidence structure by replacing each original heavily-overlapping factor $\psi_\omega(x_\omega)$ with a sum of lower-arity component factors indexed by $\tilde{\omega} \in \mathcal{S}(\omega)$, where the removed variables

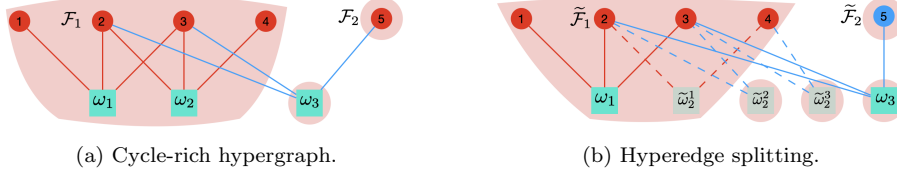


Fig. 7: (a) The cluster $\mathcal{C}_1 = \{1, 2, 3, 4\}$ contains $\omega_1 = \{1, 2, 3\}$ and $\omega_2 = \{2, 3, 4\}$ with overlap $\omega_1 \cap \omega_2 = \{2, 3\}$. Hence the induced factor graph \mathcal{F}_1 contains a cycle. (b) Hyperedge splitting replaces ω_2 with lower-arity component factors $\{\tilde{\omega}_2^1, \tilde{\omega}_2^2, \tilde{\omega}_2^3\}$ (light square nodes). Keeping only $\tilde{\omega}_2^1$ as an intra-cluster component yields $\tilde{\mathcal{E}}_1 = \{\omega_1, \tilde{\omega}_2^1\}$, for which the induced factor graph $\tilde{\mathcal{F}}_1$ becomes a tree.

$x_{\omega \setminus \tilde{\omega}}$ are frozen at reference values (taken as the latest iterates). This produces tree-structured intra-cluster couplings on which min-sum terminates in finite time.

More formally, the construction proceeds in the following three steps.

- **Step 1: Combinatorial splitting rule.** Given the hypergraph $\mathcal{G} = (\mathcal{V}, \mathcal{E})$, a *hyperedge-splitting rule* is specified by a set-valued map

$$\mathcal{S} : \mathcal{E} \rightrightarrows 2^{\mathcal{V}}, \quad \omega \mapsto \mathcal{S}(\omega) \subseteq 2^{\omega}, \quad (65)$$

where each $\tilde{\omega} \in \mathcal{S}(\omega)$ is a *component hyperedge* supported on a subset of ω . Collecting all components yields the expanded factor set

$$\tilde{\mathcal{E}} := \bigcup_{\omega \in \mathcal{E}} \mathcal{S}(\omega), \quad (66)$$

and the corresponding *split hypergraph* $\tilde{\mathcal{G}} := (\mathcal{V}, \tilde{\mathcal{E}})$, with factor graph $\mathcal{F}(\tilde{\mathcal{G}})$.

To avoid duplicated component supports, we make the following assumption.

Assumption 10 (unique-parent splitting) *The splitting map \mathcal{S} satisfies*

$$\mathcal{S}(\omega) \cap \mathcal{S}(\omega') = \emptyset, \quad \forall \omega \neq \omega' \in \mathcal{E}.$$

Under Assumption 10, for every $\tilde{\omega} \in \tilde{\mathcal{E}}$ there exists a unique $\omega \in \mathcal{E}$ such that $\tilde{\omega} \in \mathcal{S}(\omega)$; we denote this parent by $\text{par}(\tilde{\omega}) := \omega$.

We remark that Assumption 10 is not a restriction: it ensures solely that each component hyperedge admits a unique parent. The same effect can be obtained without this assumption, at the cost of heavier notation, by defining the expanded split factor set as a *disjoint union* (so that each $\tilde{\omega} \in \tilde{\mathcal{E}}$ carries its parent label).

- **Step 2: Hypertree clustering of the split factor graph $\mathcal{F}(\tilde{\mathcal{G}})$.** Given a node partition $\mathcal{V} = \bigcup_{r=1}^p \mathcal{C}_r$, we select, within each cluster, a subset of split hyperedges to be treated intra-cluster; all remaining split hyperedges are treated as inter-cluster. This is captured by the following analogue of Assumption 7.

Assumption 11 (Hypertree clusters of $\mathcal{F}(\tilde{\mathcal{G}})$) *Given a node partition $\mathcal{V} = \bigcup_{r=1}^p \mathcal{C}_r$, choose intra-cluster split hyperedges*

$$\tilde{\mathcal{E}}_r \subseteq \{\tilde{\omega} \in \tilde{\mathcal{E}} : \tilde{\omega} \subseteq \mathcal{C}_r\}, \quad r \in [p],$$

and define $\tilde{\mathcal{G}}_r := (\mathcal{C}_r, \tilde{\mathcal{E}}_r)$ with induced split factor graph $\tilde{\mathcal{F}}_r := \mathcal{F}(\tilde{\mathcal{G}}_r)$. Each $\tilde{\mathcal{F}}_r$ is a tree (singleton clusters allowed).

Unlike Def. 3, intra-cluster maximality is not required: within each cluster \mathcal{C}_r , one may keep only a subset $\tilde{\mathcal{E}}_r$ of the split components (possibly discarding some $\tilde{\omega} \subseteq \mathcal{C}_r$) so that the induced split factor graph $\tilde{\mathcal{F}}_r$ is acyclic. The discarded components are treated as inter-cluster and capture cross-cluster couplings through the corresponding condensed factor graph (defined as in Def. 3, replacing \mathcal{E} by $\tilde{\mathcal{E}}$).

• **Step 3: Surrogate split factors (freezing removed coordinates).** Splitting modifies only the *supports* of factors. To obtain an optimization method for the original problem (P), we associate to each parent factor ψ_ω a family of *surrogate component factors* supported on $\{\tilde{\omega} \in \mathcal{S}(\omega)\}$. The key idea is to freeze the coordinates removed by splitting at reference values.

Formally, for $\tilde{\omega} \in \tilde{\mathcal{E}}$, let $\omega := \text{par}(\tilde{\omega})$ and interpret $\omega \setminus \tilde{\omega}$ as the set of frozen coordinates. For a reference vector $y_{\omega \setminus \tilde{\omega}}$, introduce a component surrogate

$$\tilde{\psi}_{\tilde{\omega}}(x_{\tilde{\omega}}; y_{\omega \setminus \tilde{\omega}}),$$

which depends only on the active variables $x_{\tilde{\omega}}$ and on the frozen reference values. In the algorithm, $y_{\omega \setminus \tilde{\omega}}$ will be set to latest iterates (Jacobi-style), i.e., $y_{\omega \setminus \tilde{\omega}} = x_{\omega \setminus \tilde{\omega}}^\nu$.

Collecting all components over all parents defines the split-surrogate objective on $\tilde{\mathcal{E}}$: for any given reference vector \mathbf{y} , let

$$\tilde{\Phi}(\mathbf{x}; \mathbf{y}) := \sum_{i \in \mathcal{V}} \phi_i(x_i) + \sum_{\tilde{\omega} \in \tilde{\mathcal{E}}} \tilde{\psi}_{\tilde{\omega}}(x_{\tilde{\omega}}; y_{\text{par}(\tilde{\omega}) \setminus \tilde{\omega}}). \quad (67)$$

The constructions above decouples the *graph design* (splitting/hypertree selection) from the *analytic design* (choosing $\tilde{\psi}_{\tilde{\omega}}$). For consistency with (P), $\tilde{\Phi}(\cdot; \mathbf{y})$ shall satisfy the following regularity condition.

Assumption 12 [split-surrogate regularity] For each parent $\omega \in \mathcal{E}$ and each $i \in \omega$, choosing references consistently, $y_{\omega \setminus \tilde{\omega}} = x_{\omega \setminus \tilde{\omega}}$, yields

$$\sum_{\substack{\tilde{\omega} \in \mathcal{S}(\omega): \\ i \in \tilde{\omega}}} \nabla_{x_i} \tilde{\psi}_{\tilde{\omega}}(x_{\tilde{\omega}}; x_{\omega \setminus \tilde{\omega}}) = \nabla_{x_i} \psi_\omega(x_\omega), \quad \forall x_\omega.$$

In fact, split-surrogate regularity preserves the critical points of Φ when the reference variables are chosen consistently, which underpins the algorithmic design.

Proposition 4 Under Assumption 12, any $\bar{\mathbf{x}}$ satisfying $\nabla_x \tilde{\Phi}(\bar{\mathbf{x}}; \bar{\mathbf{x}}) = 0$ is a critical point of Φ , i.e., $\nabla \Phi(\bar{\mathbf{x}}) = 0$.

Example: We illustrate the splitting/surrogate rule (satisfying Assumption 12) on the following concrete example. Consider $\Phi(\mathbf{x}) = \sum_{i=1}^5 \phi_i(x_i) + \psi_{123}(x_1, x_2, x_3) + \psi_{234}(x_2, x_3, x_4) + \psi_{235}(x_2, x_3, x_5)$, whose corresponding factor graph is shown in Fig. 7(a). We split the factor $\omega_2 = \{2, 3, 4\}$ and keep all other factors unchanged. Consider the following valid splitting choices for ω_2 :

(i) *Pairwise split*: $\mathcal{S}(\omega_2) = \{\{2, 4\}, \{2, 3\}, \{3, 4\}\}$, and split-surrogate given by

$$\frac{1}{2} \psi_{234}(x_3, x_4) + \frac{1}{2} \psi_{234}(x_2, y_3^2, x_4) + \frac{1}{2} \psi_{234}(x_2, x_3, y_4^3). \quad (68)$$

(ii) *Two-component split*: $\mathcal{S}(\omega_2) = \{\{2, 3\}, \{3, 4\}\}$, and split-surrogate given by

$$\left(\psi_{234}(x_2, x_3, y_4^1) - \frac{1}{2} \psi_{234}(y_2^1, x_3, y_4^1) \right) + \left(\psi_{234}(y_2^2, x_3, x_4) - \frac{1}{2} \psi_{234}(y_2^2, x_3, y_4^2) \right). \quad (69)$$

(iii) *Singleton split*: $\mathcal{S}(\omega_2) = \{\{2\}, \{3\}, \{4\}\}$, and split-surrogate given by

$$\psi_{234}(x_2, y_3^1, y_4^1) + \psi_{234}(y_2^2, x_3, y_4^2) + \psi_{234}(y_2^3, y_3^3, x_4). \quad (70)$$

Fig. 7(b) depicts the pairwise split in (i), where $\mathcal{S}(\omega_2) = \{\tilde{\omega}_2^1, \tilde{\omega}_2^2, \tilde{\omega}_2^3\}$, with $\tilde{\omega}_2^1 = \{2, 4\}$, $\tilde{\omega}_2^2 = \{2, 3\}$, and $\tilde{\omega}_2^3 = \{3, 4\}$.

5.3 Algorithm design

The proposed decentralized algorithm is formally stated in Algorithm 4. It parallels Algorithm 3, with the original hypergraph replaced by the split hypergraph $\tilde{\mathcal{G}} = (\mathcal{V}, \tilde{\mathcal{E}})$ and message passing carried out only on the selected tree components $\{\tilde{\mathcal{E}}_r\}_{r=1}^p$. Compared with Algorithm 3, the additional arguments $x_{\text{par}(\tilde{\omega}) \setminus \tilde{\omega}}^\nu$ in $\tilde{\psi}_{\text{par}(\tilde{\omega})}$ encode the reference coordinates introduced by splitting and are instantiated by available iterates. When \mathcal{S} is the identity map, i.e., $\mathcal{S}(\omega) = \{\omega\}$ for all $\omega \in \mathcal{E}$ (so $\tilde{\mathcal{E}} = \mathcal{E}$ and $\tilde{\psi}_{\text{par}(\omega)} \equiv \psi_\omega$), Algorithm 4 reduces to Algorithm 3.

Algorithm 4: H-MP-Jacobi with Hyperedge Splitting

```

Initialization:  $x_i^0 \in \mathbb{R}^d$  for all  $i \in \mathcal{V}$ ; initialize  $\mu_{\tilde{\omega} \rightarrow i}^0(\cdot)$  (e.g.,  $\equiv 0$ ) for all  $r \in [p]$ ,  $\tilde{\omega} \in \tilde{\mathcal{E}}_r$ , and  $i \in \tilde{\omega}$ .
for  $\nu = 0, 1, 2, \dots$  do
    ; // (1) Jacobi-style variable update (parallel over  $i \in \mathcal{V}$ )
    each agent  $i \in \mathcal{V}$  in parallel:
        
$$\hat{x}_i^{\nu+1} \in \underset{x_i}{\text{argmin}} \left\{ \phi_i(x_i) + \sum_{\tilde{\omega} \in \tilde{\mathcal{N}}_i^{\text{in}}} \mu_{\tilde{\omega} \rightarrow i}^\nu(x_i) + \sum_{\tilde{\omega} \in \tilde{\mathcal{N}}_i^{\text{out}}} \tilde{\psi}_{\text{par}(\tilde{\omega})}(x_i, x_{\tilde{\omega} \setminus \{i\}}^\nu; x_{\text{par}(\tilde{\omega}) \setminus \tilde{\omega}}^\nu) \right\}, \quad (71a)$$

        
$$x_i^{\nu+1} = x_i^\nu + \tau_r^\nu (\hat{x}_i^{\nu+1} - x_i^\nu). \quad (71b)$$

        Sends  $x_i^{\nu+1}$  to all inter-cluster components  $\tilde{\omega} \in \tilde{\mathcal{N}}_i^{\text{out}}$  (or to their implementation);
    ; // (2) One intra-cluster min-sum (parallel) round on each split factor tree  $\tilde{\mathcal{F}}_r$ 
    foreach  $r \in [p]$  do
        foreach  $\tilde{\omega} \in \tilde{\mathcal{E}}_r$  do
            foreach  $i \in \tilde{\omega}$  do
                
$$\mu_{\tilde{\omega} \rightarrow i}^{\nu+1}(x_i) = \min_{x_{\tilde{\omega} \setminus \{i\}}} \left\{ \tilde{\psi}_{\text{par}(\tilde{\omega})}(x_i, x_{\tilde{\omega} \setminus \{i\}}^\nu; x_{\text{par}(\tilde{\omega}) \setminus \tilde{\omega}}^\nu) \right. \\ \left. + \sum_{j \in \tilde{\omega} \setminus \{i\}} \left( \phi_j(x_j) + \sum_{\tilde{\omega}' \in \tilde{\mathcal{N}}_j^{\text{in}} \setminus \{\tilde{\omega}\}} \mu_{\tilde{\omega}' \rightarrow j}^\nu(x_j) \right) + \sum_{\tilde{\omega}' \in \tilde{\mathcal{N}}_j^{\text{out}}} \tilde{\psi}_{\text{par}(\tilde{\omega}')} (x_j, x_{\tilde{\omega}' \setminus \{j\}}^\nu; x_{\text{par}(\tilde{\omega}') \setminus \tilde{\omega}'}^\nu) \right\}. \quad (72)$$

            Send  $\mu_{\tilde{\omega} \rightarrow i}^{\nu+1}(\cdot)$  to all  $i \in \tilde{\omega}$ .

```

As Algorithm 3, Algorithm 4 admits a delayed block-Jacobi representation.

Proposition 5 *Postulate Assumptions 8 and 11. Then, Algorithm 4 can be rewritten in the equivalent form: for any $i \in \mathcal{C}_r$ and $r \in [p]$,*

$$x_i^{\nu+1} = x_i^\nu + \tau_r^\nu (\hat{x}_i^{\nu+1} - x_i^\nu), \quad (73a)$$

$$\hat{x}_i^{\nu+1} \in \operatorname{argmin}_{x_i} \min_{x_{\mathcal{C}_r \setminus \{i\}}} \left\{ \begin{array}{l} \sum_{i \in \mathcal{C}_r} \phi_i(x_i) + \sum_{\tilde{\omega} \in \tilde{\mathcal{E}}_r} \tilde{\psi}_{\operatorname{par}(\tilde{\omega})} \left(x_{\tilde{\omega}}; x_{\operatorname{par}(\tilde{\omega}) \setminus \tilde{\omega}}^{\nu-d(i, \tilde{\omega})-1} \right) \\ + \sum_{j \in \mathcal{C}_r, \tilde{\omega} \in \tilde{\mathcal{N}}_j^{\text{out}}} \tilde{\psi}_{\operatorname{par}(\tilde{\omega})} \left(x_j, x_{\operatorname{par}(\tilde{\omega}) \setminus \{j\}}^{\nu-d(i, j)}; x_{\operatorname{par}(\tilde{\omega}) \setminus \{j\}}^{\nu-d(i, j)} \right) \end{array} \right\}, \quad (73b)$$

where $d(\cdot, \cdot)$ denotes variable-to-variable or variable-to-factor distance in $\tilde{\mathcal{G}}_r$.

Proposition 5 enables a convergence analysis of Algorithm 4 via essentially the same arguments as in Sec. 4. In particular, within the surrogate-regularity framework of Sec. 4.1, if the *aggregate objectives* in (73b)—the cluster-relevant portion of the split-surrogate objective (67) (playing, for $\tilde{\Phi}$, the same role that (42) plays for Φ)—are *uniformly strongly convex* in the cluster variables, uniformly over the frozen arguments, then Algorithm 4 inherits the same rate guarantees as Algorithm 3: linear convergence for strongly convex Φ , and sublinear rates for merely convex or nonconvex Φ ; see Theorem 2, 3, and 4. When the objectives in (73b) are nonconvex, the surrogate machinery can be used to ensure that the local minimizations in (71a) and (72) are well posed, and the same convergence rate conclusions (linear for strongly convex Φ , sublinear for merely convex or nonconvex Φ) follow under the standard assumptions of Sec. 4.1. We omit the technical details.

6 Numerical experiments

In this section, we evaluate our algorithms MP-Jacobi and its surrogate variants solving convex quadratic programs (and decentralized optimization) defined over pairwise graphs (Sec. 6.1 and Sec. 6.2) and hypergraphs (Sec. 6.3). All simulations are conducted in MATLAB R2025a on a Windows desktop equipped with an 8-core AMD Ryzen 7 5700G (3.80 GHz) and 64 GB of RAM.

6.1 Convex quadratic programs (pairwise graph)

We consider a convex quadratic instance of (P') with local and pairwise terms $\phi_i(x_i) = \frac{1}{2} \langle H_{ii} x_i, x_i \rangle + \langle b_i, x_i \rangle$ and $\psi_{ij}(x_i, x_j) = \langle H_{ij} x_j, x_i \rangle$. The global matrix \mathbf{H} is generated as follows: each block H_{ii}^{tmp} and H_{ij}^{tmp} is drawn with i.i.d. Gaussian entries $\mathcal{N}(0, 1)$ and then symmetrized via $\bar{\mathbf{H}}^{\text{tmp}} = \frac{1}{2}(H^{\text{tmp}} + (H^{\text{tmp}})^T)$. We set $\mathbf{H} = \bar{\mathbf{H}}^{\text{tmp}} + c\mathbf{I}$, where the scalar c is chosen so that $\kappa(\mathbf{H}) = 400$. The vector \mathbf{b} is generated with i.i.d. Gaussian entries $\mathcal{N}(0, 1)$.

We compare MP-Jacobi and surrogate MP-Jacobi against centralized block Jacobi (BJac), standard Jacobi (Jac), and gradient descent (GD), over three different graphs, as showed in Fig. 8(c). Intra-cluster edges are shown in red in the same panels. For the surrogate variant, surrogation is applied only to the message update: ϕ_i is a first-order linearization plus a proximal term, and ψ_{ij} is chosen as in Sec. 4.2(ii), with $M_{ij} = \operatorname{Diag}(H_{ij})$ and $M_i = M_j = 0$. Stepsizes are manually tuned and individually for each method, to achieve the best practical convergence.

Fig. 8(a) (resp. Fig. 8(b)) plots the optimality gap $\|\mathbf{x}^\nu - \mathbf{x}^*\|$ versus the iterations ν (resp. communications). The proposed MP-Jacobi and surrogate MP-Jacobi converge significantly faster than GD, and are competitive with Jacobi-type baselines. In particular, MP-Jacobi is close to centralized BJac and consistently

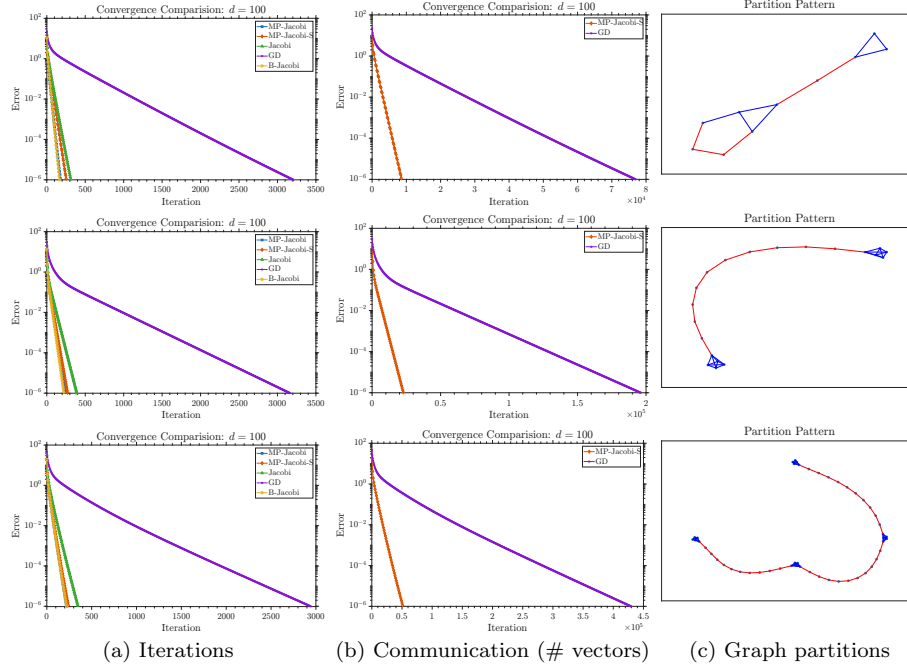


Fig. 8: Strongly convex quadratic problem: MP-Jacobi, MP-Jacobi with surrogate (MP-Jacobi-S), Gradient Descent (GD), and Block centralized Jacobi (B-Jacobi).

faster than Jac. Since BJac is not directly implementable in a fully decentralized setting, this highlights that intra-cluster message passing effectively recovers much of the benefit of centralized block coordination. Surrogate MP-Jacobi achieves similar convergence behavior with substantially reduced communication, since incidences exchange compact surrogate summaries of full functional messages.

We evaluate scalability on a ring graph. Let $m = (D+1)\lceil D^{3/2} \rceil$ and increase D progressively. We compare two clustering strategies. *Partition 1* uses two clusters: one cluster is a long path (tree) of length $\lceil m^{2/3} \rceil$, and the other is a single node. *Partition 2* uses $\lceil D^{3/2} \rceil$ clusters, each a path tree of length $D = \Theta(m^{2/5})$; see the Fig. 9(b). Our theory predicts that Partition 2 yields better scalability in m than Partition 1, and Fig. 9 corroborates this prediction numerically.

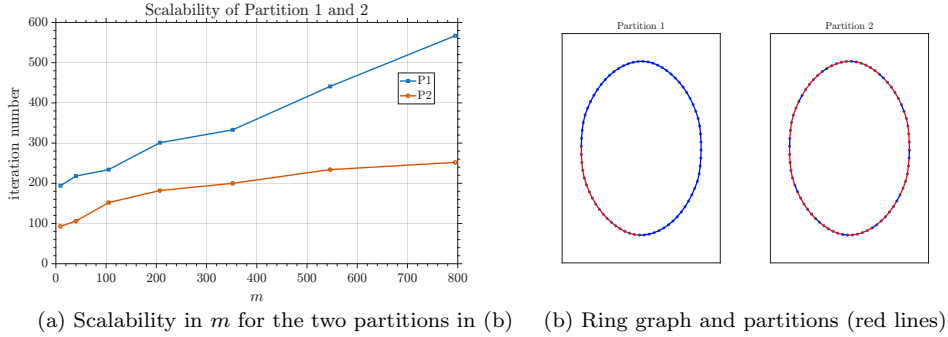
We finally remark that our method is provably convergent on loopy graphs without requiring diagonal dominance. In contrast, classical min-sum/message passing may fail in this regime; Fig. 10 shows a clear example.

6.2 Decentralized optimization (pairwise graph)

Consider the augmented formulation (5) associated with DGD-CTA. The objective in (5) can be written in the pairwise form (P') with local and coupling terms

$$\phi_i(x_i) = f_i(x_i) + \frac{1 - W_{ii}}{2\gamma} \|x_i\|^2, \quad \psi_{ij}(x_i, x_j) = -\frac{1}{\gamma} x_i^\top W_{ij} x_j. \quad (74)$$

We simulate quadratic functions f_i 's with matrices Q_{ii} generated by the MATLAB command: $B = \text{randn}(d, d); Qtmp = B' * B / m; Q_{ii} = Qtmp + c * \text{eye}(d)$; where c is



(a) Scalability in m for the two partitions in (b) (b) Ring graph and partitions (red lines)

Fig. 9: Strongly convex quadratic problem: scalability (# of iterations ν for $\|\mathbf{x}^\nu - \mathbf{x}^*\| \leq 10^{-3}$) in m under different tree-clustering strategies. *Partition 1* uses two clusters: one long tree (a path) and one singleton. *Partition 2* uses $m^{3/5}$ clusters, each a path of length $m^{2/5} - 1$ (i.e., $m^{2/5}$ nodes per cluster).

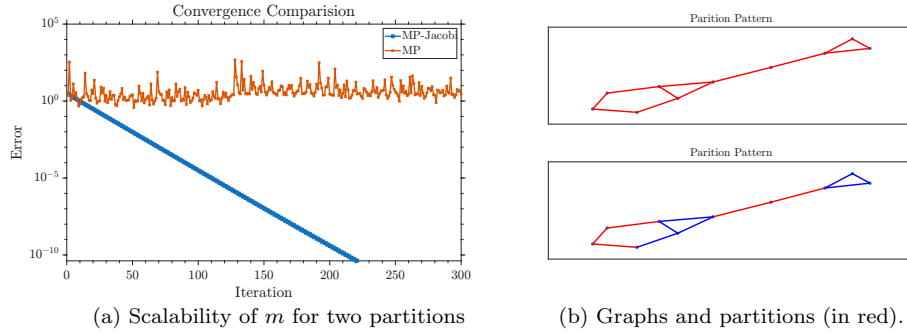


Fig. 10: Strongly convex quadratic problem on loopy graphs: min-sum splitting algorithm (MP) vs. the proposed MP-Jacobi. The min-sum splitting fails to converge on loopy graph without diagonal dominance of the objective function.

chosen such that global cost $\sum_{i=1}^m f_i(x_i)$ has condition number 100. We set $\gamma = 10^{-3}$, and W is the Metropolis weight matrix.

We compare MP-Jacobi and its surrogate variant (based on the partial linearization in (49)) against DGD-CTA [49], which is gradient descent applied to (5) with stepsize γ . The results are reported in Fig. 11. Panel (a) (resp. (b)) plots the optimality gap $\|\mathbf{x}^\nu - \mathbf{x}^*\|$ versus the iterations ν (resp. communications), while panel (c) reports the graphs and chosen partition patterns. Both MP-Jacobi and surrogate MP-Jacobi are markedly faster than DGD-CTA, with the advantage becoming pronounced on large-scale graphs (large m) and topologies with long “thin” structures (paths with large diameter). Moreover, the surrogate is essentially as effective as exact MP-Jacobi while significantly reducing per-iteration cost: incidences exchange only vectors (rather than functional messages), yielding substantial savings in communication. In terms of vector transmissions, surrogate MP-Jacobi is also consistently more communication-efficient than DGD-CTA.

To further assess scalability against existing decentralized schemes, we also consider the original consensus-based decentralized minimization $\min_{x \in \mathbb{R}^d} F(x) := \sum_{i=1}^m f_i(x)$, and solve it through its augmented CTA formulation (5), over an instance of the dumbbell graph (Fig. 12(b)). Here, F is strongly convex, quadratic.

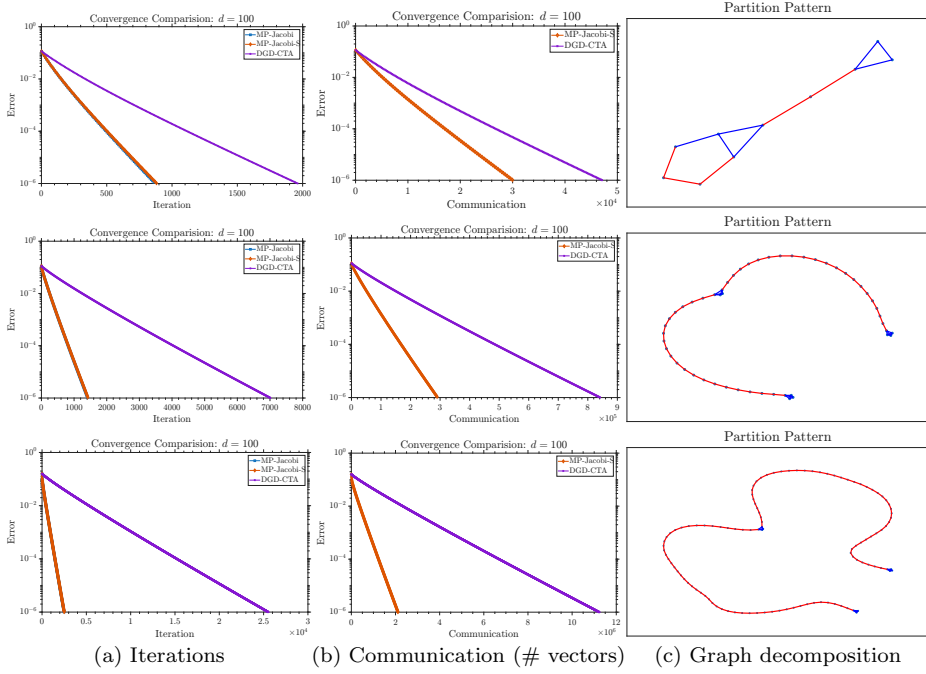


Fig. 11: Decentralized optimization in the CTA form (5): MP-Jacobi and MP-Jacobi with surrogate vs. DGD-CTA.

We simulate quadratic functions f_i 's with matrices Q_{ii} generated by the MATLAB command: $B = \text{randn}(d, d); Qtmp = B' * B/m; Q_ii = Qtmp + c * \text{eye}(d)$ with c chosen such that global cost $\sum_{i=1}^m f_i(x_i)$ has condition number 100. We fix W as the Metropolis matrix and tune γ in (5) so that the MP-Jacobi and its surrogate variant, run on this augmented problem, can achieve the same termination accuracy of existing decentralized methods minimizing directly $F(\mathbf{x})$. As representative of such methods, we simulated DGD-CTA, DGD-ATC, SONATA [39], DIGing [24], and EXTRA [36]. Let x^* be the minimizer of $F(\mathbf{x})$. All the algorithms are terminated when $\|\mathbf{x}^\nu - \mathbf{1} \otimes x^*\| / \sqrt{m} \leq 10^{-3}$, where \mathbf{x}^ν is the stacked vectors of the agents' iterates x_i^ν produced by the different algorithms.

Fig. 12(a) shows that the iteration counts of DGD-CTA and DGD-ATC grow most rapidly with m , indicating poor scalability. In contrast, MP-Jacobi and its surrogate variant exhibit the mildest dependence on m and remain consistently competitive, outperforming all baselines except EXTRA over the *full range* of values of m . While EXTRA is competitive for small networks, beyond $m \approx 100$, our methods require fewer iterations, with the advantage increasing with m .

6.3 Convex programs on hypergraphs

We report three experiments that highlight the behavior of H-MP-Jacobi and its surrogate variant H-MP-Jacobi-S solving strongly convex quadratic programs over the following hypergraphs: (i) hyper rings (no splitting); (ii) loopy hypergraphs (two hyperedge splitting strategies); and (iii) ATC-induced hypergraph (splitting).

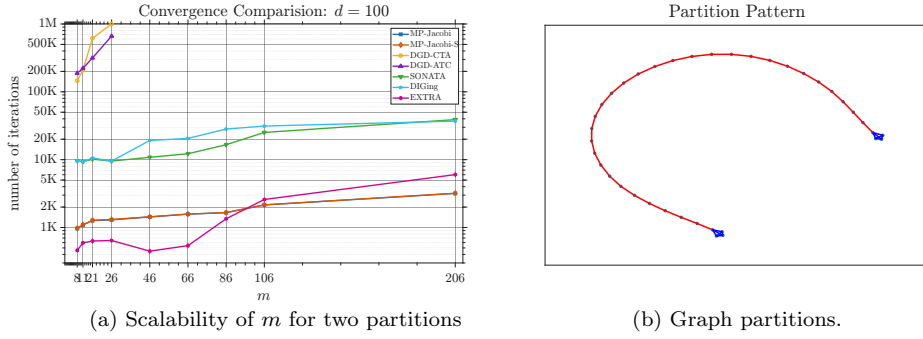


Fig. 12: Decentralized optimization $\min_x \in \mathbb{R}^d \sum_i f_i(x)$: (a) # iterations to 10^{-3} accuracy vs. m ; MP-Jacobi vs. a variety of decentralized algorithms. (b) dumbbell graph and graph partition (in red).

(i) Hyper rings (no splitting): Consider a strongly convex quadratic program on a *hyper ring*, where adjacent hyperedges overlap on (almost) one node—see Fig. 13(c). We test Algorithm 3 (H-MP-Jacobi) and its surrogate variant (H-MP-Jacobi-S). In H-MP-Jacobi-S, we apply a proximal-linear surrogate to the factor-to-variable message update (61), using the diagonal of the Hessian of the exact message, while keeping the variable update (60a) exact. As benchmark, we use the centralized GD (albeit not implementable on the hypergraph), as principled GD-type methods tailored to hypergraph couplings are not available. For clustering, we select one long path cluster containing $|\mathcal{E}| - 2$ hyperedges and all nodes incident to them, while assigning every remaining node to a singleton cluster—see Fig. 13(c). Fig. 13(a)-(b) reports the results. Both H-MP-Jacobi and H-MP-Jacobi-S converge markedly faster than GD, with the advantage increasing as $|\mathcal{E}|$ grows. Moreover, H-MP-Jacobi-S closely tracks H-MP-Jacobi, indicating that the surrogate preserves most of the performance while reducing per-iteration cost.

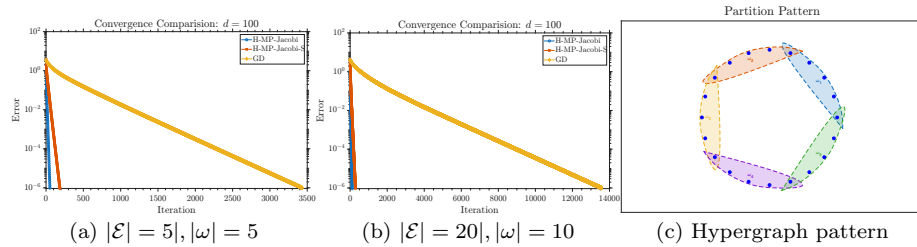


Fig. 13: Strongly convex QP over a hyperring: H-MP-Jacobi and H-MP-Jacobi-S.

(ii) Loopy hypergraphs (two hyperedge splitting strategies). We next consider a toy quadratic program on a loopy hypergraph with $\mathcal{V} = \{1, 2, 3, 4\}$ and $\mathcal{E} = \{\{1, 2, 3\}, \{2, 3, 4\}\}$ —see Fig. 14. Since the factor graph contains a short cycle, we apply the surrogate hyperedge-splitting strategy to restore an acyclic intra-cluster factor structure. We instantiate two splitting surrogates: the pairwise split (68) and the singleton split (70), denoted *H-MP-Jacobi-S1* and *H-MP-Jacobi-S2*, respectively (with stepsizes tuned for each method). Fig. 14 shows that H-MP-Jacobi-S2 converges faster than H-MP-Jacobi-S1. This is consistent with the

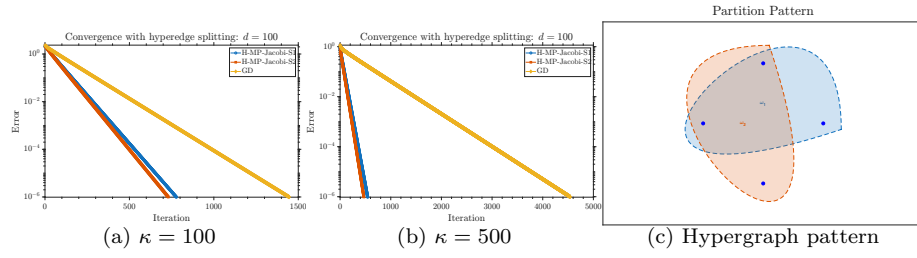


Fig. 14: Strongly convex QP: two examples of surrogate hyperedge-splitting strategies to restore an acyclic intra-cluster factor structure.

fact that the singleton split introduces fewer frozen coordinates (fewer reference points), thereby retaining more of the original coupling structure; the pairwise split is more aggressive and incurs a larger approximation error. The GD baseline is consistently, significantly slower.

(iii) ATC-induced hypergraph (splitting). Finally, we test a QP induced by the DGD-ATC model (6). Let W be the gossip matrix over the graph with $\mathcal{V} = [8]$ and edges $\{\{1, 2\}, \{1, 3\}, \{2, 3\}, \{3, 4\}, \{4, 5\}, \{5, 6\}, \{6, 7\}, \{6, 8\}, \{7, 8\}\}$, and define hyperedges $\omega_i := \{j : [W^2]_{ij} \neq 0\}$ —see Fig. 15(c). We compare two partitions/surrogates. For H-MP-Jacobi-S1, we use two clusters $\mathcal{C}_1 = \{1, 2, 3, 4\}$ and $\mathcal{C}_2 = \{5, 6, 7, 8\}$, with intra-cluster hyperedges $\omega_1 = \{1, 2, 3, 4\}$ and $\omega_2 = \{5, 6, 7, 8\}$. For H-MP-Jacobi-S2, we use $\mathcal{C}_1 = \{1, 2, 3, 4, 5\}$ and split the associated coupling into $\tilde{\omega}_1^1 = \{1, 2, 3\}$ and $\tilde{\omega}_1^2 = \{3, 4, 5\}$, while placing all remaining nodes in singleton clusters. The results in Fig. 15 show that both surrogate designs perform similarly and significantly outperform DGD-ATC (GD). Moreover, H-MP-Jacobi-S1 is slightly faster than H-MP-Jacobi-S2, consistent with the fact that S1 preserves more coupling information.

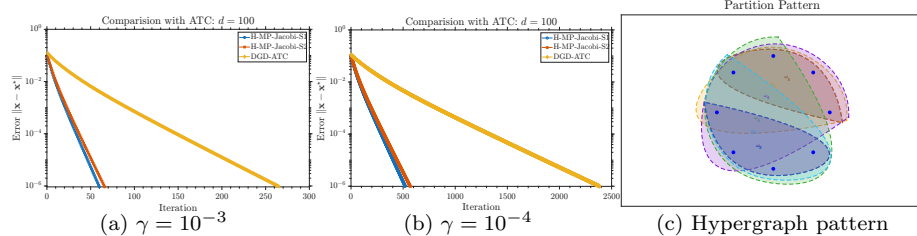


Fig. 15: DGD-ATC problem (6). Comparison of message passing-gossip algorithm and ATC over a hypergraph induced by ATC. $d = 100$.

7 Conclusions

In this work, we introduced min-sum *message passing* as an algorithmic primitive for decentralized optimization with localized couplings. Building on a fixed-point decomposition induced by a tree partition and its condensed graph, we proposed *MP-Jacobi*: at each round, every agent performs a (damped) Jacobi update using the current intra-cluster messages and the current inter-cluster neighbors variables, and then updates one-hop pairwise messages along the intra-cluster tree edges. We establish convergence for (strongly) convex and nonconvex objectives,

with topology- and partition-explicit rates that quantify curvature/coupling effects and guide clustering and scalability. To reduce computation and communication, we further developed structure-preserving surrogate algorithm and establish the analogous linear convergence for the strongly convex problem. Moreover, we extended the framework from graphs to hypergraphs; for dense hypergraphs with heavy overlaps, we proposed a hyperedge-splitting strategy that enables the algorithm to remain convergent. Extensive numerical experiments on both graph and hypergraph instances corroborate the theory, demonstrate substantial efficiency gains over decentralized gradient-type baselines, and highlight the potential of MP-Jacobi as a scalable primitive for distributed optimization.

Appendix

A Proof of Proposition 1

(a) Proof of (20b). Fix a cluster \mathcal{C}_r and a root $i \in \mathcal{C}_r$. View the tree $\mathcal{G}_r = (\mathcal{C}_r, \mathcal{E}_r)$ as oriented towards i . For every $j \in \mathcal{C}_r \setminus \{i\}$, let $\text{pa}(j)$ be the parent of j on the path to i , let $\text{sub}(j)$ be the node set of the subtree rooted at j , and let $d(i, j)$ be the hop distance from i to j . Recall the reindexed recursion

$$\mu_{j \rightarrow i}^\nu(x_i) = \min_{x_j} \left\{ \phi_j(x_j) + \psi_{ij}(x_i, x_j) + \sum_{k \in \mathcal{N}_j^{\text{in}} \setminus \{i\}} \mu_{k \rightarrow j}^{\nu-1}(x_j) + \sum_{k \in \mathcal{N}_j^{\text{out}}} \psi_{jk}(x_j, x_k^{\nu-1}) \right\}. \quad (75)$$

• **Step 1 (subtree representation):** Given $j \in \mathcal{C}_r \setminus \{i\}$, we prove by induction on the depth $d(i, j)$, that the message from j to its parent at the appropriate iteration, $\mu_{j \rightarrow \text{pa}(j)}^{\nu-d(i, j)+1}(x_{\text{pa}(j)})$, can be written as the optimal value of a local subtree problem, that is

$$\mu_{j \rightarrow \text{pa}(j)}^{\nu-d(i, j)+1}(x_{\text{pa}(j)}) = \min_{x_{\text{sub}(j)}} \left\{ \sum_{\ell \in \text{sub}(j)} \phi_\ell(x_\ell) + \psi_{\text{pa}(j), j}(x_{\text{pa}(j)}, x_j) + \sum_{\substack{(\ell, m) \in \mathcal{E}_r \\ \ell, m \in \text{sub}(j)}} \psi_{\ell m}(x_\ell, x_m) + \sum_{\substack{\ell \in \text{sub}(j) \\ k \in \mathcal{N}_\ell^{\text{out}}}} \psi_{\ell k}(x_\ell, x_k^{\nu-d(i, \ell)}) \right\}. \quad (76)$$

Base case. If j is a leaf, then $\text{sub}(j) = \{j\}$ and $\mathcal{N}_j^{\text{in}} \setminus \{\text{pa}(j)\} = \emptyset$. Evaluating (75) at iteration $\nu - d(i, j) + 1$ reads

$$\mu_{j \rightarrow \text{pa}(j)}^{\nu-d(i, j)+1}(x_{\text{pa}(j)}) = \min_{x_j} \left\{ \phi_j(x_j) + \psi_{\text{pa}(j), j}(x_{\text{pa}(j)}, x_j) + \sum_{k \in \mathcal{N}_j^{\text{out}}} \psi_{jk}(x_j, x_k^{\nu-d(i, j)}) \right\},$$

which is exactly (76) when $\text{sub}(j) = \{j\}$ (no intra-subtree edges).

Inductive step. Let j be any internal node of \mathcal{G}_r . Apply (75) with $i = \text{pa}(j)$ and ν replaced by $\nu - d(i, j) + 1$:

$$\begin{aligned} \mu_{j \rightarrow \text{pa}(j)}^{\nu-d(i, j)+1}(x_{\text{pa}(j)}) &= \\ &= \min_{x_j} \left\{ \phi_j(x_j) + \psi_{\text{pa}(j), j}(x_{\text{pa}(j)}, x_j) + \sum_{h: \text{pa}(h)=j} \mu_{h \rightarrow j}^{\nu-d(i, j)}(x_j) + \sum_{k \in \mathcal{N}_j^{\text{out}}} \psi_{jk}(x_j, x_k^{\nu-d(i, j)}) \right\}. \end{aligned} \quad (77)$$

Every child h of j satisfies $d(i, h) = d(i, j) + 1$, hence $\mu_{h \rightarrow j}^{\nu-d(i, j)}(x_j) = \mu_{h \rightarrow j}^{\nu-d(i, h)+1}(x_j)$. Applying the induction hypothesis (76) to the child h of j (i.e., replace therein j by h and $\text{pa}(h) = j$) yields

$$\mu_{h \rightarrow j}^{\nu-d(i, h)+1}(x_j) =$$

$$= \min_{x_{\text{sub}(h)}} \left\{ \sum_{\ell \in \text{sub}(h)} \phi_\ell(x_\ell) + \psi_{j,h}(x_j, x_h) + \sum_{\substack{(\ell,m) \in \mathcal{E}_r, \\ \ell,m \in \text{sub}(h)}} \psi_{\ell m}(x_\ell, x_m) \right. \\ \left. + \sum_{\ell \in \text{sub}(h), k \in \mathcal{N}_\ell^{\text{out}}} \psi_{\ell k}(x_\ell, x_k^{\nu-d(i,\ell)}) \right\}. \quad (78)$$

Substituting (78) into (77) and merging the minimizations over the pairwise-*disjoint* subtrees $\{\text{sub}(h)\}_{h: \text{pa}(h)=j}$ (together with x_j) yields

$$\mu_{j \rightarrow \text{pa}(j)}^{\nu-d(i,j)+1}(x_{\text{pa}(j)}) = \min_{x_j, \{x_{\text{sub}(h)}\}_{h: \text{pa}(h)=j}} \left\{ \phi_j(x_j) + \psi_{\text{pa}(j),j}(x_{\text{pa}(j)}, x_j) + \sum_{h: \text{pa}(h)=j} \psi_{j,h}(x_j, x_h) \right. \\ \left. + \sum_{h: \text{pa}(h)=j} \sum_{\ell \in \text{sub}(h)} \phi_\ell(x_\ell) + \sum_{h: \text{pa}(h)=j} \sum_{\substack{(\ell,m) \in \mathcal{E}_r \\ \ell,m \in \text{sub}(h)}} \psi_{\ell m}(x_\ell, x_m) \right. \\ \left. + \sum_{h: \text{pa}(h)=j} \sum_{\substack{\ell \in \text{sub}(h) \\ k \in \mathcal{N}_\ell^{\text{out}}}} \psi_{\ell k}(x_\ell, x_k^{\nu-d(i,\ell)}) + \sum_{k \in \mathcal{N}_j^{\text{out}}} \psi_{jk}(x_j, x_k^{\nu-d(i,j)}) \right\}.$$

Now note that $\text{sub}(j) = \{j\} \cup \bigcup_{h: \text{pa}(h)=j} \text{sub}(h)$ is a disjoint union, and there are no intra-cluster edges across different child subtrees other than the edges (j, h) . Regrouping the sums over $\{j\}$ and $\text{sub}(h)$ pieces, we recover exactly the structure in (76) for the subtree rooted at j . This completes the inductive step and proves the subtree representation for all $j \neq i$.

• **Step 2 (sum of messages at the root):** The primal subproblem reads

$$\hat{x}_i^{\nu+1} \in \operatorname{argmin}_{x_i} \left\{ \phi_i(x_i) + \sum_{j \in \mathcal{N}_i^{\text{in}}} \mu_{j \rightarrow i}^\nu(x_i) + \sum_{k \in \mathcal{N}_i^{\text{out}}} \psi_{ik}(x_i, x_k^\nu) \right\}.$$

For each neighbor $j \in \mathcal{N}_i^{\text{in}}$, we have $d(i, j) = 1$ and $\text{pa}(j) = i$. Therefore, (76) (with depth $d(i, j) = 1$) gives $\mu_{j \rightarrow i}^\nu(x_i)$ equal to the optimal cost value of the subproblem associated with the subtree $\text{sub}(j)$ w.r.t. $x_{\text{sub}(j)}$. The subtrees $\{\text{sub}(j) : j \in \mathcal{N}_i^{\text{in}}\}$ are pairwise disjoint and their union is $\mathcal{C}_r \setminus \{i\}$. Summing the objectives and merging the minimizations yields

$$\sum_{j \in \mathcal{N}_i^{\text{in}}} \mu_{j \rightarrow i}^\nu(x_i) = \min_{x_{\mathcal{C}_r \setminus \{i\}}} \left\{ \sum_{j \in \mathcal{C}_r \setminus \{i\}} \phi_j(x_j) + \sum_{(j,k) \in \mathcal{E}_r} \psi_{jk}(x_j, x_k) \right. \\ \left. + \sum_{j \in \mathcal{C}_r \setminus \{i\}, k \in \mathcal{N}_j^{\text{out}}} \psi_{jk}(x_j, x_k^{\nu-d(i,j)}) + \sum_{j \in \mathcal{N}_i^{\text{in}}} \psi_{ij}(x_i, x_j) \right\}.$$

Adding the terms $\phi_i(x_i)$ and $\sum_{k \in \mathcal{N}_i^{\text{out}}} \psi_{ik}(x_i, x_k^\nu)$ completes the joint intra-cluster cost and all boundary terms, now including the contribution $j = i$ (for which $d(i, i) = 0$). Therefore

$$\hat{x}_i^{\nu+1} \in \operatorname{argmin}_{x_i} \min_{x_{\mathcal{C}_r \setminus \{i\}}} \left\{ \sum_{j \in \mathcal{C}_r} \phi_j(x_j) + \sum_{(j,k) \in \mathcal{E}_r} \psi_{jk}(x_j, x_k) + \sum_{j \in \mathcal{C}_r, k \in \mathcal{N}_j^{\text{out}}} \psi_{jk}(x_j, x_k^{\nu-d(i,j)}) \right\},$$

which is exactly (20b).

(b) **Proof of (21).** By maximality (7), every edge with both endpoints in \mathcal{C}_r belongs to \mathcal{E}_r , so for any fixed external block $z_{\bar{\mathcal{C}}_r}$ the dependence of $\Phi(x_{\mathcal{C}_r}, z_{\bar{\mathcal{C}}_r})$ on $x_{\mathcal{C}_r}$ is exactly through

$$\sum_{j \in \mathcal{C}_r} \phi_j(x_j) + \sum_{(j,k) \in \mathcal{E}_r} \psi_{jk}(x_j, x_k) + \sum_{j \in \mathcal{C}_r, k \in \bar{\mathcal{C}}_r} \psi_{jk}(x_j, z_k),$$

all remaining terms being independent of $x_{\mathcal{C}_r}$. Moreover, (16) implies that each external node $k \in \bar{\mathcal{C}}_r$ is attached to a unique leaf $j_k \in \mathcal{B}_r$, so the boundary term can be rewritten as

$$\sum_{j \in \mathcal{C}_r, k \in \mathcal{N}_j^{\text{out}}} \psi_{jk}(x_j, x_k^{\nu-d(i,j)}) = \sum_{k \in \bar{\mathcal{C}}_r} \psi_{j_k k}(x_{j_k}, x_k^{\nu-d(i,j_k)}),$$

which depends on the delays only through the vector $\mathbf{d}_i := (d(i, j_k))_{k \in \bar{\mathcal{C}}_r}$ and the block $x_{\bar{\mathcal{C}}_r}^{\nu-\mathbf{d}_i} := (x_k^{\nu-d(i, j_k)})_{k \in \bar{\mathcal{C}}_r}$. Combining the two observations above, we obtain, for some constant c_i^ν independent of $x_{\mathcal{C}_r}$,

$$\sum_{j \in \mathcal{C}_r} \phi_j(x_j) + \sum_{(j, k) \in \mathcal{E}_r} \psi_{jk}(x_j, x_k) + \sum_{j \in \mathcal{C}_r, k \in \mathcal{N}_j^{\text{out}}} \psi_{jk}(x_j, x_k^{\nu-d(i, j)}) = \Phi(x_{\mathcal{C}_r}, x_{\bar{\mathcal{C}}_r}^{\nu-\mathbf{d}_i}) - c_i^\nu.$$

Thus, (20b) is equivalent to (21), which completes the proof. \square

B Proof of Theorem 2

We prove the theorem in two steps: (i) we cast Algorithm 2 as a damped surrogate block-Jacobi method with bounded delay; and then (ii) establish its convergence.

• *Step 1: Algorithm 2 as a surrogate block-Jacobi method with delays.* Fix a cluster \mathcal{C}_r and a root $i \in \mathcal{C}_r$. We view the tree $\mathcal{G}_r = (\mathcal{C}_r, \mathcal{E}_r)$ as oriented towards i (suppress the index i in the notation), and write (j, k) for the directed edge pointing to i (i.e., $d(i, k) < d(i, j)$). Following similar steps as in Section 3.1, we eliminate $\tilde{\mu}_{k \rightarrow i}^\nu$ by reapplying (41c) and repeating the substitution recursively along the branches of the tree \mathcal{G}_r . We obtain the following.

Proposition 6 *Under Assumptions 1 and 2, Algorithm 2 can be rewritten in the equivalent form: for any $i \in \mathcal{C}_r$ and $r \in [p]$,*

$$x_i^{\nu+1} = x_i^\nu + \tau_r^\nu (\hat{x}_i^{\nu+1} - x_i^\nu), \quad (79a)$$

$$\hat{x}_i^{\nu+1} \in \operatorname{argmin}_{x_i} \min_{x_{\mathcal{C}_r \setminus \{i\}}} \left\{ \sum_{j \in \mathcal{C}_r} \tilde{\phi}_j(x_j; x_j^{\nu-d(i, j)}) + \sum_{(j, k) \in \mathcal{E}_r} \tilde{\psi}_{jk}(x_j, x_k; x_j^{\nu-d(i, j)}, x_k^{\nu-d(i, j)}) \right\} \\ + \sum_{j \in \mathcal{C}_r, k \in \mathcal{N}_j^{\text{out}}} \tilde{\psi}_{jk}(x_j, x_k^{\nu-d(i, j)}; x_j^{\nu-d(i, j)}, x_k^{\nu-d(i, j)}) \quad (79b)$$

If, in addition, Assumption 3 holds, (79b) reduces to the following block-Jacobi update with delays:

$$\hat{x}_i^{\nu+1} \in \operatorname{argmin}_{x_i} \min_{x_{\mathcal{C}_r \setminus \{i\}}} \tilde{\Phi}_r\left((x_{\mathcal{C}_r}, x_{\bar{\mathcal{C}}_r}^{\nu-\delta_i}); (x_{\mathcal{C}_r}^{\nu-\mathbf{d}_i}, x_{\mathcal{E}_r}^{\nu-\mathbf{D}_i}, x_{\bar{\mathcal{C}}_r}^{\nu-\delta_i})\right), \quad (80)$$

where $\mathbf{d}_i := (d(i, j))_{j \in \mathcal{C}_r}$ and $\delta_i := (\delta_{i,k})_{k \in \bar{\mathcal{C}}_r}$ with

$$\delta_{i,k} := \begin{cases} d(i, \pi_r(k)), & k \in \mathcal{N}_{\mathcal{C}_r}, \\ 0, & k \notin \mathcal{N}_{\mathcal{C}_r}, \end{cases}$$

and $\pi_r(k) \in \mathcal{C}_r$ denotes the unique internal neighbor of k guaranteed by (16). The edge-stacked delay vector is $\mathbf{D}_i := (d(i, j); d(i, k))_{(j, k) \in \mathcal{E}_r}$. It holds $\max\{\|\mathbf{d}_i\|_\infty, \|\delta_i\|_\infty, \|\mathbf{D}_i\|_\infty\} \leq D_r$, for all $i \in \mathcal{C}_r$ and $r \in [p]$.

• *Step 2: Convergence of (80).* For any $r \in [p]$ and $i \in \mathcal{C}_r$, introduce the virtual *non-delayed* block update (used only in the analysis):

$$\bar{x}_{\mathcal{C}_r}^{\nu+1} \in \operatorname{argmin}_{x_{\mathcal{C}_r}} \tilde{\Phi}_r\left((x_{\mathcal{C}_r}, x_{\bar{\mathcal{C}}_r}^\nu); (x_{\mathcal{C}_r}^\nu, x_{\bar{\mathcal{C}}_r}^\nu, x_{\mathcal{E}_r}^\nu)\right),$$

The next two lemmas establish a descent recursion for Φ along $\{\mathbf{x}^\nu\}$. Their proofs are the analogous to Lemma 1–2 in Section 3.2, with one additional ingredient: we relate the aggregated surrogate to the aggregated objective (42) via the upper bound condition in Assumption 5.(ii).

Lemma 4 *Under Assumption 5 and any stepsize choice satisfying $\tau_r^\nu \geq 0$ and $\sum_{r=1}^p \tau_r^\nu \leq 1$, the following holds:*

$$\Phi(\mathbf{x}^{\nu+1}) \leq \Phi(\mathbf{x}^\nu) + \sum_{r \in [p]} \tau_r^\nu \left[-\frac{\|P_r \nabla \Phi(\mathbf{x}^\nu)\|^2}{2\tilde{L}_r} + \frac{\tilde{L}_r}{2} \|P_r(\hat{\mathbf{x}}^{\nu+1} - \bar{\mathbf{x}}^{\nu+1})\|^2 \right]. \quad (81)$$

Proof We first bound of the nondelay iterate for the surrogate. Note that

$$\begin{aligned} & \tilde{\Phi}_r\left(\left(\hat{x}_{\mathcal{C}_r}^{\nu+1}, x_{\bar{\mathcal{C}}_r}^\nu\right); \left(x_{\mathcal{C}_r}^\nu, x_{\bar{\mathcal{C}}_r}^\nu, x_{\mathcal{E}_r}^\nu\right)\right) \\ & \leq \tilde{\Phi}_r\left(\left(\bar{x}_{\mathcal{C}_r}^{\nu+1}, x_{\bar{\mathcal{C}}_r}^\nu\right); \left(x_{\mathcal{C}_r}^\nu, x_{\bar{\mathcal{C}}_r}^\nu, x_{\mathcal{E}_r}^\nu\right)\right) + \underbrace{\left\langle \tilde{\Phi}_r\left(\left(\bar{x}_{\mathcal{C}_r}^{\nu+1}, x_{\bar{\mathcal{C}}_r}^\nu\right); \left(x_{\mathcal{C}_r}^\nu, x_{\bar{\mathcal{C}}_r}^\nu, x_{\mathcal{E}_r}^\nu\right)\right), \hat{x}_{\mathcal{C}_r}^{\nu+1} - \bar{x}_{\mathcal{C}_r}^{\nu+1} \right\rangle}_{=0} \\ & \quad + \frac{\tilde{L}_r}{2} \left\| \hat{x}_{\mathcal{C}_r}^{\nu+1} - \bar{x}_{\mathcal{C}_r}^{\nu+1} \right\|^2. \end{aligned}$$

By definition of $\bar{x}_{\mathcal{C}_r}^{\nu+1}$ and Assumption 5.(i)(iii), we have

$$\begin{aligned} & \tilde{\Phi}_r\left(\left(\bar{x}_{\mathcal{C}_r}^{\nu+1}, x_{\bar{\mathcal{C}}_r}^\nu\right); \left(x_{\mathcal{C}_r}^\nu, x_{\bar{\mathcal{C}}_r}^\nu, x_{\mathcal{E}_r}^\nu\right)\right) \leq \tilde{\Phi}_r\left(\left(x_{\mathcal{C}_r}^\nu, x_{\bar{\mathcal{C}}_r}^\nu\right); \left(x_{\mathcal{C}_r}^\nu, x_{\bar{\mathcal{C}}_r}^\nu, x_{\mathcal{E}_r}^\nu\right)\right) - \frac{\|\nabla_{\mathcal{C}_r} \Phi(\mathbf{x}^\nu)\|^2}{2\tilde{L}_r} \\ & = \Phi_r(\mathbf{x}^\nu) - \frac{\|\nabla_{\mathcal{C}_r} \Phi(\mathbf{x}^\nu)\|^2}{2\tilde{L}_r}. \end{aligned}$$

Combining the above inequalities, we obtain

$$\tilde{\Phi}_r\left(\left(\hat{x}_{\mathcal{C}_r}^{\nu+1}, x_{\bar{\mathcal{C}}_r}^\nu\right); \left(x_{\mathcal{C}_r}^\nu, x_{\bar{\mathcal{C}}_r}^\nu, x_{\mathcal{E}_r}^\nu\right)\right) \leq \Phi_r(\mathbf{x}^\nu) - \frac{\|\nabla_{\mathcal{C}_r} \Phi(\mathbf{x}^\nu)\|^2}{2\tilde{L}_r} + \frac{\tilde{L}_r}{2} \left\| \hat{x}_{\mathcal{C}_r}^{\nu+1} - \bar{x}_{\mathcal{C}_r}^{\nu+1} \right\|^2. \quad (82)$$

By (27) and Assumption 5.(ii), we have

$$\begin{aligned} \Phi(\mathbf{x}^{\nu+1}) - \Phi(\mathbf{x}^\nu) & \leq \sum_{r=1}^p \tau_r^\nu \left(\Phi(\mathbf{x}^\nu + P_r(\hat{\mathbf{x}}^{\nu+1} - \mathbf{x}^\nu)) - \Phi(\mathbf{x}^\nu) \right) \\ & \leq \sum_{r=1}^p \tau_r^\nu \left(\tilde{\Phi}_r\left(\left(\hat{x}_{\mathcal{C}_r}^{\nu+1}, x_{\bar{\mathcal{C}}_r}^\nu\right); \left(x_{\mathcal{C}_r}^\nu, x_{\bar{\mathcal{C}}_r}^\nu, x_{\mathcal{E}_r}^\nu\right)\right) - \Phi_r(\mathbf{x}^\nu) \right). \end{aligned}$$

Combining this inequality with (82) completes the proof. \square

Lemma 5 *Under Assumption 5 and any stepsize choice satisfying $\tau_r^\nu \geq 0$ and $\sum_{r=1}^p \tau_r^\nu \leq 1$, the following holds:*

$$\Phi(\mathbf{x}^{\nu+1}) \leq \Phi(\mathbf{x}^\nu) + \sum_{r \in [p]} \tau_r^\nu \left[-\frac{\tilde{\mu}_r}{4} \|P_r(\hat{\mathbf{x}}^{\nu+1} - \mathbf{x}^\nu)\|^2 + \frac{\tilde{L}_r + \tilde{\mu}_r}{2} \|P_r(\bar{\mathbf{x}}^{\nu+1} - \hat{\mathbf{x}}^{\nu+1})\|^2 \right]. \quad (83)$$

Proof The proof follows the same steps as Lemma 2, with the exact block objective replaced by the aggregated surrogate and the final bound transferred to Φ via the upper bound condition in Assumption 5(ii) (cf. the proof of Lemma 4). We omit the details. \square

Next, we bound the discrepancy term $\|P_r(\bar{\mathbf{x}}^{\nu+1} - \hat{\mathbf{x}}^{\nu+1})\|^2$.

Lemma 6 *In the setting of Lemma 4 and Lemma 5, the following holds: for any $r \in [p]$,*

$$\|P_r(\hat{\mathbf{x}}^{\nu+1} - \bar{\mathbf{x}}^{\nu+1})\|^2 \leq \frac{2|\mathcal{C}_r|D_r}{\tilde{\mu}_r^2} \sum_{\ell=\nu-D_r}^{\nu-1} \left(\tilde{L}_{\partial r}^2 \left\| P_{\partial r}(\mathbf{x}^{\ell+1} - \mathbf{x}^\ell) \right\|^2 + \sigma_r \tilde{\ell}_r^2 \left\| P_r(\mathbf{x}^{\ell+1} - \mathbf{x}^\ell) \right\|^2 \right).$$

where $\sigma_r = \max_{i \in \mathcal{C}_r} \deg_{\mathcal{G}_r}(i)$.

Proof Define the *delayed* block update for the aggregated surrogate:

$$\hat{x}_{\mathcal{C}_r, i}^{\nu+1} := \underset{x_{\mathcal{C}_r}}{\operatorname{argmin}} \tilde{\Phi}_r\left(\left(x_{\mathcal{C}_r}, x_{\mathcal{C}_r}^{\nu-\delta_i}\right); \left(x_{\mathcal{C}_r}^{\nu+1}, x_{\mathcal{C}_r}^{\nu-\delta_i}, x_{\mathcal{E}_r}^{\nu-\mathbf{D}_i}\right)\right), \text{ thus } \hat{x}_i^{\nu+1} = [\hat{x}_{\mathcal{C}_r, i}^{\nu+1}]_i.$$

By the optimality condition,

$$\begin{aligned} 0 &= \nabla \tilde{\Phi}_r\left(\left(\bar{x}_{\mathcal{C}_r}^{\nu+1}, x_{\mathcal{C}_r}^{\nu}\right); \left(x_{\mathcal{C}_r}^{\nu}, x_{\mathcal{C}_r}^{\nu}, x_{\mathcal{E}_r}^{\nu}\right)\right) - \nabla \tilde{\Phi}_r\left(\left(\hat{x}_{\mathcal{C}_r, i}^{\nu+1}, x_{\mathcal{C}_r}^{\nu-\delta_i}\right); \left(x_{\mathcal{C}_r}^{\nu+1}, x_{\mathcal{C}_r}^{\nu-\delta_i}, x_{\mathcal{E}_r}^{\nu-\mathbf{D}_i}\right)\right) \\ &= \nabla \tilde{\Phi}_r\left(\left(\bar{x}_{\mathcal{C}_r}^{\nu+1}, x_{\mathcal{C}_r}^{\nu}\right); \left(x_{\mathcal{C}_r}^{\nu}, x_{\mathcal{C}_r}^{\nu}, x_{\mathcal{E}_r}^{\nu}\right)\right) - \nabla \tilde{\Phi}_r\left(\left(\bar{x}_{\mathcal{C}_r}^{\nu+1}, x_{\mathcal{C}_r}^{\nu-\delta_i}\right); \left(x_{\mathcal{C}_r}^{\nu}, x_{\mathcal{C}_r}^{\nu-\delta_i}, x_{\mathcal{E}_r}^{\nu}\right)\right) \\ &\quad + \nabla \tilde{\Phi}_r\left(\left(\bar{x}_{\mathcal{C}_r}^{\nu+1}, x_{\mathcal{C}_r}^{\nu-\delta_i}\right); \left(x_{\mathcal{C}_r}^{\nu}, x_{\mathcal{C}_r}^{\nu-\delta_i}, x_{\mathcal{E}_r}^{\nu}\right)\right) - \nabla \tilde{\Phi}_r\left(\left(\bar{x}_{\mathcal{C}_r}^{\nu+1}, x_{\mathcal{C}_r}^{\nu-\delta_i}\right); \left(x_{\mathcal{C}_r}^{\nu+1}, x_{\mathcal{C}_r}^{\nu-\delta_i}, x_{\mathcal{E}_r}^{\nu-\mathbf{D}_i}\right)\right) \\ &\quad + \nabla \tilde{\Phi}_r\left(\left(\bar{x}_{\mathcal{C}_r}^{\nu+1}, x_{\mathcal{C}_r}^{\nu-\delta_i}\right); \left(x_{\mathcal{C}_r}^{\nu}, x_{\mathcal{C}_r}^{\nu-\delta_i}, x_{\mathcal{E}_r}^{\nu-\mathbf{D}_i}\right)\right) - \nabla \tilde{\Phi}_r\left(\left(\hat{x}_{\mathcal{C}_r, i}^{\nu+1}, x_{\mathcal{C}_r}^{\nu-\delta_i}\right); \left(x_{\mathcal{C}_r}^{\nu}, x_{\mathcal{C}_r}^{\nu-\delta_i}, x_{\mathcal{E}_r}^{\nu-\mathbf{D}_i}\right)\right). \end{aligned}$$

Assumption 5 yields

$$\begin{aligned} &\tilde{\mu}_r \left\| \hat{x}_{\mathcal{C}_r, i}^{\nu+1} - \bar{x}_{\mathcal{C}_r}^{\nu+1} \right\|^2 \\ &\leq - \left\langle \nabla \tilde{\Phi}_r\left(\left(\bar{x}_{\mathcal{C}_r}^{\nu+1}, x_{\mathcal{C}_r}^{\nu}\right); \left(x_{\mathcal{C}_r}^{\nu}, x_{\mathcal{C}_r}^{\nu}, x_{\mathcal{E}_r}^{\nu}\right)\right) - \nabla \tilde{\Phi}_r\left(\left(\bar{x}_{\mathcal{C}_r}^{\nu+1}, x_{\mathcal{C}_r}^{\nu-\delta_i}\right); \left(x_{\mathcal{C}_r}^{\nu}, x_{\mathcal{C}_r}^{\nu-\delta_i}, x_{\mathcal{E}_r}^{\nu}\right)\right), \hat{x}_{\mathcal{C}_r, i}^{\nu+1} - \bar{x}_{\mathcal{C}_r}^{\nu+1} \right\rangle \\ &\quad - \left\langle \nabla \tilde{\Phi}_r\left(\left(\bar{x}_{\mathcal{C}_r}^{\nu+1}, x_{\mathcal{C}_r}^{\nu-\delta_i}\right); \left(x_{\mathcal{C}_r}^{\nu}, x_{\mathcal{C}_r}^{\nu-\delta_i}, x_{\mathcal{E}_r}^{\nu}\right)\right) - \nabla \tilde{\Phi}_r\left(\left(\bar{x}_{\mathcal{C}_r}^{\nu+1}, x_{\mathcal{C}_r}^{\nu-\delta_i}\right); \left(x_{\mathcal{C}_r}^{\nu+1}, x_{\mathcal{C}_r}^{\nu-\delta_i}, x_{\mathcal{E}_r}^{\nu-\mathbf{D}_i}\right)\right), \hat{x}_{\mathcal{C}_r, i}^{\nu+1} - \bar{x}_{\mathcal{C}_r}^{\nu+1} \right\rangle. \end{aligned}$$

Then,

$$\mu_r \left\| \hat{x}_{\mathcal{C}_r, i}^{\nu+1} - \bar{x}_{\mathcal{C}_r}^{\nu+1} \right\| \leq \tilde{L}_{\partial r} \left\| x_{\mathcal{N}_{\mathcal{C}_r}}^{\nu-\delta_i} - x_{\mathcal{N}_{\mathcal{C}_r}}^{\nu} \right\| + \tilde{\ell}_r \left\| x_{\mathcal{E}_r}^{\nu-\mathbf{D}_i} - x_{\mathcal{E}_r}^{\nu} \right\|.$$

Note that, for any w , $\|w_{\mathcal{E}_r}\|^2 \leq \sigma_r \|w_{\mathcal{C}_r}\|^2$, and $\left\| \hat{x}_{\mathcal{C}_r}^{\nu+1} - \bar{x}_{\mathcal{C}_r}^{\nu+1} \right\|^2 \leq \sum_{i \in \mathcal{C}_r} \left\| \hat{x}_{\mathcal{C}_r, i}^{\nu+1} - \bar{x}_{\mathcal{C}_r}^{\nu+1} \right\|^2$. Hence,

$$\left\| \hat{x}_{\mathcal{C}_r}^{\nu+1} - \bar{x}_{\mathcal{C}_r}^{\nu+1} \right\|^2 \leq \frac{2|\mathcal{C}_r|D_r}{\tilde{\mu}_r^2} \sum_{\ell=\nu-D_r}^{\nu-1} \left(\tilde{L}_{\partial r}^2 \left\| x_{\mathcal{N}_{\mathcal{C}_r}}^{\ell+1} - x_{\mathcal{N}_{\mathcal{C}_r}}^{\ell} \right\|^2 + \sigma_r \tilde{\ell}_r^2 \left\| x_{\mathcal{C}_r}^{\ell+1} - x_{\mathcal{C}_r}^{\ell} \right\|^2 \right).$$

This completes the proof. \square

We can now proceed with the proof of Theorem 2.

Let $\Delta_{\mathcal{S}}^{\nu} := \sum_{\ell=\nu-D}^{\nu-1} \left\| x_{\mathcal{S}}^{\ell+1} - x_{\mathcal{S}}^{\ell} \right\|^2$ for $\mathcal{S} \subseteq [p]$, and write $\Delta^{\nu} := \Delta_{[p]}^{\nu}$. By (81), (83), and Lemma 6, we have

$$\begin{aligned} \Phi(\mathbf{x}^{\nu+1}) &\leq \Phi(\mathbf{x}^{\nu}) - \sum_{r \in [p]} \frac{\tau}{4\tilde{L}_r} \|P_r \nabla \Phi(\mathbf{x}^{\nu})\|^2 - \sum_{r \in [p]} \frac{\tilde{\mu}_r}{8\tau} \|P_r(\mathbf{x}^{\nu+1} - \mathbf{x}^{\nu})\|^2 \\ &\quad + \sum_{r \in [p]} \tau A_r \Delta_{\mathcal{N}_{\mathcal{C}_r}}^{\nu} + \sum_{r \in [p]} \tau \tilde{A}_r \Delta_{\mathcal{C}_r}^{\nu}. \end{aligned} \tag{84}$$

By strong convexity (implying $\|\nabla \Phi(\mathbf{x}^{\nu})\|^2 \geq 2\mu(\Phi(\mathbf{x}^{\nu}) - \Phi^*)$), we have

$$\begin{aligned} \Phi(\mathbf{x}^{\nu+1}) - \Phi^* &\leq \left(1 - \frac{\tau}{2\kappa}\right) (\Phi(\mathbf{x}^{\nu}) - \Phi^*) - \sum_{r \in \mathcal{J} \cup \{s \in [p]: |\mathcal{C}_s| > 1\}} \frac{\tilde{\mu}_r}{8\tau} \|P_r(\mathbf{x}^{\nu+1} - \mathbf{x}^{\nu})\|^2 \\ &\quad + \tau A_{\mathcal{J}} \sum_{r \in \mathcal{J}} \Delta_{\mathcal{C}_r}^{\nu} + \tau \left(\max_{r: |\mathcal{C}_r| > 1} \tilde{A}_r \right) \sum_{r: |\mathcal{C}_r| > 1} \Delta_{\mathcal{C}_r}^{\nu} \\ &= \left(1 - \frac{\tau}{2\kappa}\right) (\Phi(\mathbf{x}^{\nu}) - \Phi^*) - \sum_{r \in \mathcal{J} \cup \{s: |\mathcal{C}_s| > 1\}} \frac{\tilde{\mu}_r}{8\tau} \|P_r(\mathbf{x}^{\nu+1} - \mathbf{x}^{\nu})\|^2 \\ &\quad + \tau \left(A_{\mathcal{J}} + \max_{r: |\mathcal{C}_r| > 1} \tilde{A}_r \right) \sum_{r \in \mathcal{J} \cup \{s: |\mathcal{C}_s| > 1\}} \Delta_{\mathcal{C}_r}^{\nu}. \end{aligned}$$

A standard delay-window inequality (e.g., [15, Lemma 5]) yields linear convergence under the following condition

$$2D + 1 \leq \min \left\{ \frac{2\tilde{L}}{\tau\mu}, \frac{\frac{1}{8\tau} \min_{r \in \mathcal{J} \cup \{s: |\mathcal{C}_s| > 1\}} \tilde{\mu}_r}{\tau (A_{\mathcal{J}} + \max_{r: |\mathcal{C}_r| > 1} \tilde{A}_r)} \right\},$$

with the linear rate given by (52). Using uniform stepsize values, $\tau \in (0, 1/p]$, yields (51). \square

C Proof of Theorem 3

Let $\Phi^* := \min \Phi(\mathbf{x})$ and choose any $\mathbf{x}^* \in \operatorname{argmin} \Phi(\mathbf{x})$. For any $r \in [p]$ and $i \in \mathcal{C}_r$, by Assumption 6, we have

$$\begin{aligned} & \tilde{\Phi}_r^{\text{all}} \left((\hat{\mathbf{x}}_{\mathcal{C}_r, i}^{\nu+1}, \mathbf{x}_{\bar{\mathcal{C}}_r}^{\nu-\delta_i}) ; (\mathbf{x}_{\mathcal{C}_r}^{\nu-\mathbf{d}_i}, \mathbf{x}_{\bar{\mathcal{C}}_r}^{\nu-\delta_i}, \mathbf{x}_{\mathcal{E}_r}^{\nu-\mathbf{D}_i}) \right) \\ & \leq \tilde{\Phi}_r^{\text{all}} \left((\mathbf{x}_{\mathcal{C}_r}^*, \mathbf{x}_{\bar{\mathcal{C}}_r}^{\nu-\delta_i}) ; (\mathbf{x}_{\mathcal{C}_r}^{\nu-\mathbf{d}_i}, \mathbf{x}_{\bar{\mathcal{C}}_r}^{\nu-\delta_i}, \mathbf{x}_{\mathcal{E}_r}^{\nu-\mathbf{D}_i}) \right) - \frac{\tilde{L}_r}{2} \|\hat{\mathbf{x}}_{\mathcal{C}_r, i}^{\nu+1} - \mathbf{x}_{\mathcal{C}_r}^*\|^2 \\ & \leq \Phi^* + \bar{L}_r \left\| \mathbf{x}_{\bar{\mathcal{C}}_r}^{\nu-\delta_i} - \mathbf{x}_{\bar{\mathcal{C}}_r}^* \right\|^2 + \frac{\bar{L}_r}{2} \left\| \mathbf{x}_{\mathcal{C}_r}^{\nu-\mathbf{d}_i} - \mathbf{x}_{\mathcal{C}_r}^* \right\|^2 + \frac{\bar{L}_r}{2} \left\| \mathbf{x}_{\mathcal{E}_r}^{\nu-\mathbf{D}_i} - \mathbf{x}_{\mathcal{E}_r}^* \right\|^2 - \frac{\tilde{L}_r}{2} \|\hat{\mathbf{x}}_{\mathcal{C}_r, i}^{\nu+1} - \mathbf{x}_{\mathcal{C}_r}^*\|^2 \\ & \leq \Phi^* + \frac{\bar{L}_r(\sigma_r + 1)(D_r + 1)}{2} \left(\|\mathbf{x}^{\nu} - \mathbf{x}^*\|^2 + \Delta^{\nu} \right) - \frac{\tilde{L}_r}{2} \|\hat{\mathbf{x}}_{\mathcal{C}_r, i}^{\nu+1} - \mathbf{x}_{\mathcal{C}_r}^*\|^2, \end{aligned}$$

where $\hat{\mathbf{x}}_{\mathcal{C}_r, i}^{\nu+1}$ is defined in (B). Similarly, we have

$$\begin{aligned} & \tilde{\Phi}_r^{\text{all}} \left((\hat{\mathbf{x}}_{\mathcal{C}_r, i}^{\nu+1}, \mathbf{x}_{\bar{\mathcal{C}}_r}^{\nu}) ; (\mathbf{x}_{\mathcal{C}_r}^{\nu}, \mathbf{x}_{\bar{\mathcal{C}}_r}^{\nu}, \mathbf{x}_{\mathcal{E}_r}^{\nu}) \right) \\ & \leq \tilde{\Phi}_r^{\text{all}} \left((\hat{\mathbf{x}}_{\mathcal{C}_r, i}^{\nu+1}, \mathbf{x}_{\bar{\mathcal{C}}_r}^{\nu}) ; (\mathbf{x}_{\mathcal{C}_r}^{\nu-\mathbf{d}_i}, \mathbf{x}_{\bar{\mathcal{C}}_r}^{\nu-\delta_i}, \mathbf{x}_{\mathcal{E}_r}^{\nu-\mathbf{D}_i}) \right) + \frac{\bar{L}_r(\sigma_r + 1)D_r}{2} \Delta^{\nu}. \end{aligned}$$

Next, we bound $\|\hat{\mathbf{x}}_{\mathcal{C}_r, i}^{\nu+1} - \hat{\mathbf{x}}_{\mathcal{C}_r}^{\nu+1}\|^2$. Note that

$$\|\hat{\mathbf{x}}_{\mathcal{C}_r, i}^{\nu+1} - \hat{\mathbf{x}}_{\mathcal{C}_r}^{\nu+1}\|^2 = \sum_{j \in \mathcal{C}_r} \left\| (\hat{\mathbf{x}}_{\mathcal{C}_r, i}^{\nu+1})_j - (\hat{\mathbf{x}}_{\mathcal{C}_r, j}^{\nu+1})_j \right\|^2 \leq \sum_{j \in \mathcal{C}_r} \left\| \hat{\mathbf{x}}_{\mathcal{C}_r, i}^{\nu+1} - \hat{\mathbf{x}}_{\mathcal{C}_r, j}^{\nu+1} \right\|^2.$$

Moreover, $\|\hat{\mathbf{x}}_{\mathcal{C}_r, i}^{\nu+1} - \hat{\mathbf{x}}_{\mathcal{C}_r, j}^{\nu+1}\|^2$ can be bounded exactly as in Lemma 6. Therefore,

$$\|\hat{\mathbf{x}}_{\mathcal{C}_r, i}^{\nu+1} - \hat{\mathbf{x}}_{\mathcal{C}_r}^{\nu+1}\|^2 \leq \frac{2\tilde{L}_{\partial r}^2 |\mathcal{C}_r|^2 D_r}{\tilde{\mu}_r^2} \Delta_{\mathcal{N}_{\mathcal{C}_r}^{\nu}} + \frac{2\sigma_r \tilde{\ell}_r^2 |\mathcal{C}_r|^2 D_r}{\tilde{\mu}_r^2} \Delta_{\mathcal{C}_r}^{\nu}.$$

Thus, for any $\beta > 0$,

$$\begin{aligned} & \tilde{\Phi}_r^{\text{all}} \left((\hat{\mathbf{x}}_{\mathcal{C}_r}^{\nu+1}, \mathbf{x}_{\bar{\mathcal{C}}_r}^{\nu}) ; (\mathbf{x}_{\mathcal{C}_r}^{\nu}, \mathbf{x}_{\bar{\mathcal{C}}_r}^{\nu}, \mathbf{x}_{\mathcal{E}_r}^{\nu}) \right) - \tilde{\Phi}_r^{\text{all}} \left((\hat{\mathbf{x}}_{\mathcal{C}_r, i}^{\nu+1}, \mathbf{x}_{\bar{\mathcal{C}}_r}^{\nu}) ; (\mathbf{x}_{\mathcal{C}_r}^{\nu}, \mathbf{x}_{\bar{\mathcal{C}}_r}^{\nu}, \mathbf{x}_{\mathcal{E}_r}^{\nu}) \right) \\ & \leq \left\langle \nabla_{\mathcal{C}_r} \Phi(\mathbf{x}^{\nu}), \hat{\mathbf{x}}_{\mathcal{C}_r}^{\nu+1} - \hat{\mathbf{x}}_{\mathcal{C}_r, i}^{\nu+1} \right\rangle + \frac{\tilde{L}_r}{2} \|\hat{\mathbf{x}}_{\mathcal{C}_r}^{\nu+1} - \mathbf{x}_{\mathcal{C}_r}^{\nu}\|^2 - \frac{\tilde{\mu}_r}{2} \|\hat{\mathbf{x}}_{\mathcal{C}_r, i}^{\nu+1} - \mathbf{x}_{\mathcal{C}_r}^{\nu}\|^2 \\ & \leq \beta \|\nabla_{\mathcal{C}_r} \Phi(\mathbf{x}^{\nu})\|^2 + \frac{K_{2,r}}{4\beta} \Delta^{\nu} + \frac{\tilde{L}_r}{2\tau^2} \|\mathbf{x}_{\mathcal{C}_r}^{\nu+1} - \mathbf{x}_{\mathcal{C}_r}^{\nu}\|^2 - \frac{\tilde{\mu}_r}{2\tau^2} \|\mathbf{x}_i^{\nu+1} - \mathbf{x}_i^{\nu}\|^2, \end{aligned}$$

where $K_{2,r} = \frac{2|\mathcal{C}_r|^2 D_r}{\tilde{\mu}_r^2} (\tilde{L}_{\partial r}^2 + \sigma_r \tilde{\ell}_r^2)$, and the first inequality comes from the fact that, for any μ -strongly convex and L -smooth function f ,

$$f(y) - f(z) \leq \langle \nabla f(x), y - z \rangle + \frac{L}{2} \|y - x\|^2 - \frac{\mu}{2} \|z - x\|^2.$$

Combining the above bounds all together yields

$$\begin{aligned} & \tilde{\Phi}_r^{\text{all}}\left((\hat{\mathbf{x}}_{\mathcal{C}_r}^{\nu+1}, \mathbf{x}_{\bar{\mathcal{C}}_r}^{\nu}) ; (\mathbf{x}_{\mathcal{C}_r}^{\nu}, \mathbf{x}_{\bar{\mathcal{C}}_r}^{\nu}, \mathbf{x}_{\mathcal{E}_r}^{\nu})\right) - \Phi^* \\ & \leq \frac{\bar{L}_r(\sigma_r+1)(D_r+1)}{2} \|\mathbf{x}^{\nu} - \mathbf{x}^*\|^2 - \frac{\tilde{L}_r}{2\tau^2} \|\mathbf{x}_i^{\nu+1} - \mathbf{x}_i^*\|^2 + K_{3,r} \Delta^{\nu} + \beta \|\nabla_{\mathcal{C}_r} \Phi(\mathbf{x}^{\nu})\|^2 \\ & \quad + \frac{\tilde{L}_r}{2\tau^2} \|\mathbf{x}_{\mathcal{C}_r}^{\nu+1} - \mathbf{x}_{\mathcal{C}_r}^{\nu}\|^2 - \frac{\tilde{\mu}_r}{2\tau^2} \|\mathbf{x}_i^{\nu+1} - \mathbf{x}_i^{\nu}\|^2, \end{aligned}$$

where $K_{3,r} = \frac{\bar{L}_r(\sigma_r+1)(2D_r+1)}{2} + \frac{K_{2,r}}{4\beta}$. Taking $\frac{1}{|\mathcal{C}_r|} \sum_{i \in \mathcal{C}_r}$ for both sides yields

$$\begin{aligned} & \tilde{\Phi}_r^{\text{all}}\left((\hat{\mathbf{x}}_{\mathcal{C}_r}^{\nu+1}, \mathbf{x}_{\bar{\mathcal{C}}_r}^{\nu}) ; (\mathbf{x}_{\mathcal{C}_r}^{\nu}, \mathbf{x}_{\bar{\mathcal{C}}_r}^{\nu}, \mathbf{x}_{\mathcal{E}_r}^{\nu})\right) - \Phi^* \\ & \leq \frac{\bar{L}_r(\sigma_r+1)(D_r+1)}{2} \|\mathbf{x}^{\nu} - \mathbf{x}^*\|^2 - \frac{\tilde{L}_r}{2|\mathcal{C}_r|\tau^2} \|\mathbf{x}_{\mathcal{C}_r}^{\nu+1} - \mathbf{x}_{\mathcal{C}_r}^*\|^2 \\ & \quad + K_{3,r} \Delta^{\nu} + \beta \|\nabla_{\mathcal{C}_r} \Phi(\mathbf{x}^{\nu})\|^2 + \frac{1}{2\tau^2} \left(\tilde{L}_r - \frac{\tilde{\mu}_r}{|\mathcal{C}_r|}\right) \|\mathbf{x}_{\mathcal{C}_r}^{\nu+1} - \mathbf{x}_{\mathcal{C}_r}^{\nu}\|^2. \end{aligned}$$

Now we relate $\Phi(\mathbf{x}^{\nu+1})$ to the aggregated surrogates. Note that for $\tau \in [0, 1/p]$,

$$\Phi(\mathbf{x}^{\nu+1}) \leq (1 - \tau p) \Phi(\mathbf{x}^{\nu}) + \tau \sum_{r \in [p]} \Phi(P_r(\hat{\mathbf{x}}^{\nu+1} - \mathbf{x}^{\nu})),$$

hence by Assumption 5.(ii),

$$\Phi(\mathbf{x}^{\nu+1}) \leq (1 - \tau p) \left[\Phi^* + \frac{L}{2} \|\mathbf{x}^{\nu} - \mathbf{x}^*\|^2 \right] + \tau \sum_{r \in [p]} \tilde{\Phi}_r^{\text{all}}\left((\hat{\mathbf{x}}_{\mathcal{C}_r}^{\nu+1}, \mathbf{x}_{\bar{\mathcal{C}}_r}^{\nu}) ; (\mathbf{x}_{\mathcal{C}_r}^{\nu}, \mathbf{x}_{\bar{\mathcal{C}}_r}^{\nu}, \mathbf{x}_{\mathcal{E}_r}^{\nu})\right).$$

Thus,

$$\begin{aligned} \Phi(\mathbf{x}^{\nu+1}) - \Phi^* & \leq \frac{L(1 - \tau p) + \tau p(\sigma + 1)(D + 1)}{2} \|\mathbf{x}^{\nu} - \mathbf{x}^*\|^2 - \frac{\tilde{L}_{\min}}{2C\tau} \|\mathbf{x}^{\nu+1} - \mathbf{x}^*\|^2 \\ & \quad + K_3 \tau p \Delta^{\nu} + \beta \tau \|\nabla \Phi(\mathbf{x}^{\nu})\|^2 + \frac{1}{2\tau} \left(\tilde{L} - \frac{\tilde{\mu}}{C}\right) \|\mathbf{x}^{\nu+1} - \mathbf{x}^{\nu}\|^2, \end{aligned} \quad (85)$$

where $K_3 = \max_{r \in [p]} K_{3,r}$. Moreover, by (84), we have

$$\Phi(\mathbf{x}^{\nu+1}) - \Phi^* \leq \Phi(\mathbf{x}^{\nu}) - \Phi^* - \frac{\tau}{4\tilde{L}} \|\nabla \Phi(\mathbf{x}^{\nu})\|^2 - \frac{\tilde{\mu}}{8\tau} \|\mathbf{x}^{\nu+1} - \mathbf{x}^{\nu}\|^2 + \tau K_1 \Delta^{\nu}, \quad (86)$$

where $K_1 = A_{\mathcal{J}} + \max_{r: |\mathcal{C}_r| > 1} \tilde{A}_r$. Choose $\beta = 1$ and τ such that $\frac{\tilde{L}_{\min}}{2C\tau} > \frac{L(1 - \tau p) + \tau p(\sigma + 1)(D + 1)}{2}$, and let $\nu \cdot (86) + (85)$, we have

$$V^{\nu+1} \leq V^{\nu} - \left[\frac{\tilde{\mu}\nu}{8\tau} - \frac{\tilde{L} - \tilde{\mu}/C}{2\tau} \right] \|\mathbf{x}^{\nu+1} - \mathbf{x}^{\nu}\|^2 + (\tau K_1 \nu + \tau p K_3) \Delta^{\nu},$$

where $V^{\nu} = \nu(\Phi(\mathbf{x}^{\nu}) - \Phi^*) + \frac{\tilde{L}_{\min}}{2C\tau} \|\mathbf{x}^{\nu} - \mathbf{x}^*\|^2$. For $\nu > 4(\frac{\tilde{L}}{\tilde{\mu}} - \frac{1}{C})$, $\frac{\tilde{\mu}\nu}{8\tau} - \frac{\tilde{L} - \tilde{\mu}/C}{2\tau} > 0$, by the delay-window inequality in [15, Lemma 5], if

$$(D + 1)(\tau K_1 \nu + \tau p K_3) \leq \frac{\tilde{\mu}\nu}{8\tau} - \frac{\tilde{L} - \tilde{\mu}/C}{2\tau},$$

we have

$$\Phi(\mathbf{x}^{\nu}) - \Phi^* \leq \frac{\Phi(\mathbf{x}^0) - \Phi^* + \frac{\tilde{L}_{\min}}{2C\tau} \|\mathbf{x}^0 - \mathbf{x}^*\|^2}{\nu}.$$

Consequently, for sufficiently large ν , it suffices to pick τ small enough so that the previous inequality holds; in particular,

$$\tau \leq \sqrt{\frac{\frac{\tilde{\mu}\nu}{8} - \frac{\tilde{L} - \tilde{\mu}/C}{2}}{(D+1)(K_1\nu + pK_3)}} \asymp \sqrt{\frac{\tilde{\mu}}{8(D+1)K_1}}.$$

Therefore, for sufficiently large ν , it is enough to choose τ satisfying all the above requirements, namely

$$\tau \leq \min \left\{ \frac{1}{p}, \sqrt{\frac{\tilde{\mu}}{16(D+1)K_1}}, \frac{\tilde{L}_{\min}}{CL + C(\sigma+1)(D+1)} \right\}.$$

This completes the proof. \square

D Proof of Theorem 4

By (84), we have

$$\Phi(\mathbf{x}^{\nu+1}) \leq \Phi(\mathbf{x}^\nu) - \frac{\tau}{4\tilde{L}} \|\nabla\Phi(\mathbf{x}^\nu)\|^2 - \frac{\tilde{\mu}}{8\tau} \|\mathbf{x}^{\nu+1} - \mathbf{x}^\nu\|^2 + \tau K_1 \Delta^\nu.$$

where $K_1 := A_{\mathcal{J}} + \max_{r:|\mathcal{C}_r|>1} \tilde{A}_r$. Observe that

$$\begin{aligned} & \sum_{\ell=\nu-D}^{\nu-1} [\ell - (\nu-1) + D] \|\mathbf{x}^{\ell+1} - \mathbf{x}^\ell\|^2 - \sum_{\ell=\nu+1-D}^{\nu} [\ell - \nu + D] \|\mathbf{x}^{\ell+1} - \mathbf{x}^\ell\|^2 \\ &= \sum_{\ell=\nu-D}^{\nu-1} \|\mathbf{x}^{\ell+1} - \mathbf{x}^\ell\|^2 - D \|\mathbf{x}^{\nu+1} - \mathbf{x}^\nu\|^2. \end{aligned}$$

Under the standard initialization $\mathbf{x}^{-D} = \dots = \mathbf{x}^0$, define

$$V^\nu := \Phi(\mathbf{x}^\nu) + \tau K_1 \sum_{\ell=\nu-D}^{\nu-1} [\ell - (\nu-1) + D] \|\mathbf{x}^{\ell+1} - \mathbf{x}^\ell\|^2.$$

Then, we have

$$V^{\nu+1} \leq V^\nu - \left(\frac{\tilde{\mu}}{8\tau} - \tau D K_1 \right) \|\mathbf{x}^{\nu+1} - \mathbf{x}^\nu\|^2 - \frac{\tau}{4\tilde{L}} \|\nabla\Phi(\mathbf{x}^\nu)\|^2.$$

Choose $\tau \leq \min \left\{ \frac{1}{p}, \frac{1}{2} \sqrt{\frac{\tilde{\mu}}{2DK_1}} \right\}$ so that $\frac{\tilde{\mu}}{8\tau} - \tau D K_1 \geq 0$. Since (V^ν) is nonincreasing and $V^\nu \geq \Phi^*$, summing the above inequality over ν yields (55). \square

References

1. D. Bertsekas and J. Tsitsiklis. *Parallel and distributed computation: numerical methods*. Athena Scientific, 2015.
2. A. Bretto. Hypergraph theory. *An introduction. Mathematical Engineering*. Cham: Springer, 1:209–216, 2013.
3. C. Cadena, L. Carlone, H. Carrillo, Y. Latif, D. Scaramuzza, J. Neira, I. Reid, and J. J. Leonard. Past, present, and future of simultaneous localization and mapping: Toward the robust-perception age. *IEEE Transactions on robotics*, 32(6):1309–1332, 2017.
4. X.-C. Cai and D. E. Keyes. Nonlinearly preconditioned inexact newton algorithms. *SIAM Journal on Scientific Computing*, 24(1):183–200, 2002.
5. L. Cannelli, F. Facchinei, G. Scutari, and V. Kungurtsev. Asynchronous optimization over graphs: Linear convergence under error bound conditions. *IEEE Transactions on Automatic Control*, 66(10):46044619, Oct. 2021.

6. T. Cao, X. Chen, and G. Scutari. Dcatalyst: A unified accelerated framework for decentralized optimization. (arXiv:2501.18114), Jan. 2025. arXiv:2501.18114.
7. J. Chen and A. H. Sayed. Diffusion adaptation strategies for distributed optimization and learning over networks. *IEEE Transactions on Signal Processing*, 60(8):4289–4305, 2012.
8. S. Chezhegov, A. Novitskii, A. Rogozin, S. Parsegov, P. Dvurechensky, and A. Gasnikov. A general framework for distributed partitioned optimization. *IFAC-PapersOnLine*, 55(13):139–144, 2022. 9th IFAC Conference on Networked Systems NECSYS 2022.
9. A. Daneshmand, G. Scutari, and V. Kungurtsev. Second-order guarantees of distributed gradient algorithms. *SIAM Journal on Optimization*, 30(4):3029–3068, 2020.
10. P. Di Lorenzo and G. Scutari. Next: In-network nonconvex optimization. *IEEE Transactions on Signal and Information Processing over Networks*, 2(2):120–136, 2016.
11. C. T. Dinh, T. T. Vu, N. H. Tran, M. N. Dao, and H. Zhang. A new look and convergence rate of federated multitask learning with laplacian regularization. *IEEE Transactions on Neural Networks and Learning Systems*, 35(6):8075–8085, 2022.
12. G. Even and N. Halabi. Analysis of the min-sum algorithm for packing and covering problems via linear programming. *IEEE Transactions on Information Theory*, 61(10):5295–5305, 2015.
13. F. Facchinei, L. Lampariello, and G. Scutari. Feasible methods for nonconvex nonsmooth problems with applications in green communications. *Mathematical Programming*, 164(1–2):55–90, July 2017.
14. F. Facchinei, J.-S. Pang, G. Scutari, and L. Lampariello. VI-constrained hemivariational inequalities: distributed algorithms and power control in ad-hoc networks. *Mathematical Programming*, 145(1–2):59–96, June 2014.
15. H. R. Feyzmahdavian and M. Johansson. Asynchronous iterations in optimization: New sequence results and sharper algorithmic guarantees. *Journal of Machine Learning Research*, 24(158):1–75, 2023.
16. E. Isufi, F. Gama, D. I. Shuman, and S. Segarra. Graph filters for signal processing and machine learning on graphs. *IEEE Transactions on Signal Processing*, 72:4745–4781, 2024.
17. F. R. Kschischang, B. J. Frey, and H.-A. Loeliger. Factor graphs and the sum-product algorithm. *IEEE Transactions on Information Theory*, 47(2):498–519, Feb. 2001.
18. P. Latafat and P. Patrinos. Primal-dual algorithms for multi-agent structured optimization over message-passing architectures with bounded communication delays. *Optimization Methods and Software*, 37(6):2038–2065, 2022.
19. D. M. Malioutov, J. K. Johnson, and A. S. Willsky. Walk-sums and belief propagation in gaussian graphical models. *Journal of Machine Learning Research*, 7(2):2031–2064, 2006.
20. C. C. Moallemi and B. Van Roy. Convergence of min-sum message passing for quadratic optimization. *IEEE Transactions on Information Theory*, 55(5):2413–2423, 2009.
21. C. C. Moallemi and B. Van Roy. Convergence of min-sum message-passing for convex optimization. *IEEE Transactions on Information Theory*, 56(4):2041–2050, 2010.
22. C. S. J. Nash-Williams. Random walk and electric currents in networks. In *Mathematical Proceedings of the Cambridge Philosophical Society*, volume 55, pages 181–194. Cambridge University Press, 1959.
23. A. Nedić, A. Olshevsky, and M. Rabbat. Network topology and communication-computation tradeoffs in decentralized optimization. *Proceedings of the IEEE*, 106:953–976, 2018.
24. A. Nedic, A. Olshevsky, and W. Shi. Achieving geometric convergence for distributed optimization over time-varying graphs. *SIAM Journal on Optimization*, 27(4):2597–2633, 2017.
25. A. Nedic and A. Ozdaglar. Distributed subgradient methods for multi-agent optimization. *IEEE Transactions on Automatic Control*, 54(1):48–61, 2009.
26. A. Nedic, A. Ozdaglar, and P. A. Parrilo. Constrained consensus and optimization in multi-agent networks. *IEEE Transactions on Automatic Control*, 55(4):922–938, 2010.
27. V. NK. $Lx = b$ laplacian solvers and their algorithmic applications. *Found. Tr. Theor. Comp. Sci*, 8(1–2):1–141, 2012.
28. D. Romero, M. Ma, and G. B. Giannakis. Kernel-based reconstruction of graph signals. *IEEE Transactions on Signal Processing*, 65(3):764–778, 2016.
29. S. Roth and M. J. Black. Fields of experts. *International Journal of Computer Vision*, 82(2):205–229, 2009.
30. S. Ruder. An overview of multi-task learning in deep neural networks. *arXiv preprint arXiv:1706.05098*, 2017.

31. N. Ruozzi and S. Tatikonda. Message-passing algorithms for quadratic minimization. *The Journal of Machine Learning Research*, 14(1):2287–2314, 2013.
32. A. H. Sayed et al. Adaptation, learning, and optimization over networks. *Foundations and Trends® in Machine Learning*, 7(4-5):311–801, 2014.
33. K. Scaman, F. Bach, S. Bubeck, Y. T. Lee, and L. Massoulié. Optimal algorithms for smooth and strongly convex distributed optimization in networks. In *international conference on machine learning*, pages 3027–3036. PMLR, 2017.
34. G. Scutari, F. Facchinei, and L. Lampariello. Parallel and Distributed Methods for Constrained Nonconvex OptimizationPart I: Theory. *IEEE Transactions on Signal Processing*, 65(8):1929–1944, Apr. 2017.
35. G. Scutari and Y. Sun. Distributed nonconvex constrained optimization over time-varying digraphs. *Mathematical Programming*, 176:497–544, 2019.
36. W. Shi, Q. Ling, G. Wu, and W. Yin. Extra: An exact first-order algorithm for decentralized consensus optimization. *SIAM Journal on Optimization*, 25(2):944–966, 2015.
37. W. Shi, Q. Ling, K. Yuan, G. Wu, and W. Yin. On the linear convergence of the admm in decentralized consensus optimization. *IEEE Transactions on Signal Processing*, 62(7):1750–1761, 2014.
38. S. Shin, V. M. Zavala, and M. Anitescu. Decentralized schemes with overlap for solving graph-structured optimization problems. *IEEE Transactions on Control of Network Systems*, 7(3):1225–1236, 2020.
39. Y. Sun, G. Scutari, and A. Daneshmand. Distributed optimization based on gradient tracking revisited: Enhancing convergence rate via surrogation. *SIAM Journal on Optimization*, 32(2):354–385, 2022.
40. A. Toselli and O. B. Widlund. *Domain Decomposition Methods—Algorithms and Theory*, volume 34 of *Springer Series in Computational Mathematics*. Springer, 2005.
41. M. J. Wainwright, T. S. Jaakkola, and A. S. Willsky. Map estimation via agreement on trees: message-passing and linear programming. *IEEE transactions on information theory*, 51(11):3697–3717, 2005.
42. M. J. Wainwright and M. I. Jordan. Graphical models, exponential families, and variational inference. *Foundations and Trends in Machine Learning*, 1(1–2):1–305, 2008.
43. Z. Wan and S. Vlaski. Multitask learning with learned task relationships. *arXiv preprint arXiv:2510.10570*, 2025.
44. S. Wang, A. G. Schwing, and R. Urtasun. Efficient inference of continuous markov random fields with polynomial potentials. *Advances in neural information processing systems*, 27, 2014.
45. Y.-X. Wang, J. Sharpnack, A. J. Smola, and R. J. Tibshirani. Trend filtering on graphs. *Journal of Machine Learning Research*, 17(105):1–41, 2016.
46. Y. Weiss and W. T. Freeman. Correctness of belief propagation in gaussian graphical models of arbitrary topology. *Neural Computation*, 13(10):2173–2200, Oct. 2001.
47. J. Xu, Y. Tian, Y. Sun, and G. Scutari. Accelerated primal-dual algorithms for distributed smooth convex optimization over networks. In *Proceedings of the Twenty Third International Conference on Artificial Intelligence and Statistics*, page 23812391. PMLR, June 2020.
48. K. Yuan, Q. Ling, and W. Yin. On the convergence of decentralized gradient descent. *SIAM Journal on Optimization*, 26(3):1835–1854, 2016.
49. K. Yuan, Q. Ling, and W. Yin. On the convergence of decentralized gradient descent. *SIAM Journal on Optimization*, 26(3):1835–1854, 2016.
50. K. Yuan, B. Ying, X. Zhao, and A. H. Sayed. Exact diffusion for distributed optimization and learningpart i: Algorithm development. *IEEE Transactions on Signal Processing*, 67(3):708–723, 2018.
51. Z. Zhang and M. Fu. Convergence properties of message-passing algorithm for distributed convex optimisation with scaled diagonal dominance. *IEEE Transactions on Signal Processing*, 69:3868–3877, 2021.